THE CORROSION OF CoCrMo ALLOYS FOR BIOMEDICAL APPLICATIONS

by

GEORGE BELLEFONTAINE

A thesis submitted to the University of Birmingham

for the degree of

Master of Research

School of Metallurgy and Materials

University of Birmingham

January 2010

Abstract

CoCrMo alloys have been used for biomedical implants for a number of years. They are now frequently used for the metal-on-metal hip resurfacing joints due to their high corrosion and wear performance. Thermal treatments are used on these alloys in attempt to alter the microstructure to improve the mechanical properties. However, the effect that this then has on the corrosion behaviour is less well understood. There is a concern that corrosion processes are the cause of in-vivo failures, leading to retrieval operations. The release of metal ions due to corrosion is thought to have adverse affects on the surrounding body tissue and ultimately leads to failure of the implant. The present project was carried out to investigate the feasibility of taking electrochemical measurements from hip resurfacing joints whilst articulating in a hip simulator. In this study, the effect of 'as-cast' and 'double heat-treated' CoCrMo alloys were compared for microstructure and corrosion behaviour differences while operating in a hip simulator.

Corrosion behaviour was investigated using a ProSim friction simulator with an integrated electrochemical cell in this study of tribocorrosion. OCP and potentiostat measurements were taken using 3.5% NaCl and 28% bovine in the hip simulator. Potentiodynamic polarisation curves were taken in neutral and acidified bovine serum solutions. Microstructure characterisation was carried out using SEM and EDX analysis.

The problems and changing variables that occur as a result of corrosion testing in a hip simulator were identified and discussed, most notably the change in temperature and its affect on the corrosion potential. 3.5% NaCl was shown to be a more corrosive environment than 28% bovine serum in an articulating hip simulator under load. Measurements of the OCP showed no consistent difference between the two heat-treatments; as-cast and double heat-treated. Preliminary potentiostat measurements in a hip simulator were taken, which to date, is the first of their kind.

Acknowledgements

Firstly, I would like to thank my supervisor, Dr Alison Davenport, I am tremendously grateful for all the support and time she has given me over the course of my project and writing up period. As a result of her guidance I have further developed my skills and experience, which I am sure, will be invaluable in the future. I would also like to thank the Department of Metallurgy and Materials, University of Birmingham for use of their facilities and equipment as well as their financial support during the project.

I am also grateful to my sponsors; Smith and Nephew Orthopaedics, Leamington Spa, for the use of their hip simulator, SEM and the CoCrMo hip resurfacing joints provided for use in this project. I would particularly like to thank Amir Kamali, Chenxi Li, Azad Hussain for their support and guidance during the project.

Finally I would like to thank all those in the electrochemistry group who have helped me throughout my project. I am particularly grateful to Dr Mark Ashworth for his help and support with the experimental procedures used in the project.

Table of Contents

Chapter 1 Introduction.....1

Chapter 2 Literature review.....2

2.1 Hip replacement.....2

2.2 Metallurgy of CoCrMo alloys for biomedical applications.....4

2.2.1 Physical Metallurgy.....4

2.2.2 Chemical composition.....5

2.2.3 Processing of CoCrMo alloys.....5

2.2.4 Solution treatments of CoCrMo alloys for biomedical applications; the effect on the microstructure and properties.....6

2.2.5 Carbides in CoCrMo alloys.....8

2.2.5.1 Effect of carbides on wear resistance.....8

2.2.5.2 Effect of carbides on corrosion resistance.....8

2.2.6 Summary of heat treatment results.....9

2.3 Corrosion of CoCrMo in aqueous environments.....9

2.3.1 The Corrosion Process.....9

2.3.2 Resistance to Corrosion – The Passivation of CoCrMo.....10

2.3.3 Types of Corrosion.....10

2.3.4 Tribocorrosion of CoCrMo.....11

2.3.5 Biocompatibility issues and metal ion release.....12

2.3.6 Corrosion in the body.....13

2.3.6.1 Chloride content and pH in general.....13

2.3.6.2 The influence of proteins.....13

2.4 Review of in vivo results and retrieval rates.....15

2.41 The development of Pseudotumours.....16

2.5 Review of in vitro studies.....16

2.6 Summary of Literature.....18

2.7 Project Aims and Objectives.....18

Chapter 3 Experimental Method.....19

3.1 Materials.....19

3.1.1 ASTM F75 CoCrMo alloy.....19

3.1.2 Thermal processing.....19

3.2 Microstructure characterisation.....22

3.2.1 SEM.....22

3.3 Solutions used.....22

3.4 Measuring Tribocorrosion using a Hip Simulator.....25

3.4.1 Test setup.....25

3.5 Precautions and Test parameters.....29

3.5.1 Hip simulator.....29

3.5.2 Connections and Insulation.....29

3.5.3 Test samples.....29

3.5.4 Clearance Values between the head and cup.....30

3.5.5 Experimental parameters.....30

3.6 Anodic Polarisation Measurements.....31

3.6.1 Surface preparation for electrochemical measurements.....31

Chapter 4 Results.....31

4.1 The effect of thermal treatment on the microstructure and composition of AC and DHT CoCrMo alloys.....32

4.1.1 SEM.....32

4.1.2 EDX.....33

4.2 Electrochemical Measurements – Potentiodynamic anodic polarisation curves.....34

4.3 Preliminary Hip Simulator results measuring OCP.....38

4.3.1 AC Worn in part – The difference between 3.5% NaCl and 28% Bovine Serum.....38
4.3.2 AC and DHT Worn in parts – The difference in temperature at 40°C and 20°C (room temperature).....39
4.3.3 General Overview of OCPs of worn-in as-cast and double heat treated parts.....43
4.4 Hip Simulator results measuring OCP using new AC and DHT samples.....44
4.4.1 Alternating cycles of stabilisation and abrasion.....44
4.5 Measuring the OCP over a 2.5 hour period.....50
4.5.1 Detailed examination of the OCP over a 2.5 hour period.....51
4.6 Preliminary potentiostatic measurements using a Hip Simulator.....57
4.7 Characterising the Wear Scars from the Hip Simulator.....60

Chapter 5 Discussion.....62
5.1 Microstructure and composition differences of AC and DHT.....62
5.2 Anodic polarisation curves – the difference of as-cast and double heat treated samples.....62
5.3 Feasibility of electrochemical measurements in a Hip Simulator.....64
5.3.1 The effect of Temperature in Hip simulator experiments.....64
5.3.2 Hip Simulator results measuring OCP using new AC and DHT samples.....66
5.3.2.1 Alternating cycles of stabilisation and abrasion.....66
5.3.2.2 Measuring the OCP over a 2.5 hour period.....67
5.3.3 Obtaining preliminary potentiostatic measurements using a hip simulator.....69
5.3.4 The problem of variability within hip simulator experiments.....69
5.4 The difference in solution using a Hip Simulator.....70
5.5 The clinical implications of this study.....71

Chapter 6 Conclusions.....72

Chapter 7 Further Work.....73

Chapter 8 References.....74

Chapter 9 Appendix.....80

The Corrosion of CoCrMo Alloys for Biomedical Applications

1. Introduction

Metal implants are used to replace hip joints. There was a need to increase the life expectancy of artificial hip joints as these are being implanted in younger and more active patients. One fairly new form of hip replacement is the hip resurfacing joint, which has “metal-on-metal” articulation between a metal cover on the femoral head and a metal-lined acetabular cup. These are made of CoCrMo because of its corrosion and wear resistance. However, when implanted into the body, the metal-on-metal joint will experience tribocorrosion, a form of metal degradation. There is currently concern that this may lead to the release of metal ions into the body, which can have an adverse affect on the body’s tissues. Recent work has suggested that the heat treatment of the alloy can affect its resistance to tribocorrosion and the release of metal ions. The aim of the project is to demonstrate the use of a hip simulator to take tribocorrosion measurements and investigate the effect of heat treatment on performance.

Literature review

1.1. Hip Replacement

Hip replacement surgery has been used for many decades to resolve the problem of diseased or damaged hip joints. As life expectancy increases, the demand for hip joint replacement is rising and there is a need to increase the life of prosthetic hip joints. This is especially important for younger and more active patients. Implant requirements such as high corrosion and wear resistance, biocompatibility and longevity are essential for successful hip joint replacement [1].

There are two types of metal hip prosthesis. In total hip replacements (THR), the head of the femur is cut away and a metal shaft with a replacement femoral head is inserted into the femur (Figure 2.1). Owing to the significant bone loss, this is only suitable for elderly or inactive patients. However, it is a common elective surgical procedure, with over 30,000 performed in England each year [2]. The alternative procedure, known as hip resurfacing, is more effective for younger, active patients since it conserves more bone stock and is less invasive of the femoral shaft [3]. In this case, an acetabular cup and femoral head fit together to form the hip joint, similar to a THR, but with a much shorter stem being inserted into the femur (shown in Figure 2.2). An additional advantage of resurfacing is that when the implant needs to be revised, it gives greater options than a THR as less bone will have previously been cut away [3].

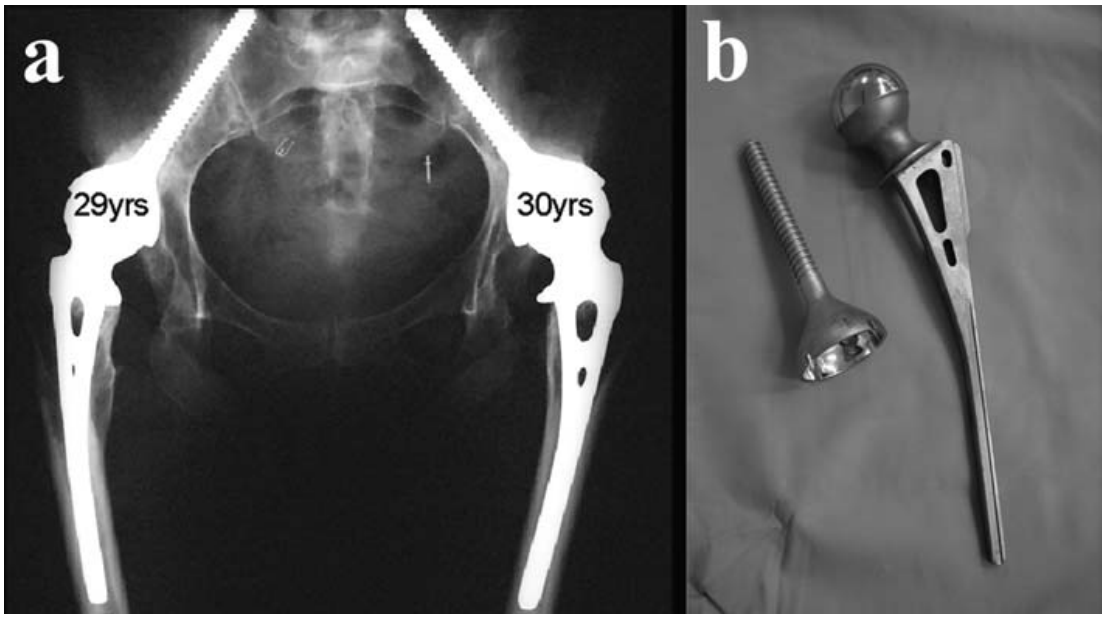

Figure 2.1:- A) An x-ray of a double total hip replacement. The shaft of the metal joint is placed down the centre of the femur. B) An example of a typical metal-on-metal total hip prosthesis [3].

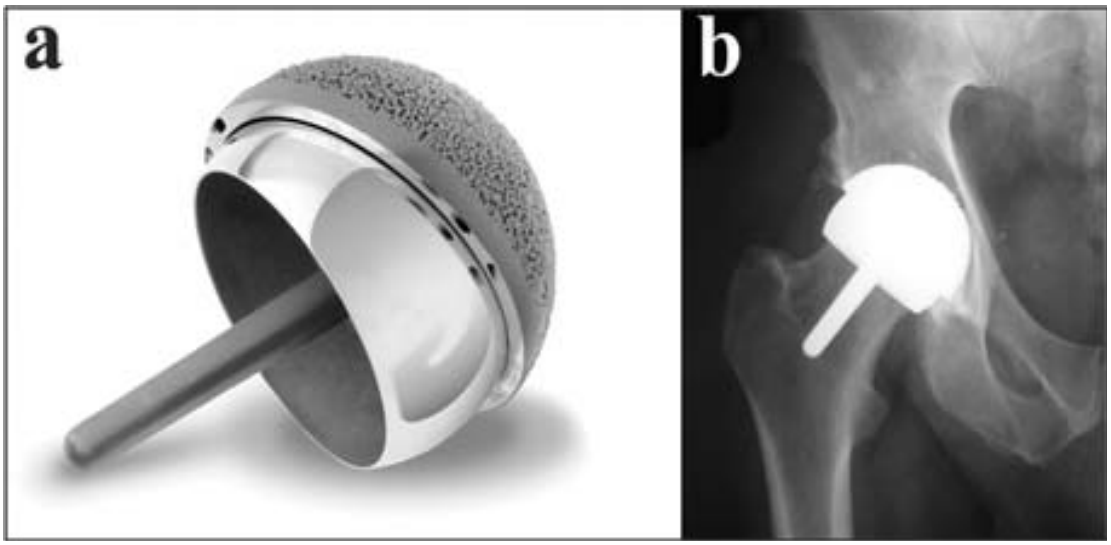

Figure 2.2:- A) An example of a typical hip resurfacing component B) An X-ray of a 7 year old hip resurfacing joint [3].

The x-ray in Figure 2.2 shows the hip resurfacing joint occupying much less space in the body compared to its counterpart in Figure 2.1. With fewer invasions of the femur and pelvic bone there is much less disruption and trauma experienced by the body and it is much easier to revise should problems arise.

In Figure 2.2a beads are present on the outside of the acetabular cup that are needed for socket fixation. These beads create a porous ingrowth surface which allows bone ingrowth giving a more natural biological fixation [4]. This is much more advantageous than the THR alternative shown in Figure 2.1b whereby a screw is inserted into the pelvic bone. CoCrMo is the alloy used in both types of hip replacement shown in Figure 2.1 and 2.2 and commonly throughout surgical procedures

A variety of head materials (both metal and ceramic) and acetabular cups (metal and polymer) have been used for THR leading to metal-on-ceramic and metal-on-polymer articulation. However, there is now increasing use of metal-on-metal articulation as it possesses superior wear resistance compared with other material combinations [5]. In the case of hip resurfacing procedures, after much research into alternative materials, metal-on-

metal bearings have been used since the mid 1990s [6, 7]. However, there is a need for further study of the tribocorrosion of metal-on-metal bearings as they have been shown in the case of CoCrMo to produce a significantly higher release of metal ions in comparison with metal-on-polyethylene bearings [8]. CoCrMo alloys are the most commonly used metal-on-metal bearing due to their high corrosion and wear resistance [9]. This is obtained largely from the addition of carbon in the alloy that results in the formation of carbides in the microstructure. Carbides give strength and wear resistance by taking up chromium and molybdenum from the surrounding area during the solidification process. However, when in articulation with another surface, in the case of a hip implant they may come into contact with the softer matrix. During the 'running in' period two-body grooving can occur where hard asperities (the carbides) make contact with their opposite surface to cause deep grooves. This can lead to the release of metal ions and wear debris. The wear debris can then lead to three-body rolling where the released particle rolls in the middle of the two articulating surfaces causing further damage. Carbides and their affect on two and three body wear will be discussed in more detail in section *2.2.5 Carbides in CoCrMo alloys*.

2.2 Metallurgy of CoCrMo alloys for biomedical applications

2.2.1 Physical metallurgy

Cobalt-based alloys have two possible crystal structures: close packed hexagonal (CPH) at low temperatures (below 417°C) and face centred cubic (FCC) at high temperatures (above 417°C). In the application of a hip resurfacing joint, however, most cobalt-based alloys will display a metastable FCC matrix structure because the thermal treatments with which these alloys are produced involve relatively fast cooling, inhibiting the formation of a CPH structure [10, 11]. This is because the kinetic transformation from FCC to CPH at room temperature is very slow [10, 11]. The rate at which this transformation occurs, however, will depend on factors such as alloying elements and specific thermal processing. When chromium and tungsten are added, this increases the transformation rate. However, when FCC stabilisers are added, such as elements like nickel and carbon this slows the transformation rate [1].

2.2.2 Chemical composition

Commonly, there are two types of CoCrMo alloys used for biomedical applications, which depend on the level of carbon added. However, both alloys have a balance of cobalt, which

can be as low as 60 wt%. There is approximately 28% chromium which forms a chromium rich passive oxide film (Cr_2O_3) that spontaneously forms on the surface of the metal [1, 5, 12, 13]. This gives good corrosion resistance by separating the metal from the air and aqueous environments [5, 9]. Typically 5-7 wt% molybdenum is used to improve the mechanical properties of the alloy as it provides solid solution strengthening and good localised corrosion resistance [1, 3, 4, 13]. The alloy has an oxide layer on its surface, which forms a thin passive film that is enriched with chromium. This is thought to be 1-4 nm thick and gives very good corrosion resistance [14, 15].

CoCrMo alloys can be termed 'high carbon' (usually 0.15-0.25 wt%) or 'low carbon' (usually less than 0.06 wt%) depending on the amount added in the casting process [13]. Carbon additions between 0.1 and 0.3 wt% have been shown to favour the formation of carbides which increase wear resistance [1, 16]. These micron-scale cast carbides that form at the surface of the alloy are much harder than the alloys matrix and so they will protect the surface from wear [17]. Experiments using cast low carbon-content CoCrMo have been shown to produce high wear rates compared with cast high carbon material [18]. High carbon has also shown to have superior corrosion and tribo-corrosion resistance [13]. Subsequently, all manufacturers have moved away from low carbon products as bearing materials in the body.

2.2.3 Processing of CoCrMo alloys

CoCrMo alloys for orthopaedic implants are primarily in the cast or wrought forms, with similar chemical compositions based on American Society for Testing and Materials (ASTM) standards. Cast alloys are often used for complicated shapes that cannot be machined, such as the acetabular cup of total hip replacements. However, this process has its limitations such as the development of inhomogenous microstructures as a result of un-equal cooling rates. This can lead to wrought alloys being a favourable alternative whereby large castings are hot forged and thermo-mechanically processed and re-worked into a smaller size [1, 19, 20]. This result in the microstructure being refined is due to any shrinkage voids which existed being closed up. This then gives superior mechanical and fatigue properties to the same metallic material [20]. For example, simple modular femoral heads can be machined from a wrought alloy with high carbon in it.

This project will focus on the use of cast ASTM F75, which has the composition given in Table 2.1.

Table 2.1 List of compositions and major elements of Cast ASTM F75 CoCrMo alloy [1, 20]

Name	Condition	Hardness HV or R*	Nominal compositions of major elements (approximate wt %)				
			Co	Cr	Mo	C	Others (≥ 1 wt %)
ASTM F75	Cast	310 HV	Bal	28	6	0.35	Ni-1, Si-1, Mn-1

*HV = Hardness Vickers, R = Hardness Rockwell, Bal = Balance

2.2.4 Solution treatments of CoCrMo alloys for biomedical applications: the effect on the microstructure and properties

The manufacturing process, solution treatment and solidification process can cause a number of different transformations to occur in the alloy. These variations in the microstructure have a strong influence of properties such as strength, fracture toughness, corrosion and wear resistance. An “as-cast” Co-Cr alloy has a coarse dendritic structure characteristic of investment casting with carbides present in the matrix. When the Co-Cr alloy is heat-treated it serves to homogenise the microstructure causing some of the carbides to dissolve into the matrix [21].

Hot isostatic pressing (HIPping) is sometimes used to reduce microporosity resulting from casting. Such treatments have been used for Birmingham Hip Resurfacing devices: in 1994 HIPping was used alone, then in 1995 devices were solution heat-treated, before a combination of both hot isostatic-pressing and solution heat-treatment was used in 1996 [3].

Heat treatments for biomedical CoCrMo vary with different manufacturing companies. The alloys used in this project were obtained from Smith and Nephew Orthopaedics who supplied “as-cast” and “double heat-treated” samples. Double heat treatment involves solution heat treatment followed by HIPping. Full details of the heat treatment procedures are given in Chapter 3. There are two main effects of heating the metal to this temperature; Firstly, the overall carbide volume fraction of the alloy is reduced, and secondly, the original large blocky carbides can dissolve leaving smaller particles in the matrix [17, 18]. The corrosion resistant carbides are broken up by this dissolving making them easier to dislodge under abrasive conditions [3]. Kauser [1] also found similar results

whereby heat treating the alloy reduced the carbide area fraction as well as the number of carbides in the alloy. However, with the reduced carbide area fraction it has been found that the HIPping of sintered materials gives fewer pores in the microstructure and so improves the fatigue strength [21]. This is also supported by Kauser who found that the amount of porosity seen in solution treated samples that had undergone HIPping first has been generally smaller than that of as-cast samples [1].

Currently, there is concern that solution-treated prostheses (prostheses that have undergone further solution treatments post the casting process) do not perform as well as as-cast prostheses. The advantage of double heat-treating, whereby solution treatment (ST) followed by hot isostatically pressing (HIP) is carried out on the component (full details of double heat treating process are in the Experimental Method, Section 3.1.2 *Thermal Processing*), is that subsurface microporosity is removed, and the alloy's ductility and homogeneity is improved [17, 22]. However, the concern is that HIP-ST may lead to increased metal wear owing to the decrease in size and area fraction of carbides [17, 23]. However, ST is carried out to homogenise the matrix leading to a more stable, uniform oxide layer compared with a more inhomogeneous highly dendritic (as-cast) structure [13].

There is also evidence that the double heat treating of the alloy causes a molybdenum depleted region to surround the molybdenum rich precipitates that are seen in DHT CoCrMo samples [1, 24, 25]

2.2.5 Carbides in CoCrMo alloys

2.2.5.1 Effect of carbides on wear resistance

Cobalt-based alloys owe their wear resistance to the hard macroscopic carbides present in the microstructure. Carbides are harder than the surrounding alloy and so are more resilient to the two and three body abrasive wear that can be experienced in a metal-on-metal hip joint [1]. The wear rate depends on the carbide volume fraction as well as their size and distribution, which is known to be affected by the thermal processing of the alloy. Carbide size distribution refers to the different morphologies that can exist such as blocky, particulate agglomerated or lamella eutectoid carbides depending on the thermal treatment undergone [20]. For example it has been shown that the carbides of an as-cast (AC) CoCrMo alloy

possess a large, irregular and blocky morphology within the grains and at the grain boundaries, whereas those alloys that have been more extensively heat treated exhibit an agglomeration of particulate carbides which are finely dispersed at grain boundaries [18, 20].

The AC bearings (those that have had no solution treatment post casting) have a higher carbide volume fraction as well as a greater abrasive wear resistance compared with the “single” or “double heat-treated” (DHT) alloys [20]. This is because during the casting process the carbon concentrates with molybdenum and chromium to form these carbides. Heat treatments vary between manufacturing processes, but it is evident that a combination of solution treatment and hot isostatic pressing leads to smaller carbides and a reduction in the number of visible carbides (using SEM) within the matrix [18]. However in a comparative study, Kauser saw carbides in all AC, single and DHT alloys but found that the carbide size and distribution was reduced once samples had undergone heat-treatment [1].

2.2.5.2 Effect of carbides on corrosion resistance

Carbides themselves are very good at resisting corrosion. During solidification of the alloy carbides take up chromium away from the matrix which deprives it of a highly corrosion resistant element. This preferential leaching of chromium causes a chromium depleted zone adjacent to carbide, which is known as sensitisation. These surrounding areas of the carbide are then open to localised attack [26]. Pits and crevices can then form in the matrix which can accelerate the rate of corrosion. As the matrix starts to corrode at a faster rate than the carbides areas of small asperities will develop on the surface due to non-uniform attack. These asperities (the corrosion resistant carbides) stick out and can cause deep grooves in the softer matrix of the opposing surface, which is termed two body abrasive wear. These deep grooves remove the protective oxide film as well as damaging the sub surface layers in the alloy. A larger asperity may cause a smaller asperity to break out of the articulating surface. This can remain in between the two surfaces and cause three-body rolling wear. The harder carbide can remain in the middle of the two surfaces or can get embedded into the opposing surface’s softer matrix. This disturbs the subsurface layers as well as the protective oxide film allowing the solution to come into contact with the bare metal and accelerate the corrosion process. Once CoCrMo alloys have undergone heat-treatment the carbides then remain richer in chromium and molybdenum. This then deprives the softer matrix of these important corrosion resistant elements [18, 20]. Moreover, Kauser [1] found that DHT samples had a

higher corrosion rate than AC samples which was attributed to the molybdenum depletion as a result of the heat-treatment.

2.2.6 Summary

Currently work done on the heat-treatment of CoCrMo alloys has shown AC alloys to have superior wear properties over DHT [15, 18, 20, 27]. Generally, it is considered that AC microstructures have a higher carbide fraction and this results in them having lower wear rates. The effect that the heat treatment has on the carbides in the matrix is considered an important factor in how the alloy behaves under wear and in corrosive environments. The greater amount of wear a component experiences causes a greater amount of bare metal to be exposed to the environment. This will then accelerate the rate at which corrosion can occur.

2.3 Corrosion of CoCrMo in aqueous environments

2.3.1 The Corrosion Process

Corrosion is an electrochemical process whereby metal atoms are oxidised and are released into a solution [1]:

$$M \rightarrow M^{n+} + ne^{-} \quad (2.1)$$

The electrons that are produced in the oxidation reaction must be consumed in a cathodic reaction such as the reduction of oxygen or water. The type of cathodic reaction that can occur is normally dependant on the nature of the corrosive environment; the most common cathodic reactions are as follows:-

Oxygen reduction in an acidic environment: $O_2 + 4H^{+} + 4e^{-} \rightarrow 2H_2O$ (2.2)

Oxygen reduction in a neutral/alkaline environment: $O_2 + 2H_2O + 4e^{-} \rightarrow 4OH^{-}$ (2.3)

Water reduction (neutral/alkaline environment): $2H_2O + 2e^{-} \rightarrow H_2 + 2OH^{-}$ (2.4)

Proton reduction (acidic environment): $2H^{+} + 2e^{-} \rightarrow H_2$ (2.5)

These reactions can occur at any position over the metal surface but commonly some areas are dominated by anodic reactions and others are dominated by cathodic reactions [28]. For an isolated piece of metal, however, the total rate of oxidation must equal the total rate of reduction for corrosion to take place. The potential at which the rate of the anodic reaction is

equal to the rate of the cathodic reaction is termed free corrosion potential (*Ecorr*) or open circuit potential (OCP).

2.3.2 Resistance to Corrosion – The Passivation of CoCrMo

Due to the formation of a chromium rich passive oxide film (Cr_2O_3) on CoCrMo alloys, they show a high resistance to corrosion. When a metal is in a passive state it will still corrode in a slow and uniform mode, but it will resist the thermodynamic tendency to rapidly dissolve. This condition is achieved when a passive oxide film is formed at the metal surface. Passive oxide films can vary in thickness, chemical composition as well as in oxidation states and are affected by a number of factors, including pH, electrode potential and composition of the electrolyte [29, 30]. When an alloy is placed in an electrolyte, the oxide film undergoes continual dissolution/depassivation and growth/repassivation processes. However, if the dissolution rate is high then active dissolution of the metal ions will occur accelerating the rate of corrosion [1].

Changes in the pH of the electrolyte, can destabilise the passive film. They result from local anodic reactions where the pH drops meaning that there is an increased concentration of H^+ ions in the electrolyte due to the hydrolysis of cations. This makes passivation and the formation of a new oxide film harder and dissolution easier meaning further dissolution of the oxide film occurs [1].

2.3.3 Types of Corrosion

Corrosion may be general or localised. General corrosion involves the uniform dissolution of the metal surface. In contrast, localised corrosion can take place on a passive metal surface in the presence of aggressive ions. Here, localised attack occurs in specific sites where there are high local dissolution rates, which lead to high rates of penetration [31]. Chloride ions will enhance the localised corrosion process and occur at local sites caused by imperfections where there are pits or inclusions [1]. There are several forms of localised corrosion, but pitting, crevice corrosion, fretting, and tribocorrosion are the most relevant types for artificial hip joints.

Pitting corrosion is confined to a point or small hole within the metal. Pitting can initiate at sites where there are small surface defects such as a scratch or a dent, a small change in chemical composition of the alloy or damage to the oxide film. In the pit there is a rapid depletion of oxygen, and the pit becomes a net anode, undergoing rapid dissolution.

This anodic reaction produces electrons that are used in oxygen reduction reactions at the external surface. The generation of metal ions in the pit cavity leads to a net positive charge in the pit, resulting in an influx of chloride ions to maintain the charge balance. Hydrolysis of metal cations causes a decrease in pH. These factors promote pit growth, as high concentrations of chloride and hydrogen ions promote metal dissolution [1].

Crevice corrosion is associated with the formation of stagnant solution in crevices or occluded areas such as those formed under washers, fastener heads, lap joints and clamps. The mechanism of crevice corrosion is similar to that of pitting corrosion: depletion of oxygen, more acidic conditions and build-up of aggressive ionic species such as chloride enhance metal dissolution and produce accelerated attack within the crevice. However, the difference is that an external crevice former is required to initiate corrosion on the surface [1].

Fretting corrosion can also occur where micro-motion between two surfaces causes depassivation leading to localised corrosion. These small amplitude displacements occur when the total amplitude of movement is smaller than the contact width of the prosthetic joint [32, 33]. The micromotion between the faying surfaces, which can often happen over a crevice, causes depassivation followed by a period of active dissolution during the repassivation process, increasing the concentration of metal ions in the cavity leading to acidification through hydrolysis and ingress of chloride ions for charge balance. Minor movements of the hip joint frequently occur when people adjust or change position and so fretting corrosion can accelerate wear.

2.3.4 Tribocorrosion of CoCrMo

Tribocorrosion describes the synergistic interaction of abrasion with corrosion to accelerate the degradation of an alloy [5]. The two processes combined have a bigger effect on the alloy than if they were to occur separately. For example, it has been demonstrated that by applying a load to the surface of the materials the corrosion potential shifts from a passive region to a more active region. This is a result of the physical removal of the passive film during sliding under load, allowing corrosion to proceed at an accelerated rate [34]. Metal ions can be released as a result of tribocorrosion, and their hydrolysis can lower the pH locally, which can further increase anodic dissolution and the susceptibility for corrosion. Metal debris can also be released and can build up in the body's tissues. If they are not engulfed and excreted by the body's immune response they can then cause adverse physiological effects.

The articulating motion within an artificial joint damages the protective oxide layer and leads to the formation of corrosion products more rapidly than if there was no motion at

all. The underlying active bare metal is then exposed to an electrochemical reaction with the tissue fluid, which then results in more material loss. This is two-body wear which involves the friction of two surfaces only. In between periods of motion where the joint is static, it is generally assumed that a depassivation-repassivation process can occur whereby a new protective oxide layer can be formed where the previous one had been damaged. This can be dependent on how quickly the materials ability to reform the oxide layer and the length of time the joint is static for.

Three body wear involves the two articulating surfaces mentioned as well as an abrasive third body particle. This third body particle can increase the abrasion of the two surfaces, causing scratching and further damage to the protective oxide. Third body particles can be generated from articulating surfaces (Two-body wear) as well as reverse surfaces if joint/cement/bone movement occurs. Corrosive wear can also be caused by third body wear, where the corrosion debris acts as an abrasive third body [5] and can cause deep grooves in the bearing surfaces. It is accepted that wear particles from prosthetic implants can cause an inflammatory response as well as loosening of the joint and ultimately failure. However, it has been revealed that retrieved metal-on-metal hip replacements have predominantly failed (i.e. removed due to detrimental effect to the patient) due to two and three body wear [15].

2.3.5 Biocompatibility issues and metal ion release

The biocompatibility of CoCrMo alloy is closely linked to its high resistance to corrosion, which is attributed to the spontaneous formation of a passive oxide film. The integrity of this oxide film has been strongly correlated with the chemical and mechanical stability of the alloy once implanted into the body [35]. However, CoCrMo alloys can still have an adverse effect on the body's tissues when the implant undergoes tribocorrosion (covered more in Section 2.3.6 - Corrosion in the Body). When a hip-resurfacing joint is placed in the body the two articulating surfaces will cause tribocorrosion to occur and this will then lead to metal ion release.

2.3.6 Corrosion in the body

2.3.6.1 Chloride content and pH

The chloride content of the environment is an important factor to consider when looking at the corrosion of an alloy. Chloride ions are aggressive species which can lead to localised corrrosion processes in the form of pitting and crevice corrosion (described in more detail in

Section 2.3.3). If the chloride ions are present in an aerated solution, this is believed to increase the corrosion rate further [36].

The pH of the environment can also affect the corrosion rate of the alloy. The pH can be lowered by changes in local anodic reactions by the increase in the concentration of H^+ ions through the hydrolysis of cations. This makes passivation a lot harder and dissolution easier resulting in the dissolution of the oxide film meaning passivity is destabilised. This is described as an autocatalytic process [1]. Conversely, where cathodic reactions dominate, the solution becomes more alkaline (the pH increases due to the generation of OH^- ions by the consumption of H^+ ions). The more acidic the solution is, as a consequence of hydrolysis, the higher the corrosion current of the alloy will be when compared with a neutral pH [14].

Inside the body, the pH is generally homeostatically regulated to a value of 7.4 [37]. However, it is thought that at sites of inflammation, which can often happen at the site of an implanted metal-on-metal hip joint (see section *2.6 The development of Pseudotumours* for more detail), can lead to a transient "acid tide" where the pH may fall to as low as 4.5 [38]. Another important aspect to consider is the oxygen saturation levels of tissues within the body. Currently it is considered that the cells of healthy individuals are saturated to 97-99% which could have a major influence on the oxidation reduction reactions that take place [1]. With regards to in-vitro testing in a hip simulator there is no information currently in the literature regarding the oxygen saturation levels of NaCl and bovine serum solutions.

2.3.6.2 The influence of proteins

When a hip-resurfacing joint is placed in the body it comes into contact with synovial fluid, which lubricates the joint. This can be an aggressive environment due to the proteins which constitute 5% of the synovial fluid [1]. The biomaterials surface (and the released degradation products) can combine with the proteins to form a proteinacious film, which in the literature can be referred to as a biofilm [30, 39]. The film can exist on the surface of the metal-on-metal bearings and is often considered to have a beneficial effect, as it is thought that the proteins in the bovine serum adsorb to the bearings surfaces, creating solid films which provide lubricating surface layers [40].

The presence of proteins can either decrease or increase the corrosion rate of the alloy. Contu [14] suggested that the proteins present in calf serum inhibit the hydrogen evolution reaction and form a diffusion barrier that causes the anodic dissolution of the alloy to be under a diffusion control. This barrier prevents metal ion release and access of aggressive species such as chloride ions, which would accelerate the corrosion rate of the joint [1, 14]. In

contrast, Yan et al. [9, 30] observed that the proteins can enhance ion release and passive film breakdown in static corrosion conditions for both high and low carbon CoCrMo alloys. This occurred when there was a reduction in the passive region following proteins adsorbing to the sample surface.

However, generally it is believed that the proteins in synovial fluid are beneficial to the effect of tribology as they provide boundary lubrication within the joint and reduce friction [30, 31, 36, 41, 42]. This is also supported by Sun et al. [15] who found that anodic currents were lower for protein solutions than inorganic solutions, reducing the potential for corrosion. The same is considered for amino acids, whereby they have been found to react with materials under tribological contact and form organometallic/oxides, which lubricate the metallic sample surface [13].

CoCrMo alloys are a relatively passive metal with a low dissolution rate. However, over time the effect of tribocorrosion in a biological system can lead to the release of metal ions in-vivo that will cause adverse physiological effects such as toxicity, carcinogenicity, genotoxicity, and metal allergy [43]. Most proteins are negatively charged, whereas cobalt and chromium are positively charged ions. Once a metal is bound to a protein it can be systematically transported and either stored or excreted. Cobalt has been shown to be transported from the tissues to the blood and usually eliminated in the urine within 48 hours, which does not cause too much of a health risk to the patient. However, chromium has been reported to have built up in the tissues and red blood cells [43] and this accumulation of metal ions can cause adverse physiological effects such as osteolysis and metallosis [44]. Metal debris can also be associated with tumour formation, hypersensitivity [31, 45]. High levels can also cause fibrosis, granulomatosis, bone resorption, necrosis of the bone and loosening of the implant [31, 46].

2.4 Review of in vivo results and retrieval rates

The “failure” of CoCrMo hip resurfacing joints leading to the need for retrieval of the implant and revision surgery has been attributed to many different reasons such as head and neck fractures, cup loosening and the orientation of load [47]. These all result to the bearing being subjected to adverse stresses increasing its wear rate, which ultimately results in revision surgery. From a tribocorrosion perspective, it is important to examine the retrievals specific to wear, corrosion and the release of metal ions and wear debris into the body.

Investigation into the heat-treatment and microstructure can also help to explain the wear and corrosion properties of the implant and why it may fail.

In March, 2007, a woman testified that her Corin hip resurfacing device came loose after 5 years with opposition from Smith and Nephew suggesting that failure was due to the double heat treating process the alloy was subjected to in the manufacturing process. This sparked media interest and was brought to the attention of FDA Orthopaedic and Rehabilitation Device Panel, where the influence of heat-treatment on its performance in-vivo has since been a hot topic of debate [48].

In a study of 15 retrieved metal-on-metal implants of Weber Metasul hips were studied at 10-81 months after implantation. The average was 33 months before retrieval with patients experiencing pain, squeaking of the joint and limping, with half of which having radiological evidence of osteolysis [49]. These symptoms were attributed to the release of cobalt and chromium ions into the tissue, which can be the result of tribocorrosion processes.

There has long been concern that metal-on-metal hip arthroplasties may develop problems associated with metal sensitivity. The disadvantage of metal-to-metal bearings is that they shed many more wear particles which is thought to produce local tissue concentrations that can be ten times higher than those found in metal-on-polymer joints. It is thought that this sensitivity can lead to loosening of the joint [50], as well as groin pain [51] and pain in and around the soft tissues of the joint [52], which can ultimately lead to revision surgery.

Evidence exists that retrieval operations have been caused by corrosion failure, whereby the CoCrMo alloy head experienced localised attack around molybdenum-rich phases. This was thought to be the result of molybdenum-depletion in the alloy [25]. Unfortunately, no evidence of any chemical analysis was shown to support their theory.

2.4.1 The development of *Pseudotumours*

There is increasing concern that CoCrMo metal-on-metal hip resurfacing possesses a number of health risks resulting from metal sensitivity. It has been reported 17 women who have undergone metal-on-metal hip resurfacing have developed a soft tissue mass, termed a pseudotumour. The symptoms that have been experienced with the development of these pseudotumours have been discomfort in the region of the hip, spontaneous dislocation, nerve palsy and the development of a noticeable mass or rash at the hip joint, which can present itself after a mean time of only 17 months [45]. Further research into this has found that

cobalt nanoparticles and ions have cytotoxic effects on macrophages in an in-vitro environment, which is believed to be a contributing factor to the development of pseudotumours [53]. In several other cases pseudotumour masses have also been seen to develop with the deposit of metal wear debris around the hip joint [47, 54-56] . The solution to pseudotumour development is normally to have revision surgery on the implant, and in some cases THRs [54] and metal-on-polyethylene bearings [57] have been preferred. Although there is a growing concern about pseudotumour development as a result of metal-on-metal hip resurfacings it does not affect that many implant patients. It is estimated that approximately only 1% of patients who have a metal-on-metal resurfacing develop a pseudotumour within five years [45]. Another source describes the risk of developing a pseudotumour to be as low as 0.15% [57]. However, the literature suggests that the wear debris generated by the tribocorrosion of the two articulating surfaces is linked to the development of pseudotumours. This is why it is important to limit the tribocorrosion of an implant to prevent the release of wear debris and metal ions.

2.5 Review of in vitro studies

When examining the materials suitable for hip resurfacing prosthesis there are generally two types of in-vitro experiments; pin-on-disc/friction-test setups which look at the tribo-contact between two surfaces and is often combined with electrochemical measurements [5, 12-14, 20, 30, 58-60]. The other alternative is to use hip simulators [17, 61-64]. To date these hip simulator experiments have measured the wear rate of alloys by measuring the ion release rate and weight loss of the bearing materials. Recently however, a study has been done that has looked at direct instrumentation of electrochemical measurements in a hip simulator [42], which this project aims to replicate.

Hip joint simulator studies show that metal-on-metal bearing hip prostheses have two discrete wear phases, which are; ‘running in’ and ‘steady state’. The running in phase is the initial phase where the two surfaces co-adapt. There are high wear rates at this point as the two surfaces meet for the first time causing large amounts of friction. This stage is normally completed after the first 10^6 cycles [31]. Several simulator studies have demonstrated that initial wear rates are higher and then decline once the bearings have bedded in [31, 61, 65, 66] . It is thought that during the ‘running in’ phase the surface becomes smoother, where sharp peak asperities wear off [31]. This smoother surface topography produced from the

‘running in’ phase is then easier to lubricate than the original surface, causing wear rates to be much lower [31].

Bowsher et al. [62] compared ‘normal walking’ and ‘fast jogging’ conditions in a hip simulator experiment using high carbon metal-on-metal CoCrMo bearings. The result was that ‘fast jogging’ conditions generated a twenty-fold increase in the total wear particle surface area, concluding that highly active metal-on-metal patients may exhibit greater ion release than in less active patients. This greater level of ion release would increase the corrosion susceptibility for those patients that are more active.

Several studies have taken place looking at the wear of AC and DHT components in a hip simulator. Contrary to some studies mentioned earlier, Bowsher et al. [17] found no statistical difference between the two heat-treatments under both ‘running in’ and ‘steady state’ conditions. It was concluded that changes in the microstructure caused by heat-treatments do not appear to influence the wear behaviour of high carbon metal-on-metal articulations with similar chemical compositions.

It has been shown that the ion release rate increases as the swing phase load increases in a hip simulator. This is consistent with the increased severity of the metal-to-metal contact [42]. To minimise the risks of these conditions the release of metal ions and more specifically the exposure to wear needs to be reduced. However, over time it is considered that the release of Co ions in particular should decrease due to the implant going from ‘running-in’ to a ‘steady state’ condition causing less wear [31].

Although retrievals of revised components show much variability in the metals microstructure it has been found that those with the highest wear occur in components with a lower volume fraction of carbides [3]. This suggests that an AC microstructure (with a higher proportion of carbides) should have superior wear properties compared with a heat-treated implant. Nevelos et al, [67] found a comparable result in-vitro where unidirectional pin on plate studies of heat-treated cobalt chromium showed two and half times higher wear than AC cobalt chrome. It could be suggested that in both cases the heat treatment caused carbide depletion and as a result suffers higher wear rates. However, in another study by Nevelos et al, [67] they found no difference in the wear rates of heat-treated cobalt chrome and AC cobalt chrome in a hip simulator study [3].

Taking potential measurements in a hip simulator machine is as yet a relatively new phenomenon. So far, studies have been done obtaining potential controlled measurements from CoCrMo alloys in other devices [1, 9, 13, 30, 34, 59]. To date, only one other paper exists obtaining potential measurements from a hip simulator machine [42] which is

comparable to this study. Yan et al., [42] obtained results from a ProSim friction simulator with an integrated electrochemical cell under a variety of loads peaking at 2 kN. NaCl solution, 25% serum and Bovine synovial fluid were the solutions used to obtain OCP measurements. The main finding was that in comparison with a reciprocating pin-on-plate tester the OCP is nobler in the friction simulator, meaning less mechanical and electrochemical damage is experienced. To my knowledge this is the first study to produce potentiostatic measurements from a hip simulator.

2.6 Summary of Literature

Currently there has been concern that although CoCrMo metal-on-metal hip resurfacing joints have superior wear and strength to other metallic combinations as well as polymer and ceramic options, they still release metal ions into the body. This is the result of the tribocorrosion between the two articulating surfaces of the head and the cup under load. Although work has been done on the electrochemistry of the alloy, little work has currently been done on the electrochemistry of the CoCrMo hip resurfacing joint while operating in a hip simulator. As yet, there is no literature that specifically focuses on the corrosion properties of AC and DHT CoCrMo alloy operating in a hip simulator.

2.7 *Project Aims and Objectives*

The aim of this work is to carry out electrochemical measurements on the tribocorrosion of CoCrMo hip implants in a hip simulator and to investigate whether there is any difference in the behaviour of as-cast and double heat-treated components.

2. Experimental Method

3.1 Materials

3.1.1 ASTM F75 CoCrMo alloy

The material investigated was a cast cobalt-chromium-molybdenum (CoCrMo) alloy produced in accordance with American Society for Testing (ASTM) F75-98, which is a Standard Specification for vacuum cast cobalt chromium molybdenum alloy for surgical implant applications. Smith and Nephew Orthopaedics Ltd. (Leamington Spa) provided the

CoCrMo hip resurfacing bearings. Samples were provided as a hip resurfacing joint consisting of a head and a cup in both as-cast and double heat-treated form. The nominal chemical composition provided by the manufacturer is listed in Table 3-1.

Table 3.1 Nominal chemical composition of the ASTM F75 CoCrMo alloy (supplied by Smith and Nephew Orthopaedics Ltd).

Element	**C**	**Si**	**Mn**	**S**	**Al**	**Co**	**Cr**
(Wt %)	0.28	0.95	0.36	0.004	<0.01	Bal	28.31

Fe	**Mo**	**Ni**	**Ti**	**W**	**N ppm**
0.24	5.92	0.73	0.03	0.04	100

3.1.2 Thermal processing

Two different cast CoCrMo alloys were examined; “double heat-treated” and “as-cast”. The thermal processing for the double heat-treated alloy was carried out by Smith and Nephew Orthopaedics, Leamington Spa. Both the as-cast and the double heat-treated alloys were from the same batch and can be classed as high carbon alloys (approximately 0.28%). The only difference in the two alloys was the difference in thermal processing undertaken. This only applied to the double heat-treated alloy and is shown below.

Table 3.2: Thermal treatments applied to produce a ‘Double heat-treated’ CoCrMo alloy (Information supplied by Smith and Nephew Orthopaedics, Leamington Spa).

Process number	**Heat treatment procedures**
1	Solution annealed at 1200°C for 4 hours (in a soft vacuum $<5x10^{-1}$ Pa), then quenched in nitrogen gas from 1200°C to 800°C at a cooling rate of 50°C/min minimum, then air cooled.

2	Heat treated to 1200 ± 10°C in vacuum and subjected to a pressure of 103 ± 5 MPa for 4 hours (HIPping), then cooled in argon at a rate of 8-10°C/min and combined with Process 1.

Table 3.3: Thermal processing for the two types of CoCrMo samples provided.

Abbreviation	**Sample description**	**Processing applied**
AC	"As-Cast"	No treatment
DHT	"Double Heat-treated"	1 + 2

Table 3.4: Hip resurfacing joint sample number and process history (for hip simulator tests).

Test history	**Heat treatment**	**Sample name**	**Experiment used/section**
Worn-in (unknown, scratches evident)	As-cast	WN AC 1	Difference in solution
Worn-in (unknown, scratches evident)	As-cast	WN AC 2	Difference in temperature

Worn-in (unknown, scratches evident)	Double heat-treated	WN DHT 1	
Worn-in (unknown, scratches evident)	As-cast	WN AC 3	Preliminary potentiostatic measurements
New (polished)	As-cast	NW AC 1	Alternating abrasion/stabilisation (Section 4.4)
New (polished)	Double heat-treated	NW DHT 1	
New (polished)	As-cast	NW AC 2	Single abrasion test (Section 4.5)
New (polished)	Double heat-treated	NW DHT 2	

Table 3.5: Disc sample number and process history (for anodic polarisation tests)

Test history	**Heat treatment**	**Sample name**	**Experiment used/section**
New (polished) – cut from the stem of NW AC1	As-cast	DC NW AC 1	Polarisation Curves (Section 4.2)
New (polished) – cut from the stem of NW DHT1	Double heat-treated	DC NW DHT 1	

Tables 3.4 and 3.5 below show information on each sample joint used for each test in the project and its sample name that it is referred to in the text.

3.2 Microstructure Characterisation

3.2.1 SEM

For high resolution surface investigations Scanning Electron Microscopy (SEM) equipped with EDX were used. Imaging was carried out using both backscattered electron (BEI) and secondary electron imaging (SEI) modes at an accelerating voltage of 20 keV and a working distance of approximately 10 mm. Analysis of the data using EDX was carried out using INCA software (Oxford Instruments, UK) to determine composition of the microstructure.

3.3 Solutions used

Two solutions were used over the course of the project with each one being freshly prepared on each day of testing. The two different solutions provided different environments for the comparison of AC and DHT specimens.

Newborn Calf Serum (NCS) (Harlan Sera Lab, UK) was used at 28% concentration in deionised water, as recommended in the ISO standards [68]. At present this is considered the most representative simulation of proteins that exist for synovial fluid and was pH8. The major protein constituents of the solution are listed in Table 3.6.

3.5 % Sodium Chloride (NaCl) (Fisher Scientific Ltd, UK) was used at 3.5% concentration in deionised water and was pH5. A higher percent of sodium chloride was used than is normally comparable to body fluids (around 1%) in order to create a solution which was slightly more acidic simulating periods when a joint may be infected [38]. This solution was mainly used in preliminary experiments, as well as giving a comparison with the protein containing Newborn calf serum and to provide a different environment where a difference between AC and DHT may be seen.

Table 3.6: Major protein fractions of newborn calf serum (supplied by Harlan Sera Lab, UK)

Protein	**%**
Albumin	46.2

Alpha 1 and 2 globulin	29.1
Beta globulin	12.97
Gamma globulin	11.8

"Full Strength' Ringers Solution" with 10% Concentrated Newborn Calf Serum (NCS) acidified to pH2

Full strength Ringers solution (90% volume) (Fisher Scientific Ltd, UK) was combined with concentrated NCS (10% volume) to again closely simulate the protein constituents in synovial joint fluid. This is based on a study by Kauser [1], who also looked at the effect of heat treatment in simulated body environments.

The solution was then acidified in order to simulate the effect of a drop in pH in vivo possibly caused by the effects of surgery, infection or by hydrolysis reactions resulting from crevice corrosion [38]. Concentrated HCl (Fisher Scientific Ltd, UK) was used to adjust the solution to pH2. The pH was measured using a pH 210 Microprocessor pH Meter (Hanna Instruments Ltd, UK), which was calibrated using two buffer solutions, pH 4 and 7, prior to any experiments. Acidifying the solution gave another environment where any differences between AC and DHT samples could possibly be seen.

Table 3.7: Ringers' solution chemical composition (supplied by Fisher Scientific Ltd, UK)

Chemical	Formula	Concentration (mM)
Sodium hydrogen carbonate	$NaHCO_3$	1
Potassium chloride	KCl	4

Sodium chloride	NaCl	154
Calcium chloride	$CaCl_2$	5

3.4 Measuring Tribocorrosion using a Hip Simulator

3.4.1 Test Setup

The metal-on-metal friction tests were executed using a ProSim Friction Simulator (ProSim Ltd, Stockport-Manchester). Figure 3.21 below shows the single-station servo-hydraulic machine set up for measuring friction and corrosion. The friction simulator has two controlled axes of motion: rotation and load.

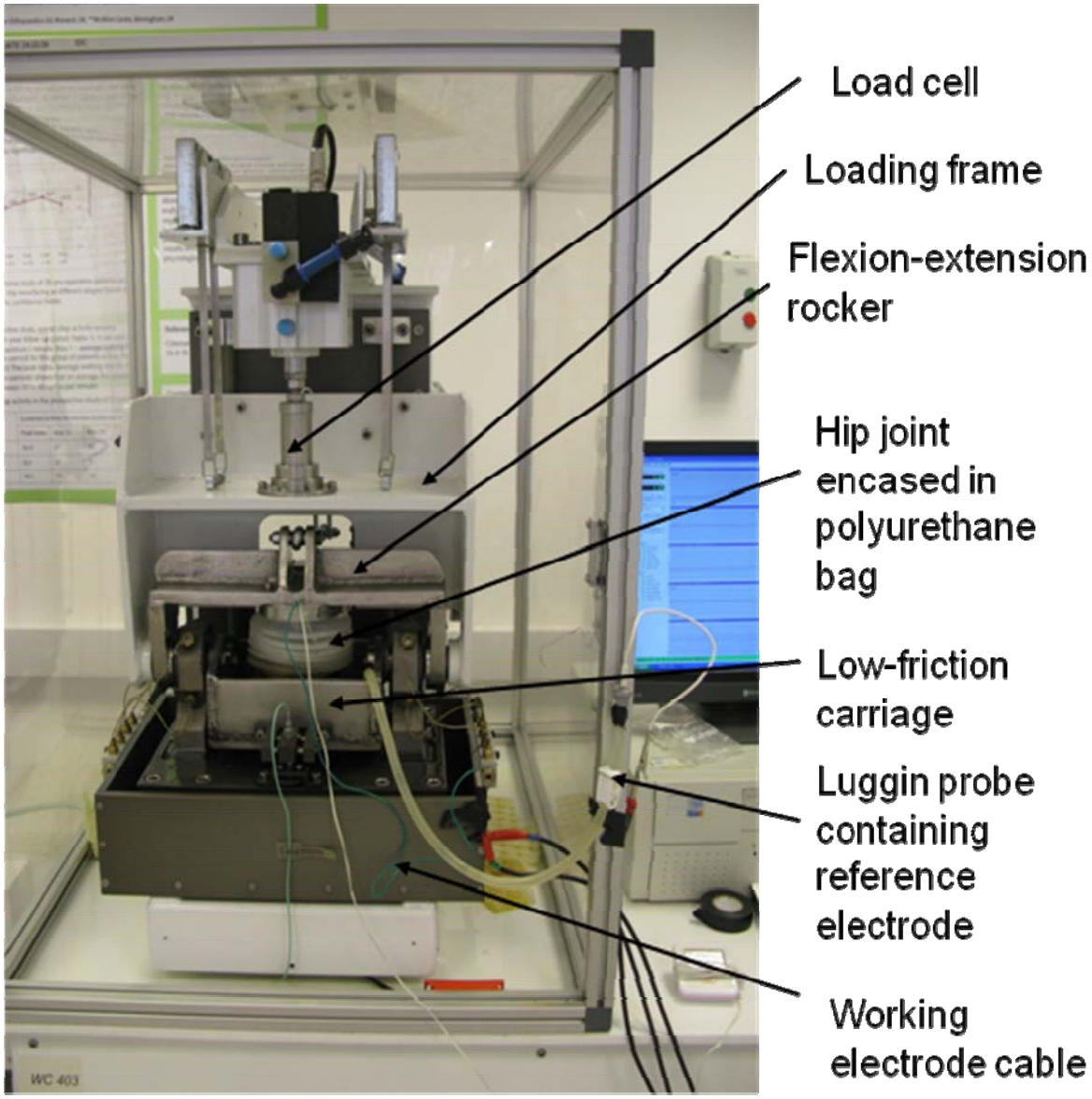

Figure 3.1: Test setup for taking OCP measurements of the head and cup during contact and abrasion in a ProSim Friction Simulator.

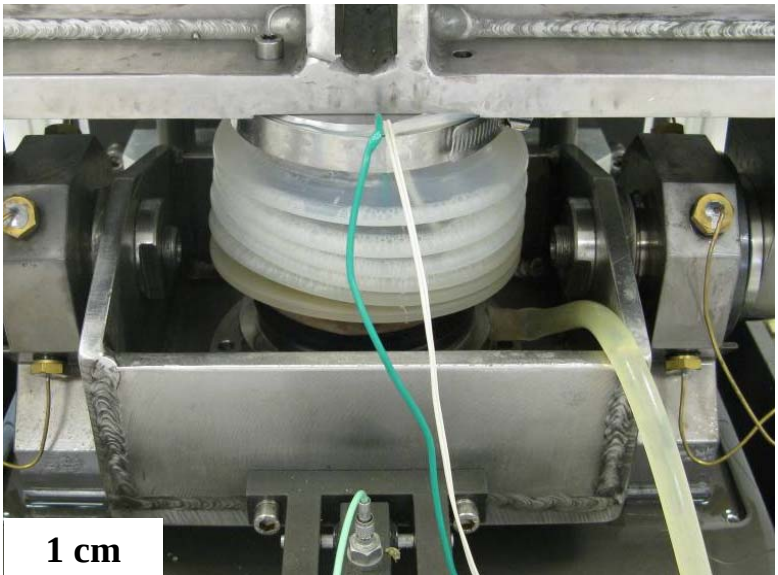

Figure 3.2: Close up of OCP setup showing the joint encased in a polyurethane sealed bag. The working electrode cable (green), temperature monitor (white) and Luggin probe are also shown.

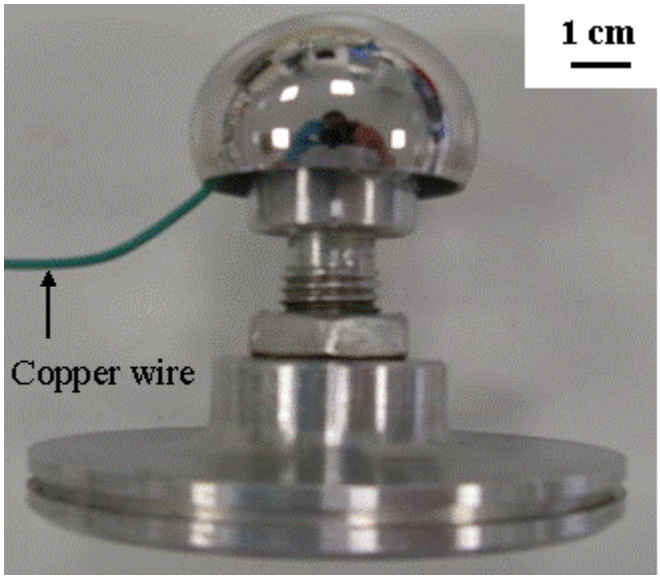

Figure 3.3: Stainless steel fixture and sample head attached with working electrode cable.

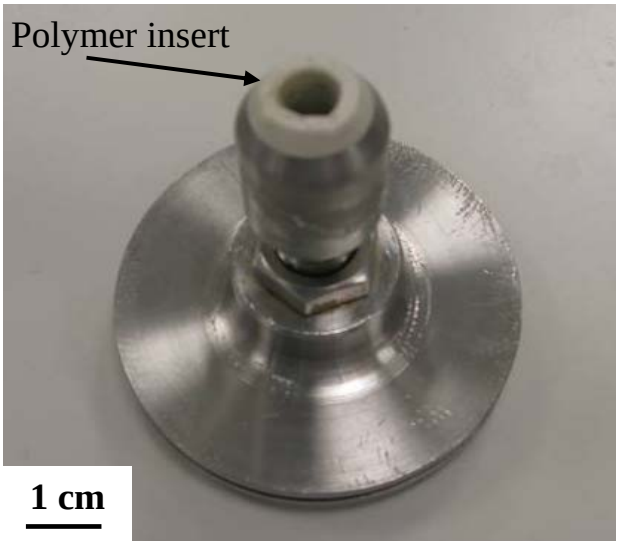

Figure 3.4: Stainless steel holder for the head modified with a polyethylene insert.
The polymer insert goes down 3cm in the head fixture where the stem of the joint and contacting copper wire are placed. This insulates the head and the copper wire (the working electrode) from any other metal-on-metal contact.

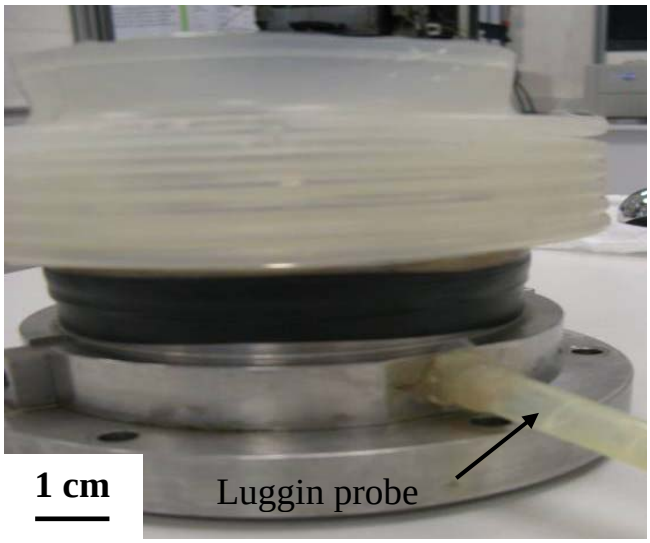

Figure 3.5: Stainless steel holder showing Luggin probe for reference electrode.
The Luggin probe is attached to the fixture with silicon sealant. This enables the solution in the holder to drain through a hole into the tube to provide a wet environment in a continuous path so that the corrosion potential can be measured.

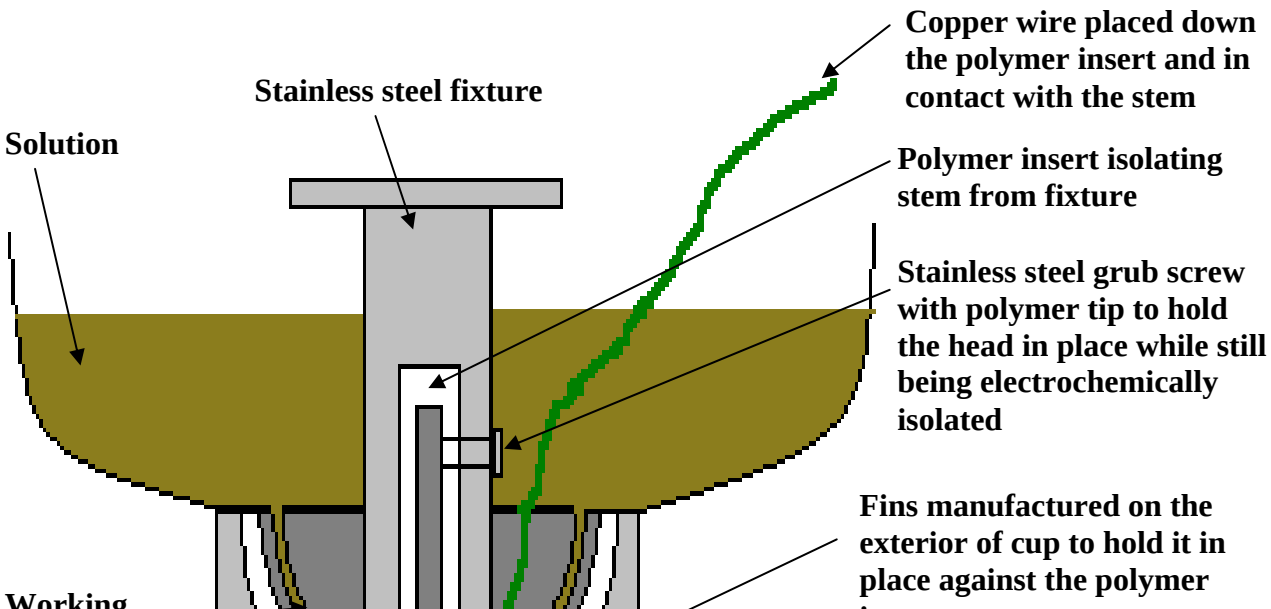

Figure 3.6: Schematic diagram of the positions of the head and cup in the hip simulator. The copper wire acts as the working electrode by being placed down the polymer sleeve and is in direct contact with the stem. The stem is joined to the reverse of the head making its exterior surface the working electrode. The interior of the cup is in contact with the solution as well as the exterior of the head, meaning that the working electrode is made up of the two articulating surfaces on the head and cup, connected via the head stem and copper wire. It should also be noted that the parts of the fixture that are shown to be in contact with the solution (i.e. interior surface of the head and the stainless steel fixture and holder) were lacquered before the beginning of each test to prevent it from being electrochemically active.

3.5 Precautions and Test parameters

3.5.1 Hip Simulator

In order to simulate the dominant flexion/extension action of the natural hip joint in the hip friction simulator, the motion arm of the loading frame is used to flex and extend the femoral head through a range of up to 45° (-15° to +30°). The flexion/extension motion of the femoral head operated at a frequency of either 1 or 0.5 Hz, which are the slowest available settings. Peak loads of 2000 N were applied to the joint during abrasion cycles, obtained from ISO

standards and is comparable to other studies in this area [42, 69, 70]. During stabilisation periods, the hip joint was static with a load applied at either 0 N or 1000 N, which is stated with the results of each experiment.

3.5.2 Connections and Insulation

To ensure that no other metal surfaces were exposed to the solution both fixtures for the head and the cup were lacquered (45 stopping-off lacquer, MacDermid plc, Birmingham) as well as the back of the cup and the inside of the head. This ensured that the only two metal surfaces that were exposed to the solution were those that come into contact when the head and cup are articulating.

A copper wire was placed down the polymer sleeve, so that it was in direct contact with the stem of the head (acting as the working electrode, as the head and cup are in direct metal-on-metal contact). A voltmeter was used to check these connections as well as the isolation of the fixtures. The sample head was held in stainless steel fixture shown above in Figure 3.4. A polymer insert was used to prevent metal-on-metal contact between the stem of the head and fixture, also shown. The head and cup were then encased in a sealed polyurethane bag. A Luggin probe (polyurethane tube) was used which was 70 cm long (as short as possible) where solution could proliferate to and be in contact with the reference electrode. The exterior of the head and the interior of the cup that articulated were the only exposed metallic areas that acted as the working electrode. This had a combined area of approximately 78 cm^3.

3.5.3 Test Samples

To ensure new test samples were in the same condition prior for each experiment a series of procedures were carried out. Firstly, test specimens were cleaned using deionised water and propanol before and after each experiment. Secondly, a check was carried out on the alignment of the centres of rotation of the femoral head and acetabular cup with the simulator's centre of rotation. This made sure that the point at which the head and cup are in contact was zero. The cup was fixed in the holder using polymer insert brackets at an angle of 35° to be comparative to other studies [17, 42, 62] and as physiologically relevant as possible.

3.5.4 Clearance Values between the head and cup

Clearance is the gap that exists between the head and cup and the lower this is the better fit the two components will have. The amount of clearance between the head and the cup is thought to be a key parameter in controlling wear behaviour [41, 63, 71]. Wear experienced by the alloys surface can damage the passive film and leave the alloy more susceptible to corrosion. Due to this the average difference in clearance was kept as low as possible between the AC and DHT samples with a difference of 5.3 microns. The clearance values for each individual joint are shown in the appendix.

3.5.5 Experiment Parameters

Experiments which focused on the effect of temperature on the corrosion potential (results shown in section 4.3.2) used two operating temperatures; 20°C ± 1° (room temperature) and 40°C ± 1°. Before the beginning of each test the solution was maintained at its desired temperature for 1 hour in an incubator and then directly placed in test situ. The maximum time between coming out of the incubator and the start of each test was approximately 90 seconds.

To ensure consistency, measurements were alternated between the two different parameters. For example, the bovine serum and NaCl solutions were alternately tested; solutions at 40°C and 20°C were alternately tested as well as as-cast and double heat-treated samples being alternately tested. The amount of solution used was kept constant by using 200 ml for every hip simulator test which was enough to fully submerse the joint and the electrodes.

For both OCP and potentiostatic tests a saturated calomel electrode (SCE) was used as the reference electrode which was placed down a Luggin probe (polymer tube) where it was immersed in solution of the test set up. When taking potentiostatic measurements a platinum mesh was used acting as a counter electrode. This had the same area as the head and cup added together (the working electrode) and was joined together with platinum wire. Care was taken to ensure that the platinum was free standing in the solution surrounding the head and cup and was not in contact with any other metal surface. The potential applied was -0.05 V which was based on being slightly above the OCP that had been found in previous experiments examining OCP. In between tests the counter electrode (platinum mesh) was cleaned by immersing in nitric acid for 2 minutes prior to testing.

3.6 Anodic Polarisation Measurements

3.6.1 Surface preparation for electrochemical measurements

Disc samples 4 mm thick were cut from the stems of the as-cast and double heat treated heads to avoid any sample to sample variation resulting from the casting process. This also enabled them to be compared with results obtained from the hip simulation study. The discs were then cold mounted in epoxy resin with an electrical connection to the unexposed side of the disc. Prior to testing, samples were polished to 1 μm and degreased using Teepol. The samples were then ultrasonically cleaned in ethanol for 1 minute, washed with deionised water and dried to remove any contaminants on the metal surface. Before the beginning of each test, the sample was pre-warmed on a Microsoft Stage Heater (Brunel Microscopes Ltd, UK) to 37 ± 0.5° for 20 minutes. All equipment was washed with deionised water and dried before use.

The tests were carried out using a computer controlled potentiostat 1280 (Solartron Instruments, UK) and Gill AC43 potentiostat (ACM Instruments Ltd, UK). The electrochemical setup consisted of a 3 electrode cell which included a working electrode, counter electrode and reference electrode. The counter electrode was a platinum mesh that was comparable to the area exposed on the working electrode. Between tests this was cleaned by immersing in nitric acid for 2 minutes. A saturated colomel electrode (SCE) was used as the reference. OCP was measured for 15 minutes prior to the anodic polarisation curves. For anodic sweeps a reference potential of -500 to 900 mV with a scan rate of 1 mV/sec and a sweep rate of 60 mV per second was used.

4. Results

4.1 The effect of thermal treatment on the microstructure of cast CoCrMo alloys

4.1.1 SEM

As-cast (AC) and double heat-treated (DHT) heads were examined using SEM prior to testing to observe any differences in the microstructure. The images shown are taken from the

top and in the centre of each head. Images from the sides showed no obvious differences in the microstructure compared with the centre.

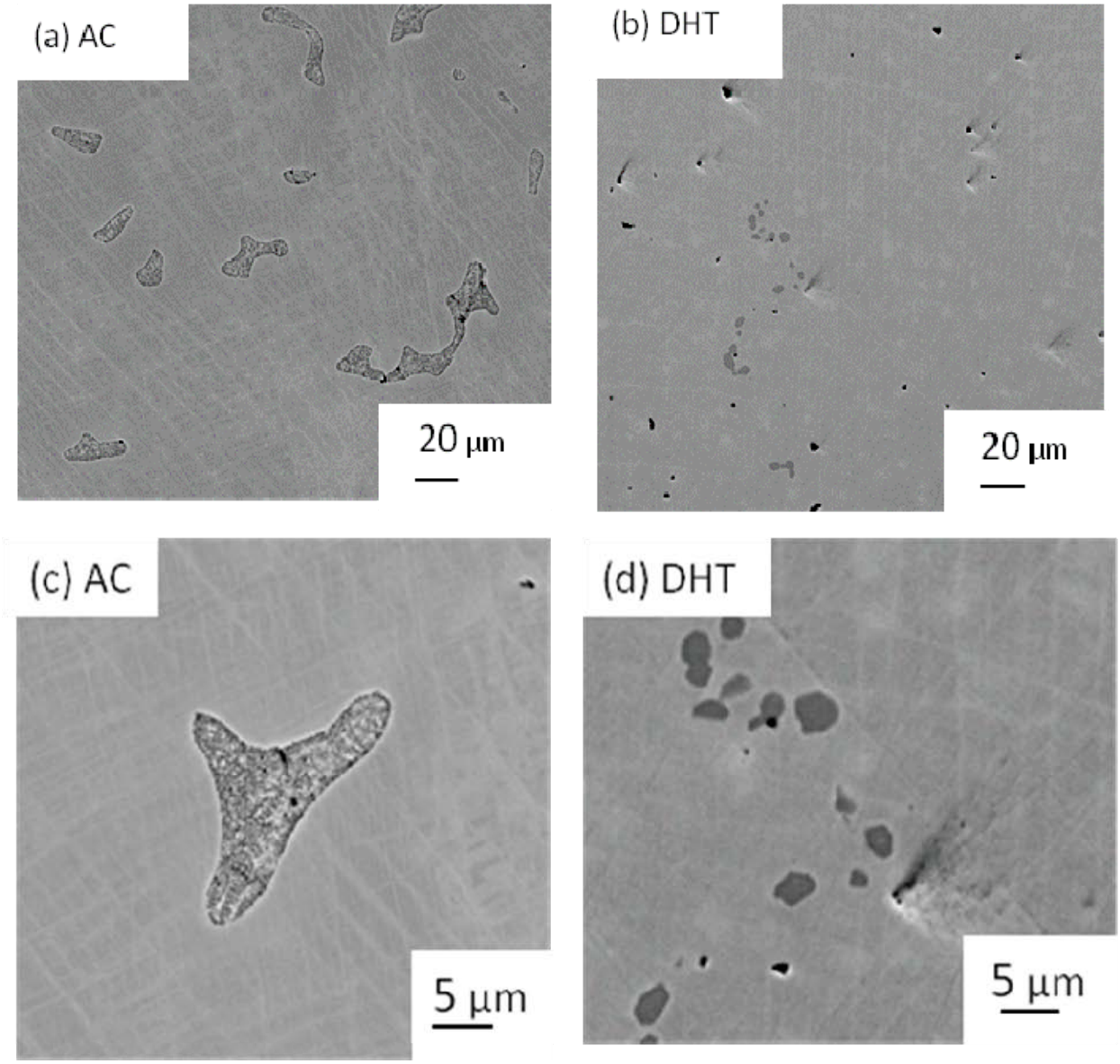

Figure 4.1: SEM images of the microstructure of AC (NW AC1) **(a)** and **(c)** and DHT (NWDHT1) **(b)** and **(d)** heads. The AC samples were obtained from the same batch as the DHT samples prior to heat-treatement.

Figure 4.1 shows microstructure that was typical for all AC and DHT head samples examined. In image **(b)** and **(d)** the carbides are much smaller and irregular following partial dissolution of the large as-cast carbides (images **(a)** and **(c)**). The carbides are typically less than 5 µm wide in comparison with the AC sample, which are typically much bigger with one being approximately 20 µm wide in Figure 4.1**(c)**. Porosity is shown in DHT images **(b)** and **(d)** but this was not a consistent difference that was seen between AC and DHT samples.

4.1.2 EDX

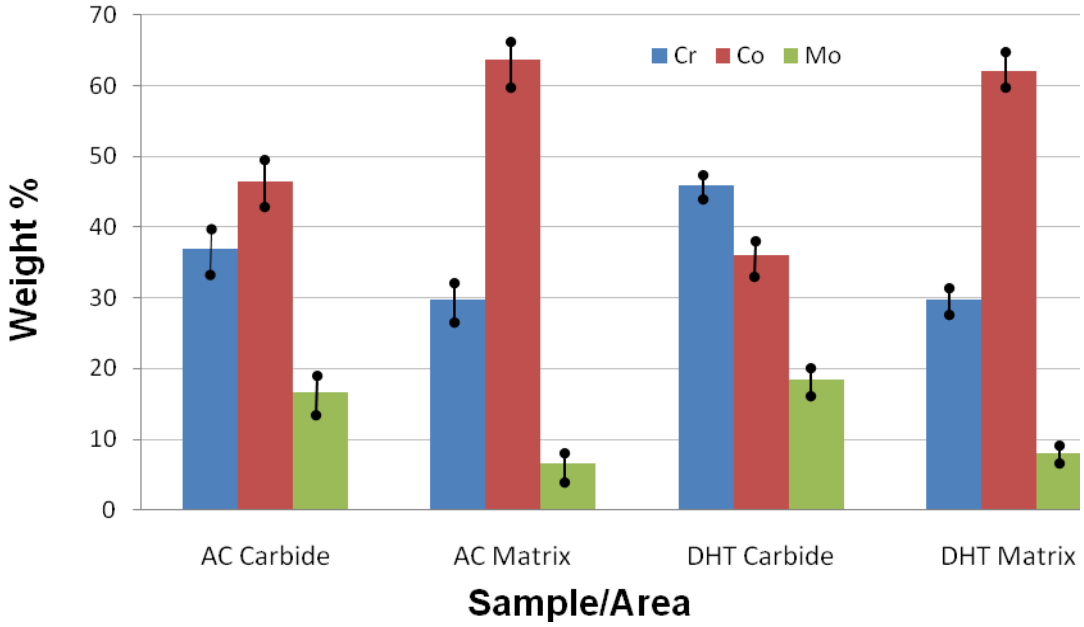

Figure 4.2: Summary of SEM EDX spot analysis in both the matrix and carbide areas of NW AC1 and NW DHT1 samples, showing the average and standard deviation of 15 measurements. Results are normalised to 100% for the elements selected. Analysis was carried out on polished head surfaces and carbon content was excluded from the data due to high carbon contamination using SEM EDX analysis.

In all samples, the carbides were primarily chromium-molybdenum-rich and lower in cobalt content compared with the matrix. On average the double heat-treated carbides had a higher percentage of chromium and a lower percentage of cobalt in them compared with the as-cast carbides. The molybdenum levels appear similar for both the matrix and carbide in the as-cast and double heat-treated samples. EDX was taken from the same sample heads shown in Figure 4.1.

In summary, the double heat-treatment resulted in a reduction of the carbide size and number with less of a dentritic structure exhibited in the matrix, compared with the as-cast structure (shown in Figure 4.1).

4.2 Electrochemical Measurements – Potentiodynamic anodic polarisation curves

All polarisation curves were performed at 37°C.

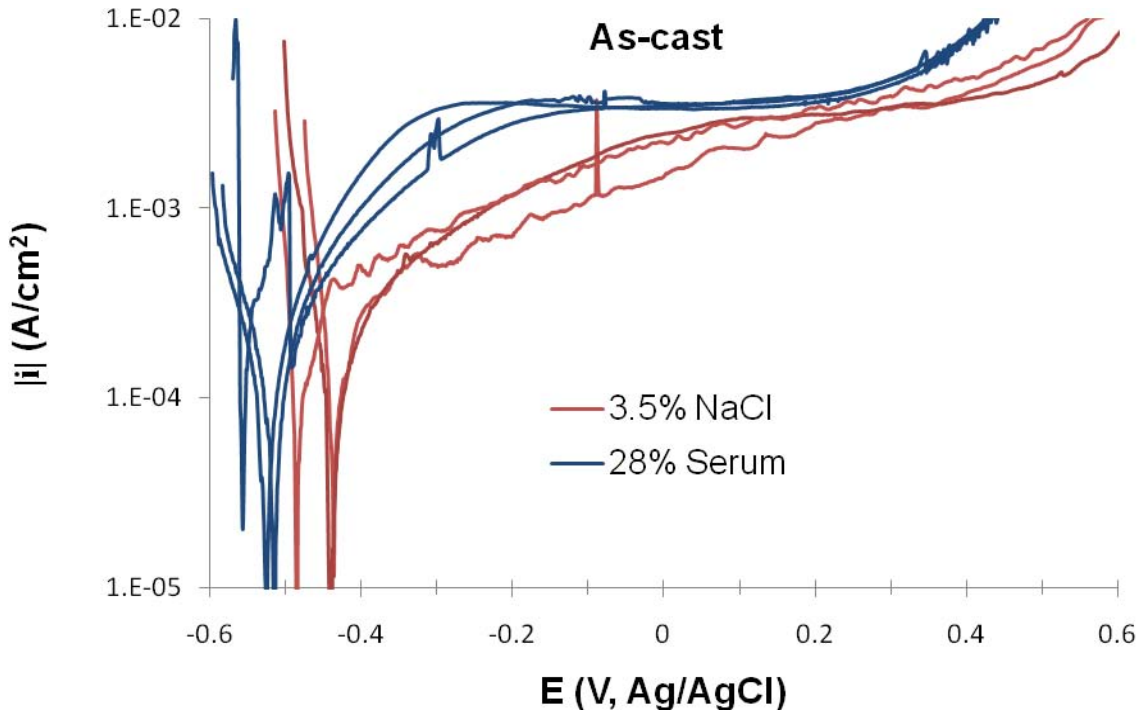

Figure 4.3: Potentiodynamic anodic polarisation curves measured from DC NW AC1 in 3.5% NaCl and 28% bovine serum at 37± 0.5°C. The measurements were alternated between the two solutions.

The as-cast sample shows greater anodic reactivity (higher current density at -0.3 V) in the bovine serum compared with 3.5% NaCl. The OCP (Ecorr) for bovine serum is more negative than the NaCl. It is interesting to note that the static potentiodynamic tests (figures 4.3-5 consistently have a more negative OCP compared with hip simulation tests (figures 4.7-19) under abrasion. The hip simulator tests are much nobler with OCPs of around 0--0.1 where as the potentiodynamic tests were around -0.4--0.6.

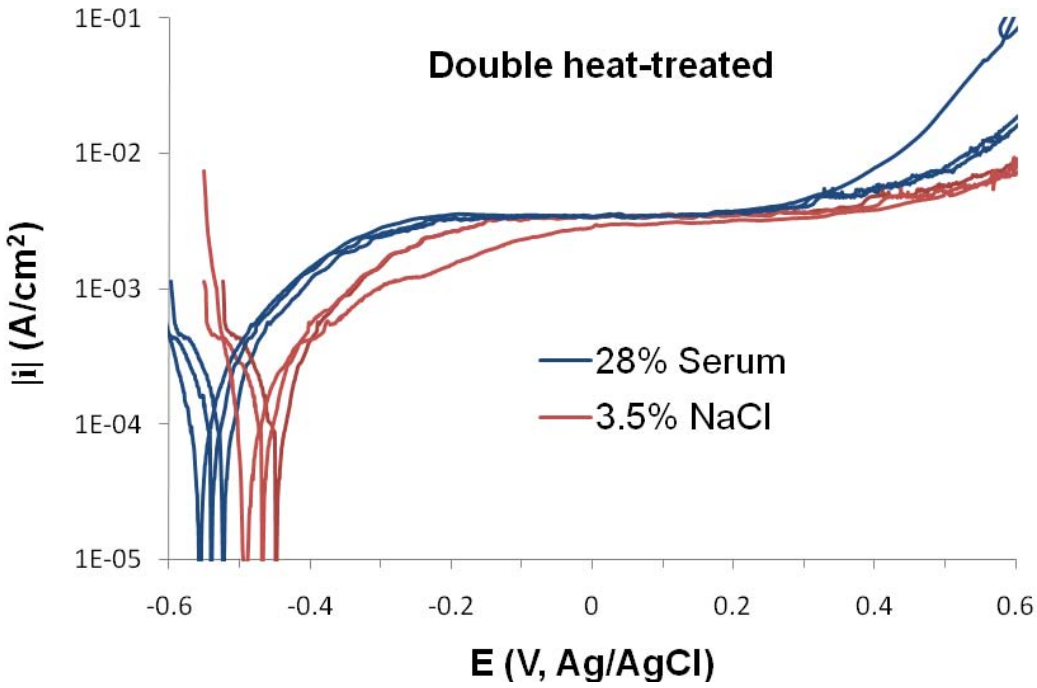

Figure 4.4: Potentiodynamic anodic polarisation curves measured from DC NW DHT1 in 3.5% NaCl and 28% bovine serum at 37± 0.5°C. The measurements were alternated between solutions.

For the double heat-treated sample again there is greater anodic reactivity in 28% bovine serum solution than in 3.5% NaCl.

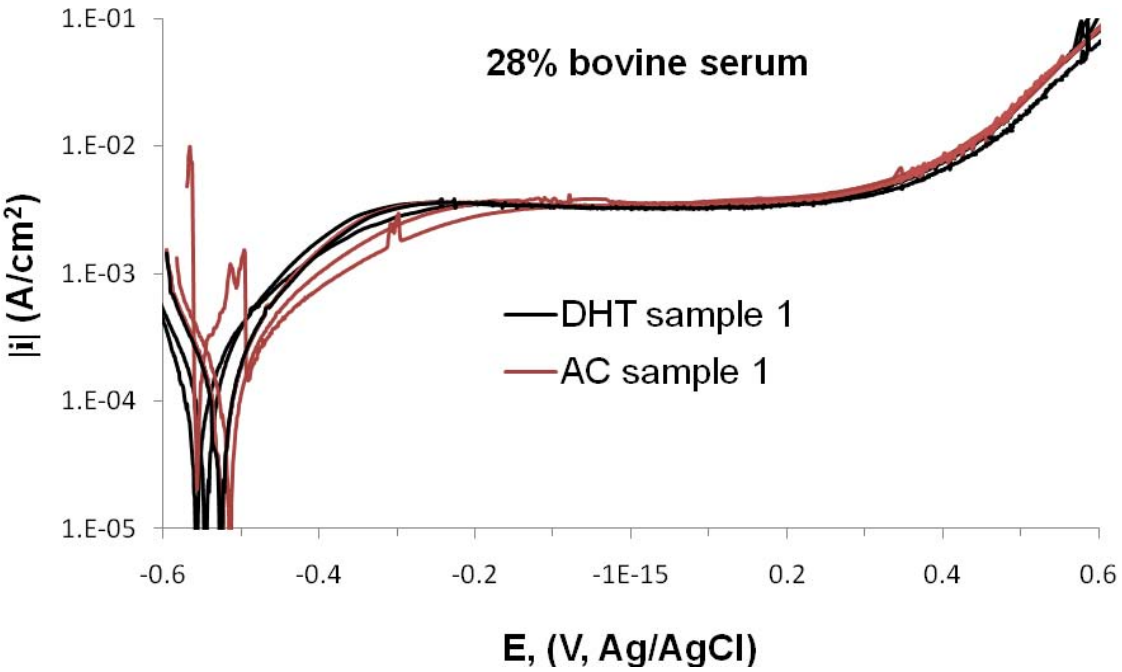

Figure 4.5: Potentiodynamic anodic polarisation curves for DC NW AC1 and DC NW DHT1 in 28% bovine serum at 37± 0.5°C. Measurements were alternated between samples.

In 28% bovine serum the as-cast and double heat-treated samples are fully overlapped suggesting a very similar level of anodic reactivity.

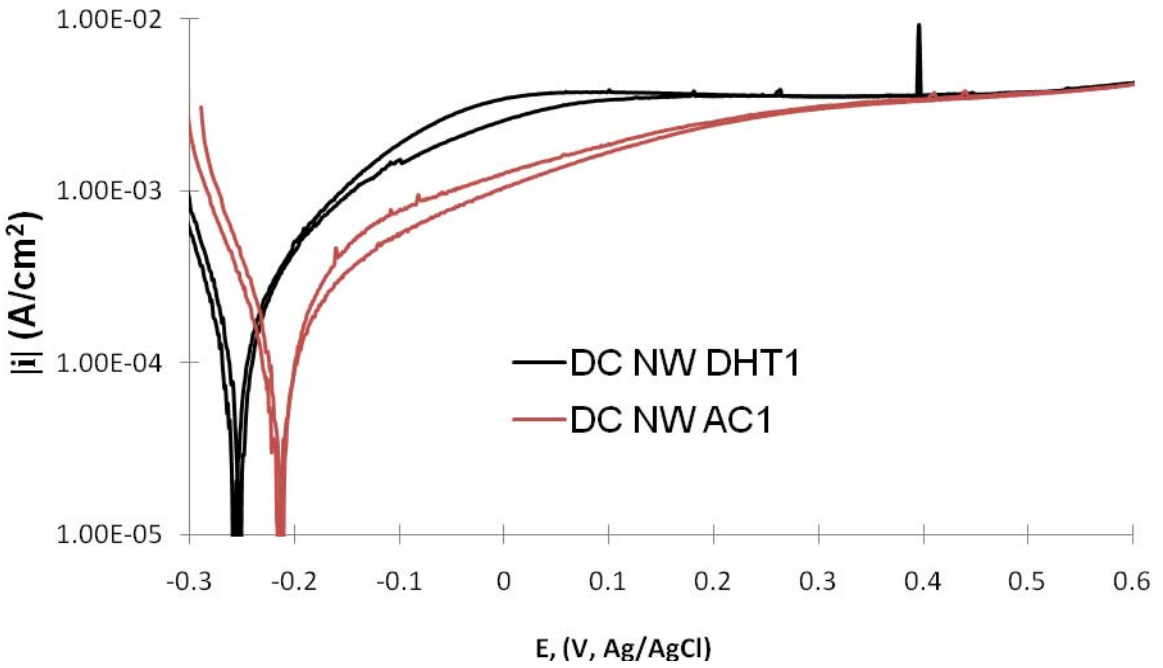

Figure 4.6: Potentiodynamic anodic polarisation curves in 90% Ringers solution and 10% bovine serum acidified to pH2 (adjusted using concentrated HCl) at 37± 0.5°C for Disc New AC1 and Disc New DHT1. Measurements were alternated between samples.

In pH2 Ringers solution and 10% Bovine serum there is a consistent difference shown whereby the double heat-treated sample shows higher anodic reactivity.

4.3 Preliminary Hip Simulator results measuring OCP

4.3.1 AC Worn in part – The difference between 3.5% NaCl and 28% Bovine Serum

The following results were obtained from tests that lasted 1500 seconds with periods of abrasion at 300 and 900 seconds. Each period of abrasion consisted of 100 cycles at a speed of 1 Hz, which lasted approximately 100 seconds. During this period the cup was stationary and the head moved through an angle of 45° while under a downward load of 2000 N. When not in a period of abrasion, the head and cup were stationary and were subjected to a vertical load of 1000 N.

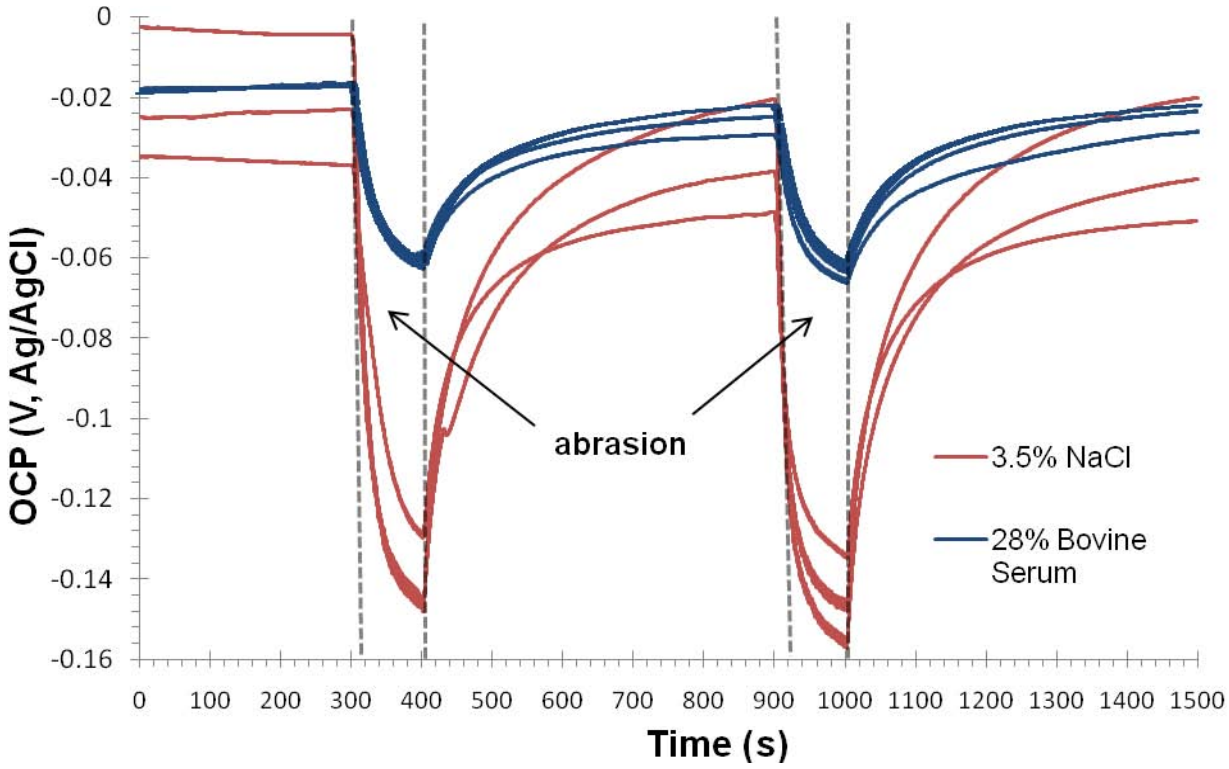

Figure 4.7: OCP as a function of time for a worn-in AC 1 part over a 1500 second period in 28% Bovine serum and 3.5% NaCl at room temperature (20 °C). The measurements were alternated between 3.5% NaCl and 28% bovine serum to eliminate any time-dependent changes in the articulating surfaces.

During the abrasion period (the sharp drops in potential) the sample shows a greater drop in OCP during depassivation when in the 3.5% NaCl solution compared with the 28% Bovine serum solution. The same sample was used for all of the measurements but the solutions were

alternated so that the difference between the two is consistent and not a consequence of time-dependent changes in the articulating surfaces.

The greater drop in OCP during abrasion suggests a greater increase in anodic reactivity for CoCrMo in 3.5% NaCl compared with 28% Bovine serum. This is somewhat surprising since the anodic reactivity in the absence of abrasion was found to be higher for 28% Bovine serum than 3.5% NaCl in Figure 4.3 (anodic polarisation curves). However, the polarisation curves were measured at 37 °C whereas the abrasion measurements in Figure 4.7 were carried out at approximately 20°C.

4.3.2 AC and DHT Worn-in parts – The difference in temperature at 40°C and 20°C (room temperature)

Before investigating the difference between as-cast and double heat-treated samples in the hip simulator the effect that temperature could have on potential was examined. This was to find out if it was needed to be regulated in future tests.

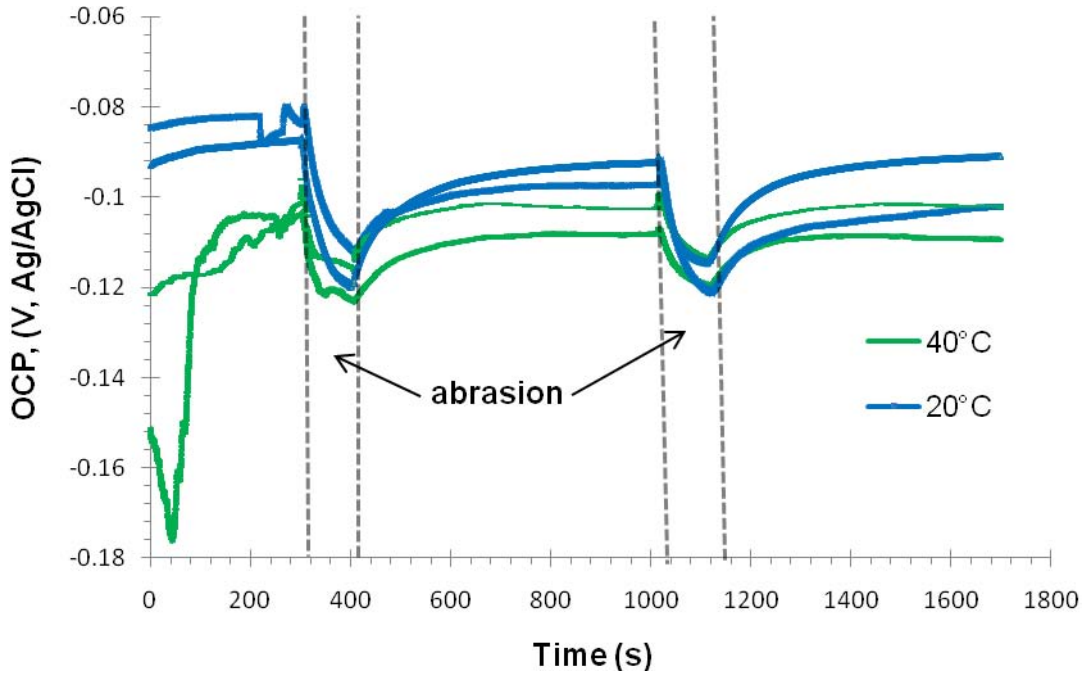

Figure 4.8: OCP as a function of time for a worn-in AC 2 part in 28% bovine serum at 40°C and 20°C. The measurements were alternated between 20°C and 40°C with the solution being changed each time.

These results were obtained from tests that lasted 1700 seconds. Two abrasion periods were used consisting of 100 cycles at a speed of 1 Hz. During this period the cup was held

stationary while the head was moved through an angle of 45° under a downward load of 2000 N. In the periods that abrasion did not take place the head and cup were stationary and were under a downward load of 1000 N (these test parameters were the same used for the results shown in Figures 4.9, 4.10, 4.11).

At the start of each test each solution was at its specified temperature. However by the end of the test the solutions at 40°C had cooled to an average of 31°C. The solutions at 20°C had increased slightly to 22°C. These changes in temperature were typical for the following tests shown in Figures 4.9-11 where temperatures of 40°C cannot be maintained and the increases in temperature being attributed to the heat generated from the powering of the movement arm by the machine. Figure 4.8 shows the start potentials at 40°C to be lower than those at 20°C. Before the first period of abrasion there is a difference of approximately 20 mV, however there is no difference between the temperatures in both abrasion periods. This could be due to the solution at 40°C cooling down closer to 20°C to give a similar depassivation value.

Also the 40°C experiment which starts of at -0.15 and then dramatically increases to - 0.11V may have cooled down towards room temperature at 300 seconds, explaining why the potential shoots up. Overall temperature does not have a definite affect for this worn-in as-cast sample in 28% bovine serum.

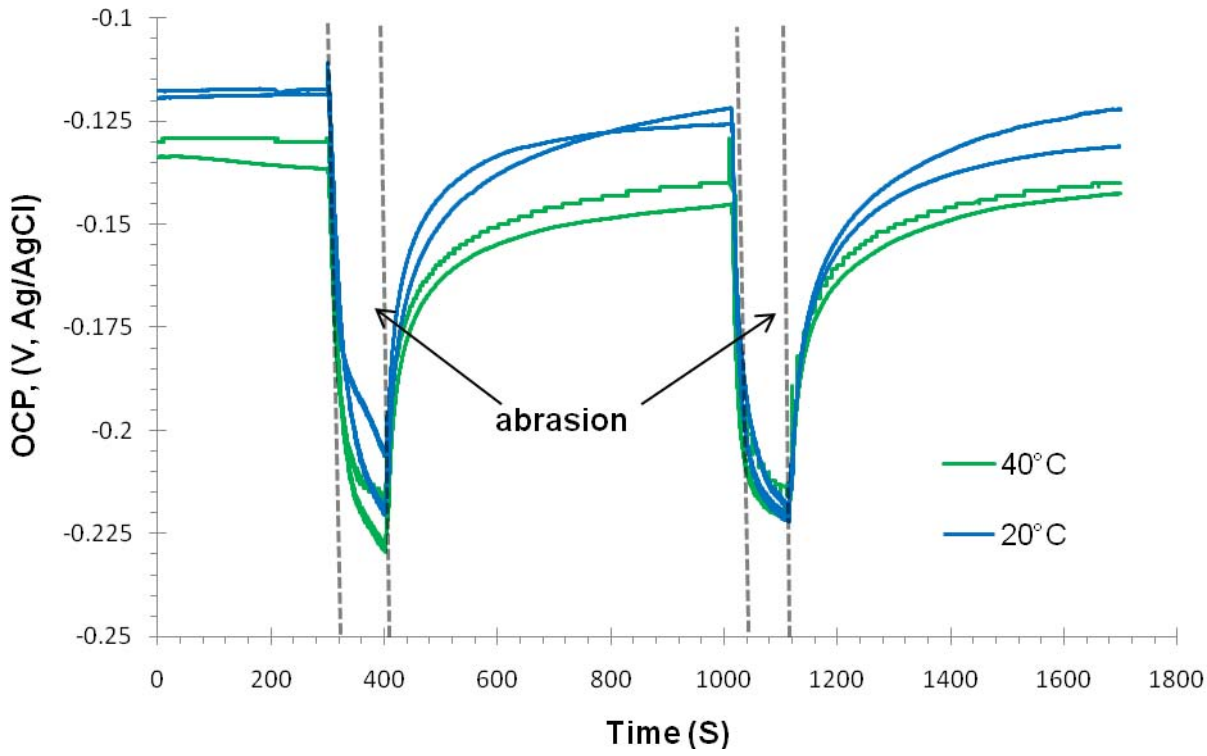

Figure 4.9: OCP as a function of time for a worn-in AC 2 part in 3.5% NaCl solution at 40°C and 20°C. Measurements were alternated between 40°C and 20°C.

At the start of each test, each solution was at its specified temperature. However by the end of the test the solutions at 40°C had cooled to an average of 29°C. The solutions at 20°C had increased slightly to 22°C. At 40°C the starting potential is 50 mV more negative and gives a lower depassivation potential in the first abrasion. Also when repassivating, the solution at 20°C repassivates quicker and to a less negative value. However this difference is very slight and in the second abrasion period there is no difference in the OCPs. This could be due to the solution having cooled down to nearer 20°C by this point (1000 seconds into the experiment), meaning the depassivation rates would be similar. Overall the differences in the OCPs at 40°C and 20°C for the as-cast sample in 3.5% NaCl solution is not enough to be considered significant.

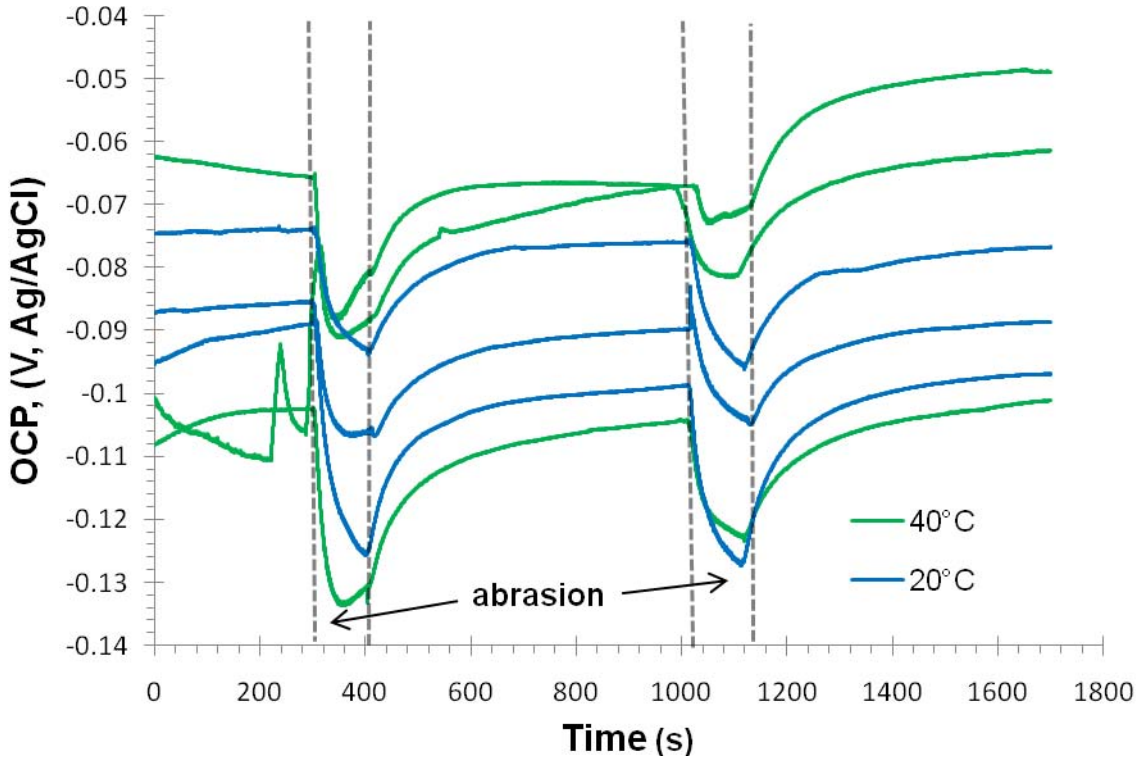

Figure 4.10: OCP as a function of time for the worn in DHT 1 part in 28% bovine serum at 40°C and 20°C. The measurements were alternated between 40°C and 20°C.

At the start of each test, each solution was stable at its specified temperature. However, for the tests conducted at 40°C the solution actually went on to cool during the experiment giving an average of 28°C by the end of the test. The tests conducted at 20°C actually increased in temperature to an average of 22°C by the end of the test. Figure 4.10 shows for DHT 1(worn-in double heat-treated sample) in 28% Bovine serum, there is considerable scatter with no systematic trend in the behaviour with temperature. The green line which appears most negative could be an anomaly as it was the last test run in the sequence; however more testing would be required to confirm this.

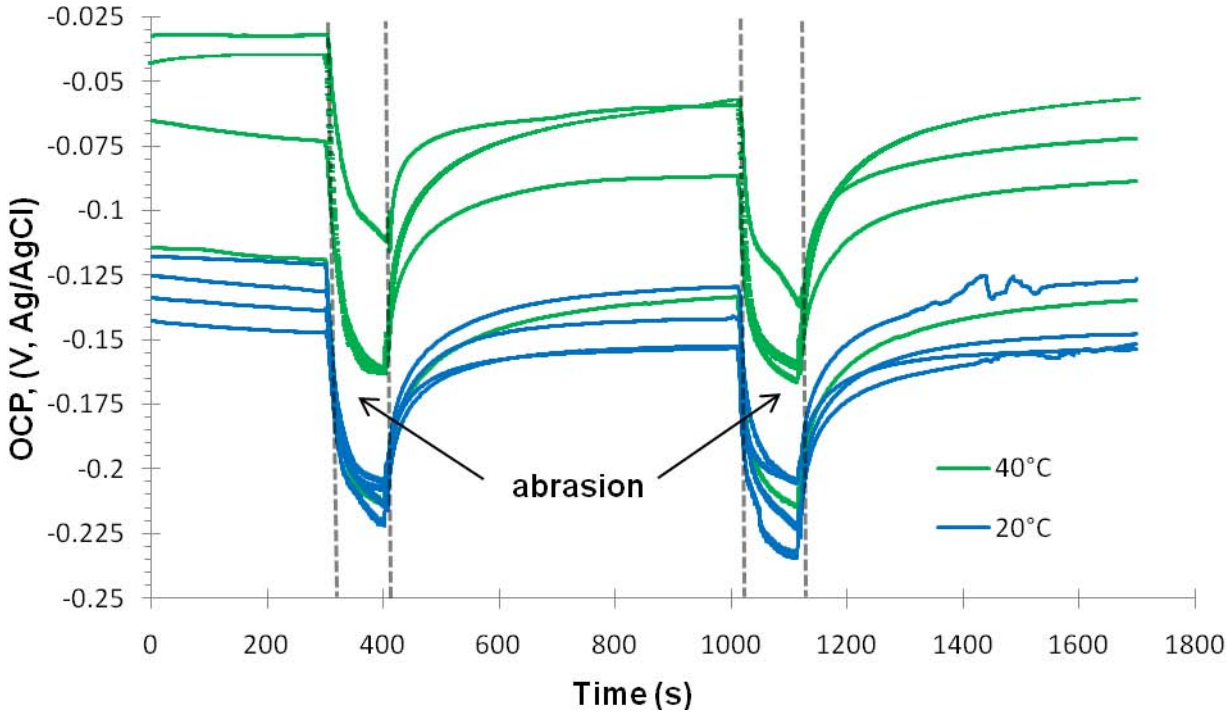

Figure 4.11: OCP as a function of time for the worn-in DHT 1 part in 3.5% NaCl solution at 40°C and 20°C. Measurements were alternated between 40°C and 20°C.

At the start of each test, each solution was stable at its specified temperature. However by the end of tests conducted at 40°C the temperature had cooled to an average of 32°C whereas the solutions at 20°C had increased slightly to 22°C. Figure 11 shows that 3.5% NaCl is less negative when it is at 40 degrees when compared with room temperature. The starting potential for 3/4 of the experiments at 40°C is significantly higher than when conducted at 20°C. The green curve that falls in the middle of blue curves was the last experiment in the sequence. This could be the result of previous experiments before which may have impacted the surface's reactivity if not enough time had been left for the alloy's surface to repassivate.

4.3.3 General Overview of OCPs of worn-in as-cast and double heat treated parts

It is evident that Figures 4.8-4.11 show a large degree of scatter, as there is not always a clear difference in OCP between the two temperatures. However, one consistent difference is seen between the different solutions used. In Figures 4.8 and 4.10 examining bovine serum, increased temperature did not appear to have any effect. However, in Figures 4.9 and 4.11 both experiments show a consistent difference in temperature (if only small), when tested in 3.5% NaCl. However, these results contradict each other as for the AC sample (Figure 4.9)

40°C gives a more negative OCP whereas for the DHT sample (Figure 4.11) 20°C gives a more negative OCP. It is important to note that in these experiments the temperature has never constant throughout any of the experiments. As a general trend the solutions at 40°C would cool by around 10°C during the 1700 second period as it was exposed to room temperature (20°C). The solutions tested at room temperature were more consistent, increasing each time to 22°C by the end of the experiment. This can be attributed to the frictional heat generated during these short abrasion periods.

The major finding from these experiments is the issue of irreproducibility within the hip simulator. Although consistent trends were seen in Figures 4.9 and 4.11 in 3.5% NaCl, however these trends contradicted each other and so it is not possible to draw any reliable conclusions. The issue of irreproducibility could be the result of sample-to-sample variation as these worn-in samples may have different abraded areas as a result of wear previously experienced, which may in-turn affect the corrosion potential. The other significant factor is that it was not possible to regulate the temperature of the solution throughout the duration of the test, which could contribute to the irreproducibility of the results. The difficulty of keeping the temperature of the solution constant at either 20°C or 40°C in the hip simulator means that for the following experiments temperature will only be monitored, with all experiments taking place at room temperature.

4.4 Hip Simulator results measuring OCP using new AC and DHT samples

4.4.1 Alternating cycles of stabilisation and abrasion

The following experiments lasted 4000 seconds (approximately 66 minutes), consisting of alternating cycles of stabilisation followed by abrasion, with each period lasting 500 seconds. During the stabilisation period the joint was completely stationary but was under a downward load of 1000 N. During the abrasion period a downward load of 2000 N was applied and movement by the head through a 45° angle at a speed of 1 Hz. Each as-cast and double heat-treated sample was put through 8 runs with all experiments beginning at room temperature (20°C). In this experiment the temperature was monitored and the periods of abrasion caused an increase in temperature of the solution, surrounding the joint. This is shown in Figures 4.13 and 4.15.

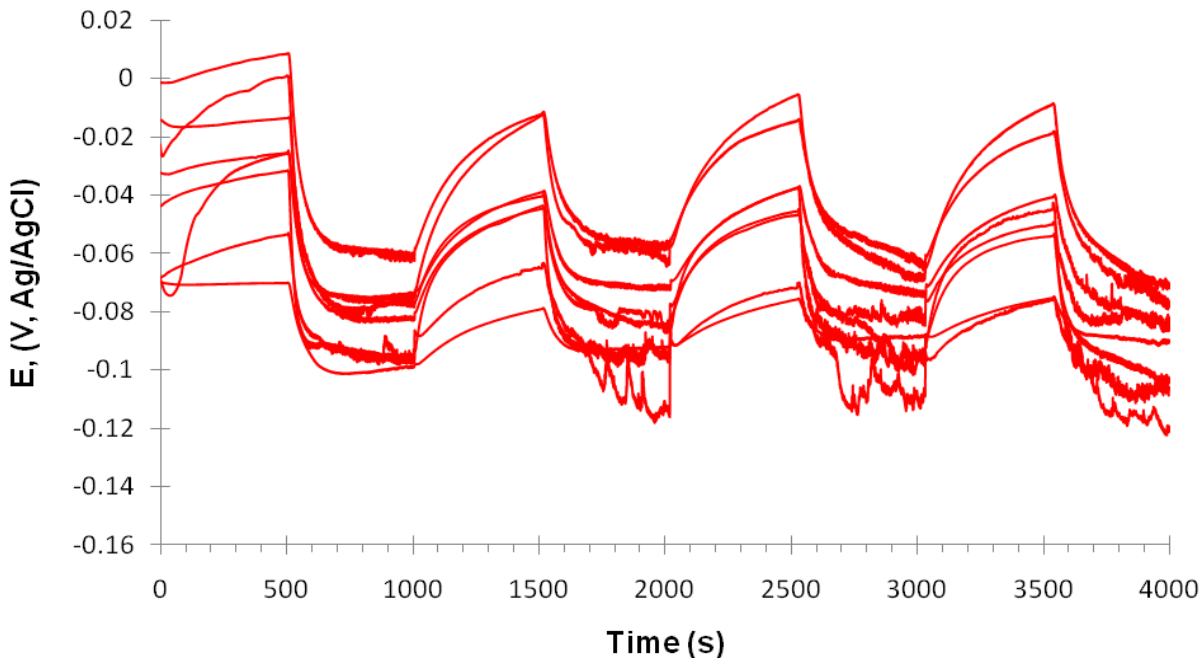

Figure 4.12: OCP as a function of time for runs 1-8 on the New AC 1 joint in 28% Bovine serum. As-cast measurements were removed and alternated with the double heat-treated measurements that follow, with new solution being used for each experiment. Due to preliminary issues of irreproducibility experiments were alternated to eliminate any time dependant effects.

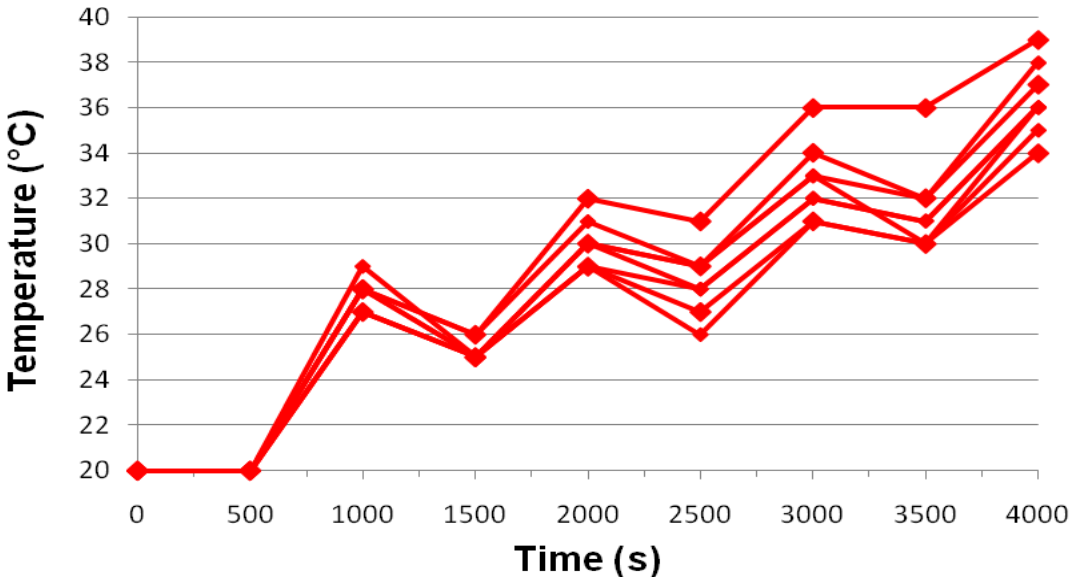

Figure 4.13: Temperature increase as a result of abrasion for runs 1-8 of the bovine serum surrounding the New AC1 joint. Temperature readings were taken every 500 seconds. Note that abrasion occured for 500 seconds, starting at 500, 1500, 2500 and 3500 second time periods.

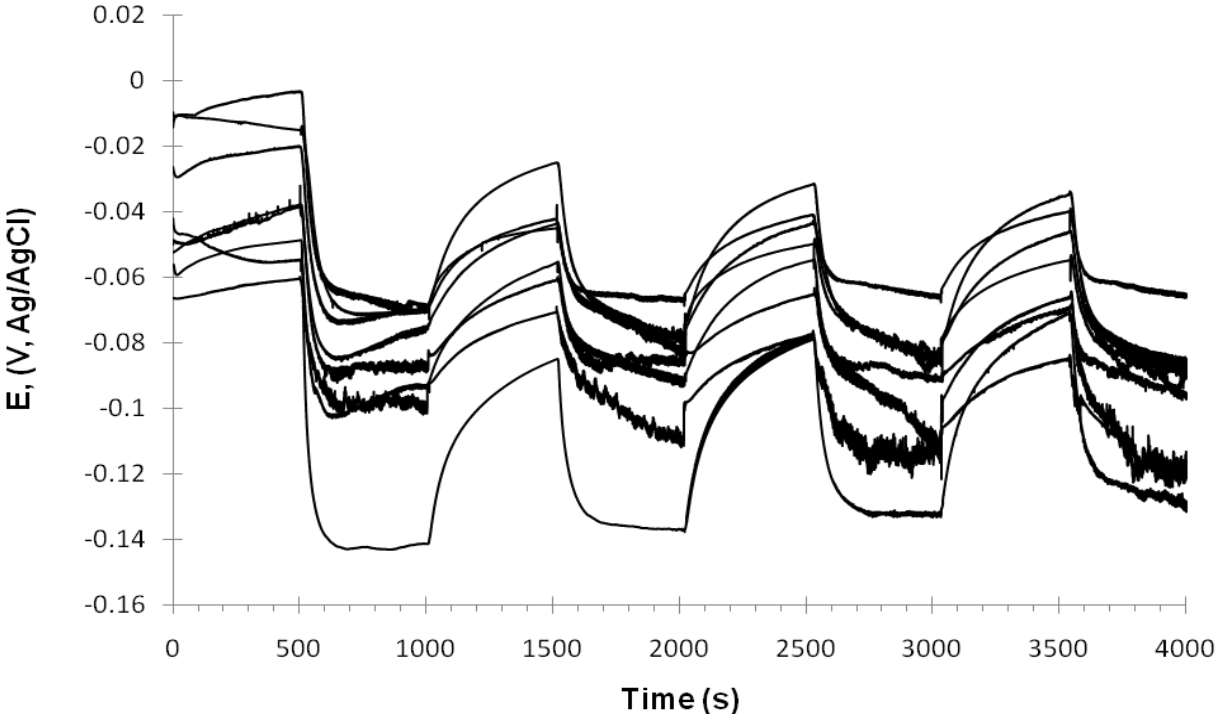

Figure 4.14: OCP as a function of time for runs 1-8 on the New DHT 1 part in 28% bovine serum. Double heat-treated experiments were alternated with the as-cast experiments shown above with fresh solution being used each time.

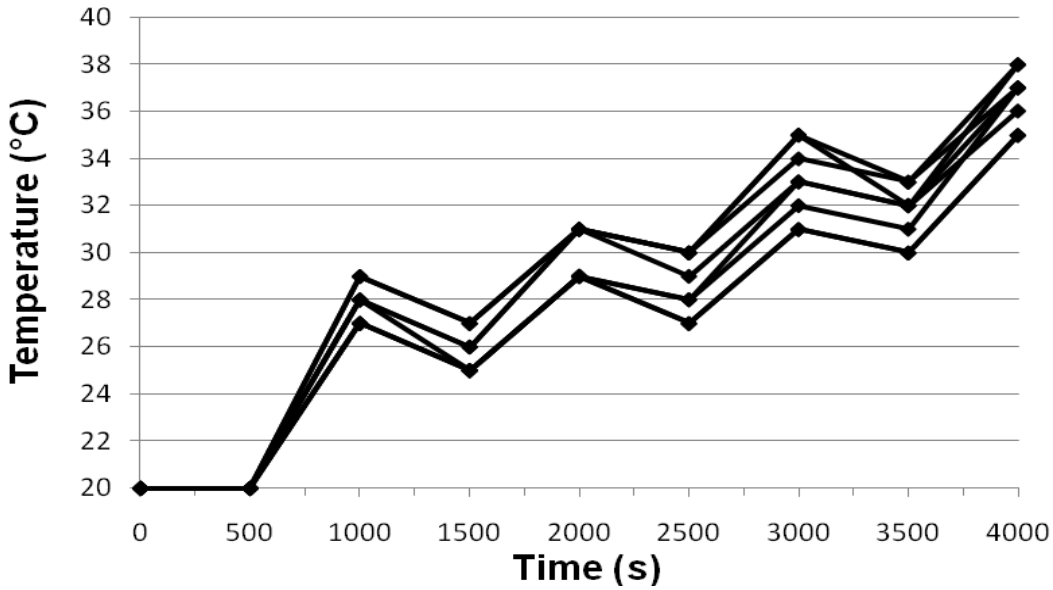

Figure 4.15: Temperature increase as a result of abrasion of the bovine serum surrounding the New DHT 1 joint for runs 1-8. Temperature readings were taken every 500 seconds. Note that abrasion occured for 500 seconds, starting at 500, 1500, 2500 and 3500 time periods.

Figures 4.12 and 4.14 have been shown on the same scale for easy comparison. A large degree of scatter for both as-cast and double heat-treatments is evident. There is some consistency with the start potentials between the two heat-treatments in the first stabilisation period but once the surfaces have undergone abrasion there is little consistency between the OCPs.

It is evident that the New DHT sample 1 (Figure 4.14) is generally at a more negative potential than the New AC sample 1 (Figure 4.12). Figures 4.13 and 4.15 show the temperature increase in the solution as a result of articulation. There appears to be no distinct difference between the temperature at the two different heat treatments as most of the runs follow a similar trend. The important aspect to note regarding Figures 4.13 and 4.15 is that during a 500 cycle abrasion period the temperature can increase up to 8 or 9 °C, which may then affect the corrosion potential.

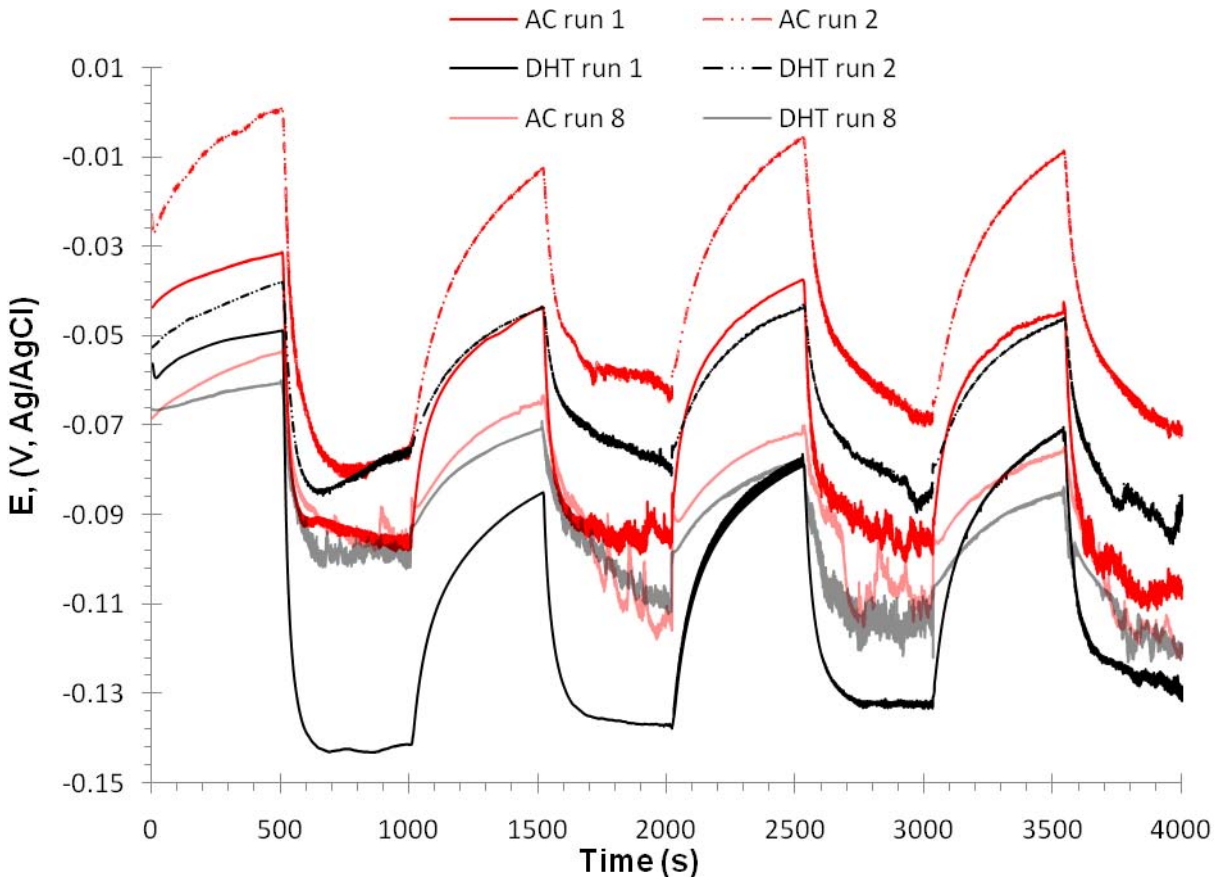

Figure 4.16: OCP as a function of time for NW AC 1 and NW DHT 1 joints for runs 1, 2 and 8 in 28% bovine serum.

Figure 4.16 shows NW DHT 1 depassivating to a more negative potential when comparing runs 1 and 2 with NW AC 1. Also the starting potentials are higher for NW AC 1 in both runs 1 and 2 compared with NW DHT 1. After 8 runs there is little difference in the corrosion potential between AC and DHT. However, given the scatter of the results the difference is not very convincing.

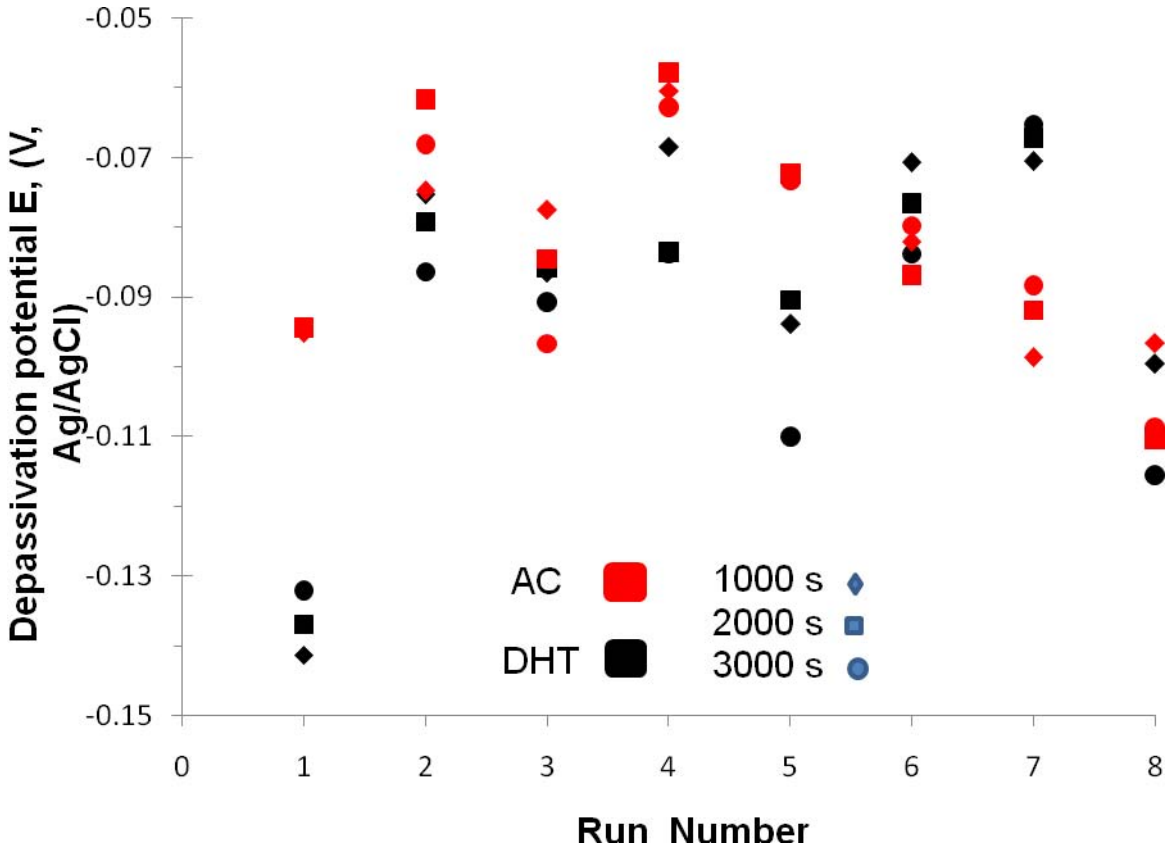

Figure 4.17: The OCP at the end of the abrasion cycle showing the depassivation potentials between NW AC 1 and NW DHT 1 for runs 1-8 in 28% bovine serum. Depassivation values were taken at 1000, 2000 and 3000 seconds for each sample explaining why there are 3 values for each run number.

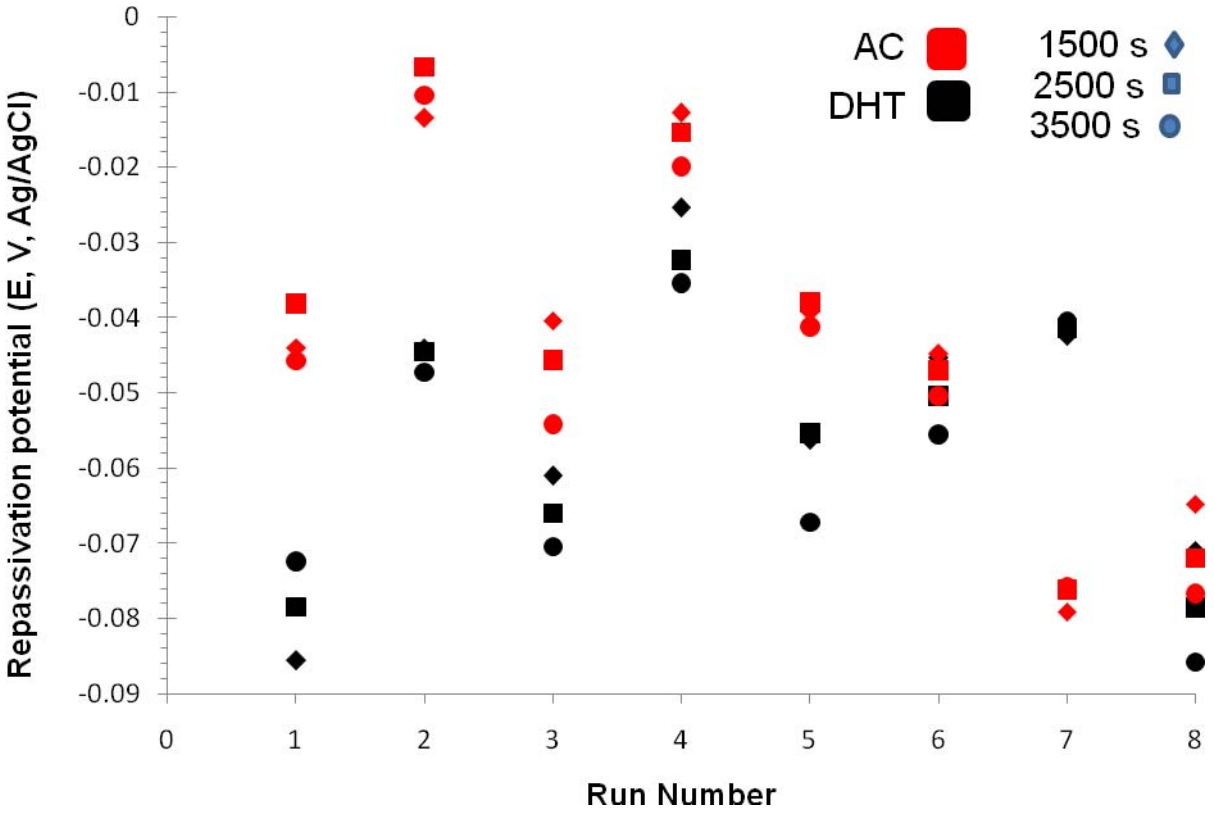

Figure 4.18: The OCP at the end of the stabilisation cycle showing the repassivation potentials for NW AC 1 and NW DHT 1 in runs 1-8 in 28% bovine serum. Repassivation values were taken at 1500, 2500 and 3500 seconds for each sample explaining why there are 3 values for each run number.

Figures 4.17 and 4.18 show the maximum depassivation and maximum repassivation values in each test run respectively. In the tests shown in Figures 4.12 and 4.14 there were three periods of abrasion at 1000 s, 2000 s and 3000 s for each test run. The depassivation values at these points for both heat treatments are plotted on Figure 4.17. Generally, DHT depassivates to a more negative potential during abrasion, however runs 3, 6 and 8 give very similar values. For the stabilisation periods shown in Figures 4.12 and 4.14 repassivation values have been taken at the end of this period at 1500 s, 2500 s and 3500 s for each test run. The repassivation values at these points for both heat treatments are plotted on Figure 4.18. In 5 runs out of 8 the AC sample repassivates to a greater potential than the DHT sample, however runs 6 and 8 are very similar and run 7 shows the opposite of this trend. Run 7 in both Figures 4.17 and 4.18 could be an anomaly against the general trend as AC shows greater depassivation and less repassivation compared with DHT.

4.5 Measuring the OCP over a 2.5 hour period

Brand new polished as-cast and double heat-treated samples were used to perform an OCP experiment over a 2.5 hour period (9000 seconds). The experiment consisted of a 3000 second (50 minute) stabilisation period at the start. During this period no load was applied, but the surfaces were in contact and the joint was completely stationary. After the first 3000 seconds, there were 1500 cycles of abrasion that lasted another 3000 seconds. This was under a vertical load of 2000 N and through a 45° angle at a speed of 0.5 Hz. At the end of the 3000 seconds of abrasion, another period of stabilisation followed with no vertical load applied and the joint remaining completely stationary and still in contact for 3000 seconds. All experiments were conducted at room temperature (20°C). These parameters were based on a similar test conducted by the Yan et al. [42].

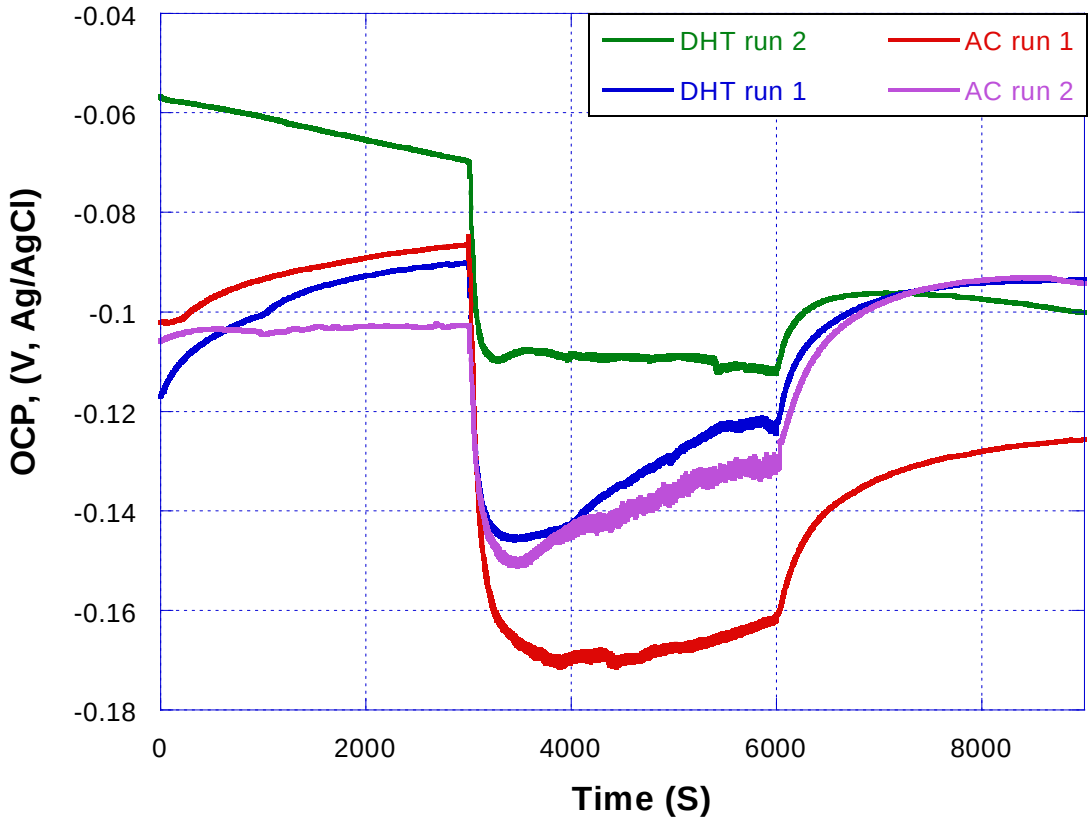

Figure 4.19: OCP as a function of time for a single period of the NW AC 2 and NW DHT 2 joints for runs 1 and 2 in 28% bovine serum. Measurements of NW AC 2 and NW DHT 2 were alternated with fresh solution used for each test.

The relatively constant OCP trace at the start of each experiment represents the initial period of 3000 seconds when the potential was stabilising in a static environment under no load. The

potential then drops to more negative values during abrasion. This is due to the combined effect of a downward load of 2000N being applied and the joint moving through an angle of 45° at 0.5 Hz.

Each test regardless of AC or DHT, showed the same overall shape. For both NW AC 2 and NW DHT 2 run 1, a bigger drop in potential is seen compared to run 2. The AC sample depassivates to a more negative potential than the DHT sample in both runs 1 and 2. However, previous experiments have shown there to be sample-to-sample variation this must be taken into account when interpreting the data.

4.5.1 Detailed examination of the OCP over a 2.5 hour period

The following Figures (4.20-4.23) show detailed examination of the OCP of the experiments shown in Figure 4.20. Image (a) shows the start of abrasion at 3000 seconds and images (b) and (c) show the mid-points of abrasion at 4000 and 5000 seconds respectively. This was done to see if fluctuations in the OCP were related to the movement of the head. This was under a vertical load of 2000 N and through a 45° angle at a speed of 0.5 Hz.

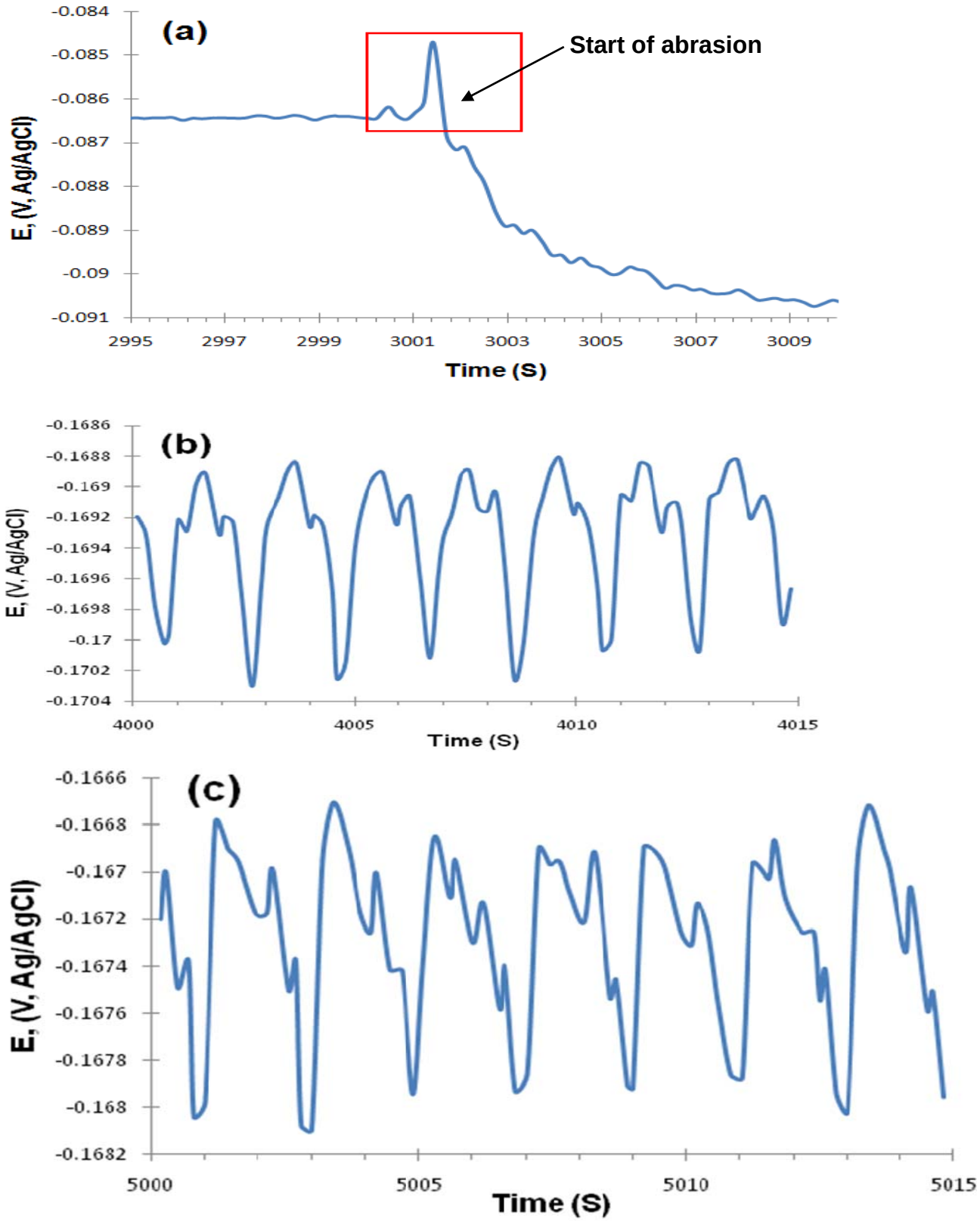

Figure 4.20: The OCP pattern for NW AC 2 run 1 at **(a)** the start of the abrasion cycle **(b)** 1000 seconds in to the abrasion period **(c)** 2000 seconds into the abrasion period

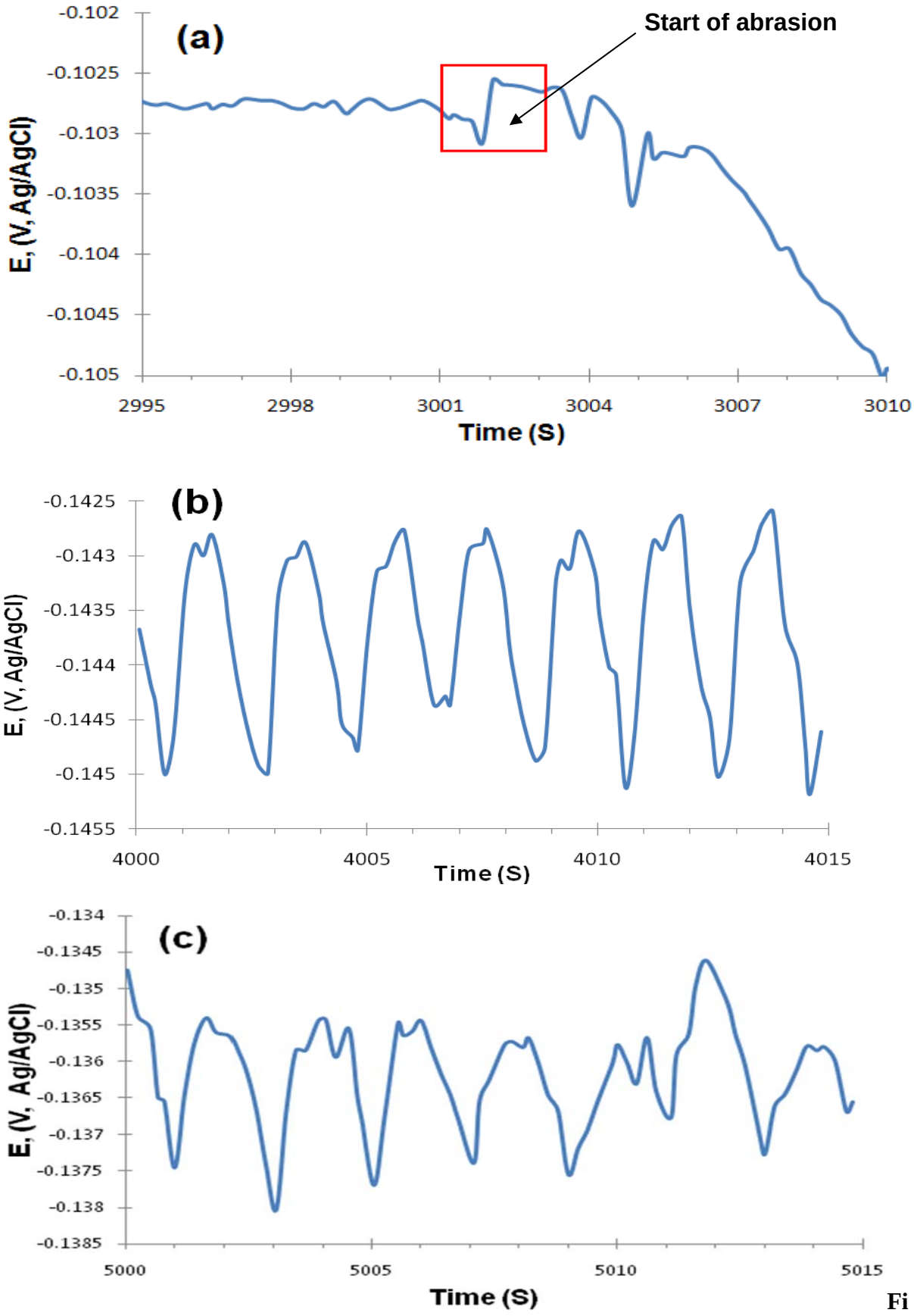

Figure 4.21: The OCP pattern for NW AC 2 run 2 at **(a)** the start of the abrasion cycle **(b)** 1000 seconds in to the abrasion period **(c)** 2000 seconds into the abrasion period

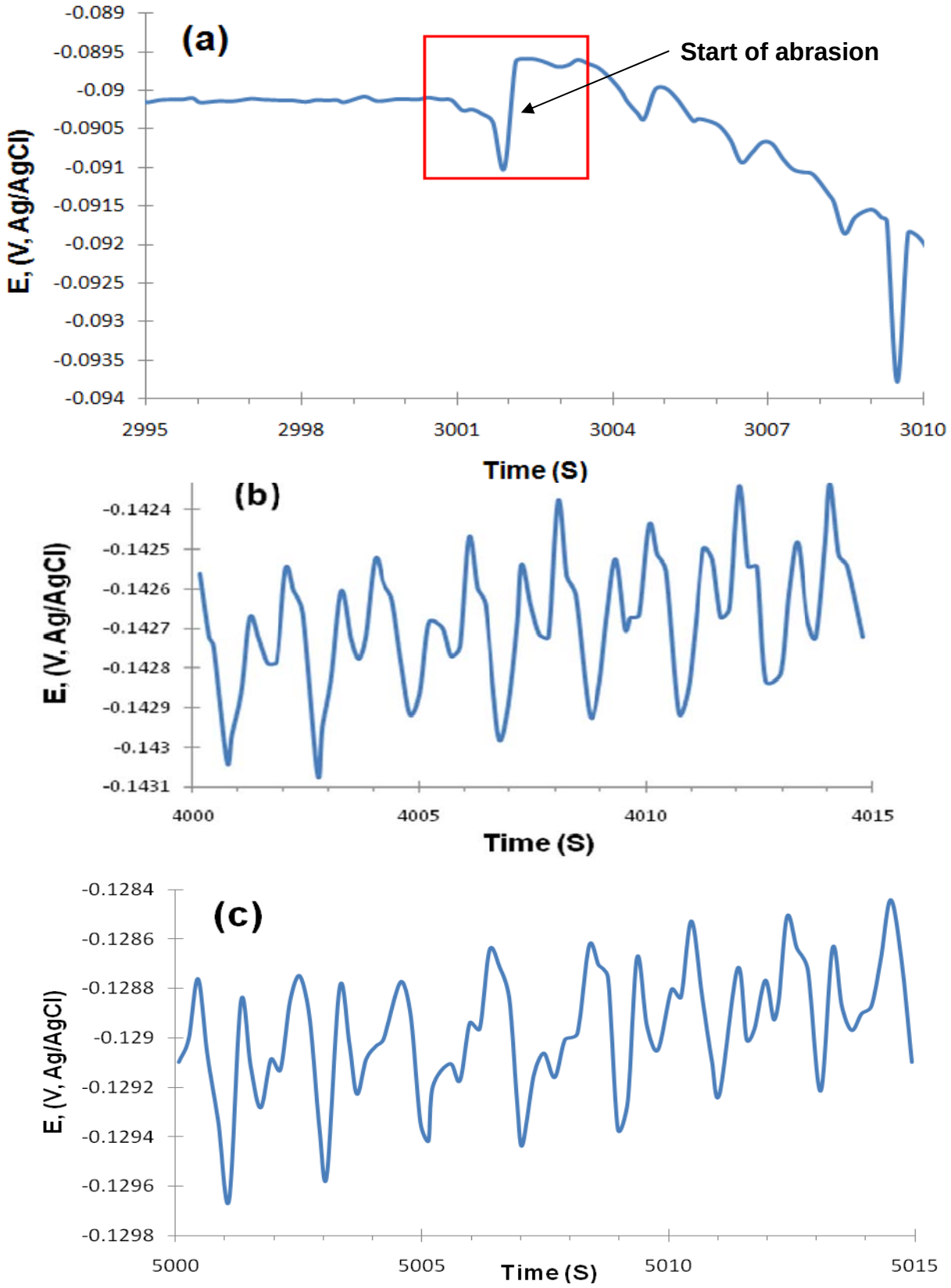

Figure 4.22: The OCP pattern for NW DHT 2 run1 at **(a)** the start of the abrasion cycle **(b)** 1000 seconds in to the abrasion period **(c)** 2000 seconds into the abrasion period.

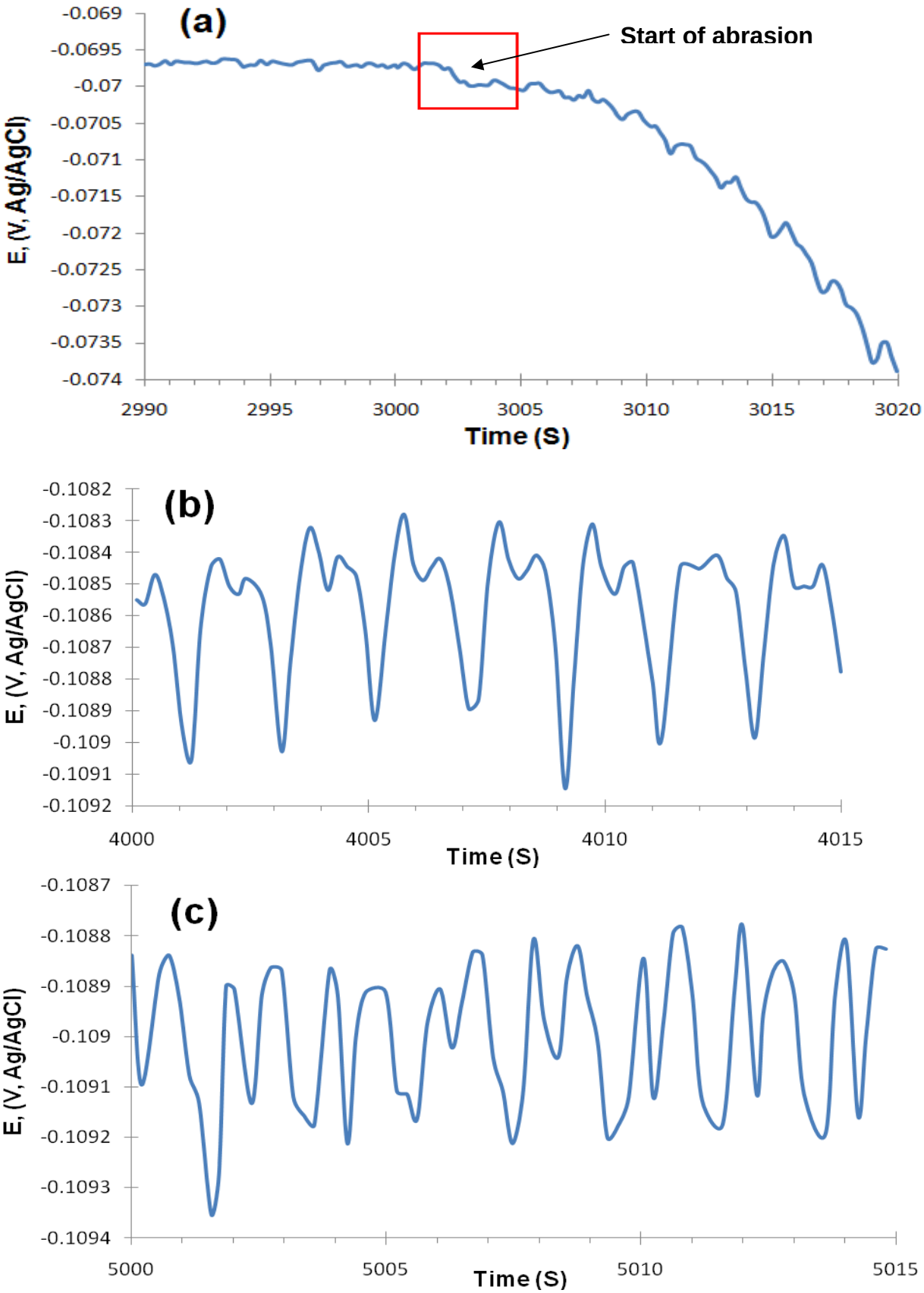

Figure 4.23: The OCP pattern for NW DHT 2 run 2 at **(a)** the start of the abrasion cycle **(b)** 1000 seconds in to the abrasion period **(c)** 2000 seconds into the abrasion period.

Figures 4.20-3 show the OCP fluctuation with the movement of the joint. The frequency of the oscillation was set at 0.5 Hz for this experiment (slowest available), meaning that each cycle takes 2 seconds to complete. In Figures 4.21-4, graphs (b) and (c) all show a relative pattern in that every 2 seconds the OCP has a similar shape to other periods in its own sequence. This highlights that the back and forth motion definitely affects the shape of the OCP.

There is a slight difference between graphs (b) and (c) for Figures 4.20-3 in that the OCP pattern in all (c) graphs are less defined compared with the (b) graphs. Both graphs (b) and (c) were taken from the same abrasion period for each figure, although graph (c) was 1000 seconds later (500 cycles later) into the cycle.

There is also relative inconsistency with the OCPs at the start of each abrasion period. Figures 4.21 and 4.22 follow the same trend at the start of abrasion where a sharp dip is followed by a sharp rise in potential. Alternatively, Figure 4.20 has small rise in potential followed by another bigger, sharper rise in potential. However, Figure 4.23 shows no real change in the OCP at the start of abrasion, when comparing it with the rest of the OCP in the graph.

There is a symmetrical pattern seen in Figures 4.20-3 which corresponds to the back and forth motion of the head in the hip simulator, however it was not clearly defined throughout the graphs.

4.6 Preliminary potentiostatic measurements using a Hip Simulator

The following experiment took potentiostatic measurements from WN AC 1 joint.

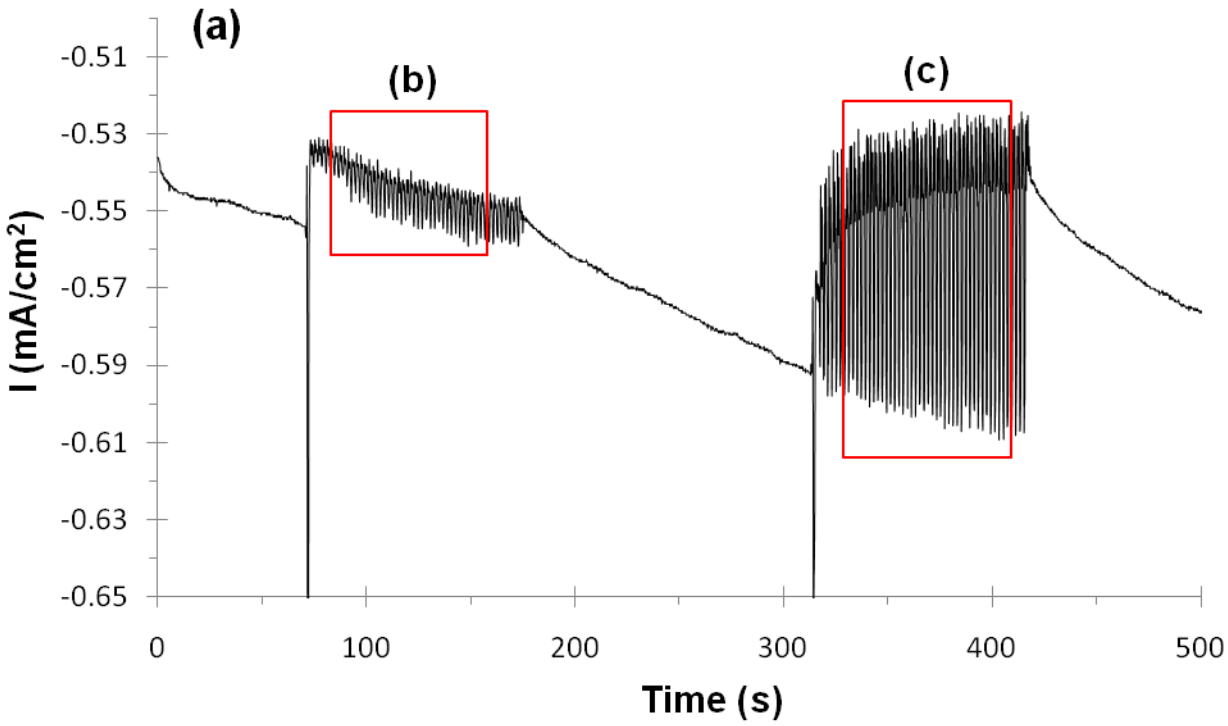

Figure 4.24: Current flowing as a function of time for worn-in AC 3 in 28% bovine serum at room temperature. There are two different stages of abrasion shown **(b)** 15° angle of movement subjected to a 2000 N downward load and **(c)** a 45° angle of movement subjected to a 2000 N downward load.

Figure 4.24 shows that when the joint is articulating the current increases during both abrasion periods. The increase in current released in abrasion period **(b)** compared with abrasion **(c)** can be correlated to the 30° increase in angle of movement by the hip simulator, mentioned in the caption.

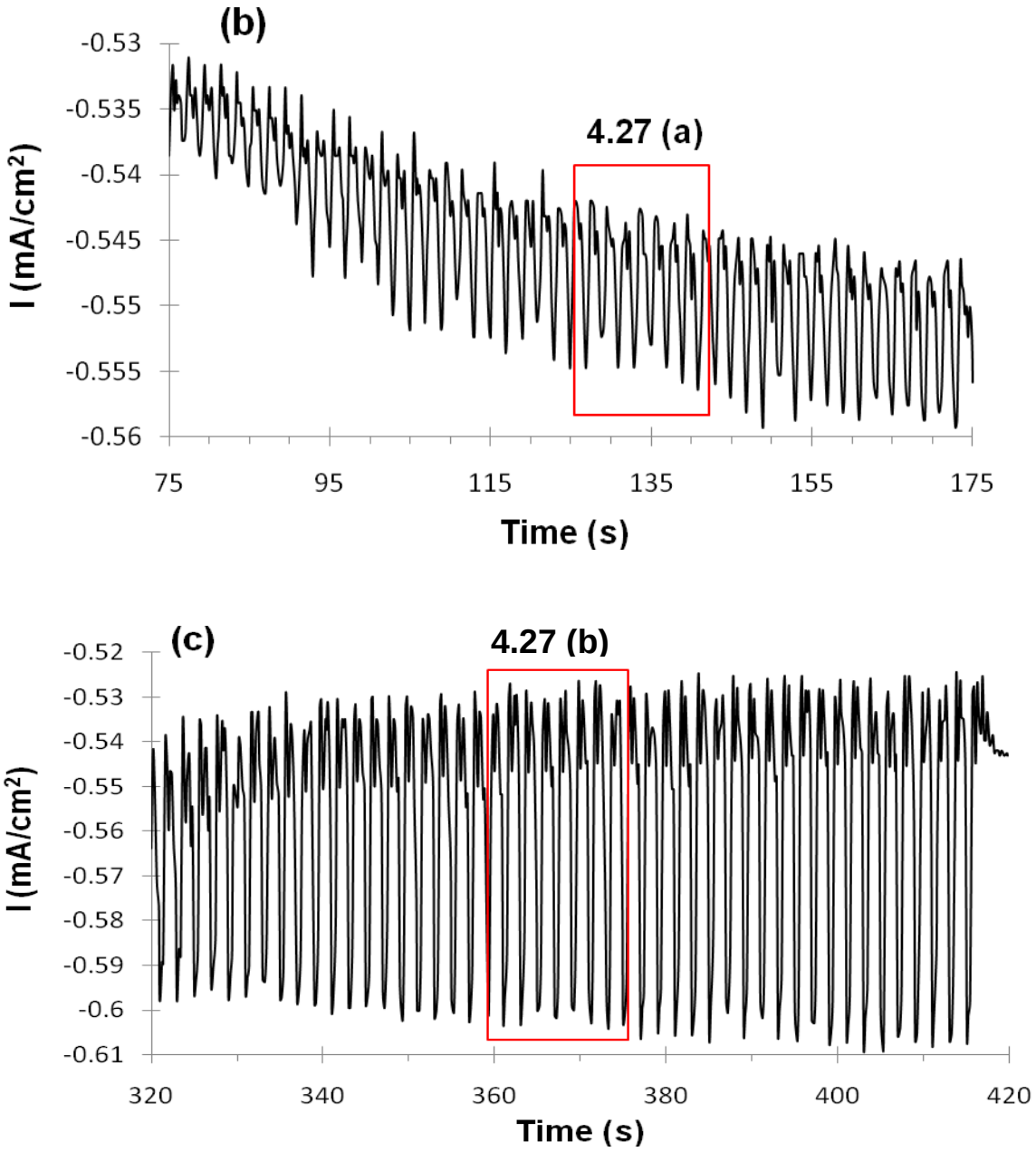

Figure 4.25: The difference in current as a function of time during abrasion period **(b)** under 2000 N load with a 15° range of movement and **(c)** under 2000 N load with a 45° range of movement.

Figures (b) and (c) 4.25 show the difference in current fluctuations with an increased angle of abrasion. Figure (b) shows current fluctuations with a difference of approximately 0.01 (mA/cm^2) whereas with (c) the increased angle gives current fluctuations of approximately 0.07 (mA/cm^2). The current for the increased angle of abrasion generally more negative suggesting a greater abrasion angle may mean the alloy is more susceptible to corrosion.

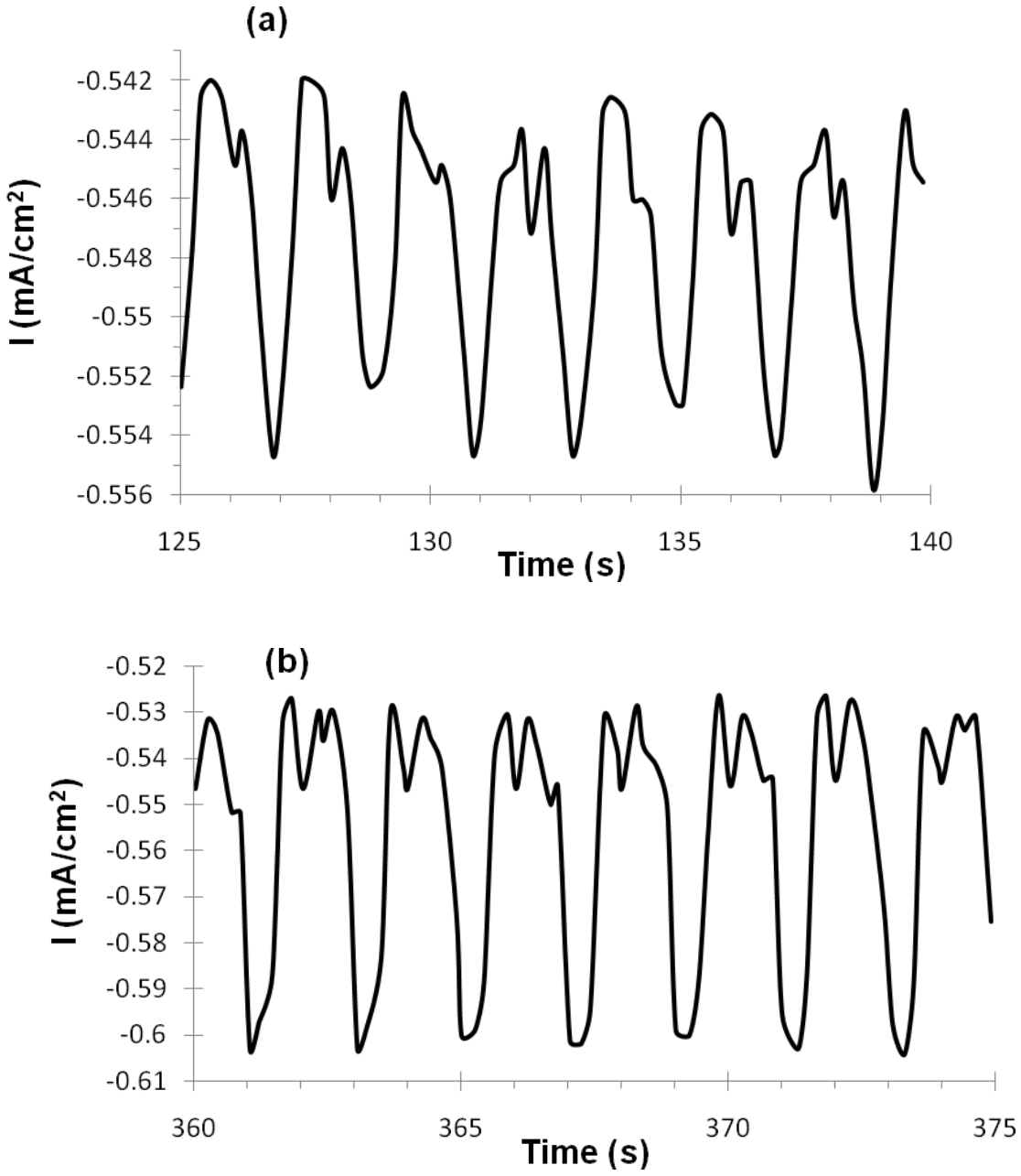

Figure 4.26: The current fluctuations over 15-seconds of abrasion in sections a) and b). Both sections have 2000 N load applied but abrasion **a)** has a 15° range of movement whereas abrasion **b)** has a 45° range of movement.

Figures (a) and (b) 4.26 were taken from the middle of each abrasion period and the 15-second period shown in the figure shows the typical shape of the current flow throughout the whole period. It has been difficult to obtain consistent and reproducible measurements from this experiment. The preliminary results shown here is a promising start from a single sample. However, to compare as-cast and double heat-treated samples more work needs to be done on

the procedure to reproduce similar results. It may also be difficult to obtain true results for the comparison of AC and DHT due to the sample-to-sample variation already observed.

4.7 Characterising the Wear Scars from the Hip Simulator

After each experiment in the hip simulator heads were examined using an SEM to observe surface damage as a result of abrasion. The following figures are typical of what was seen after the surface had experienced abrasion.

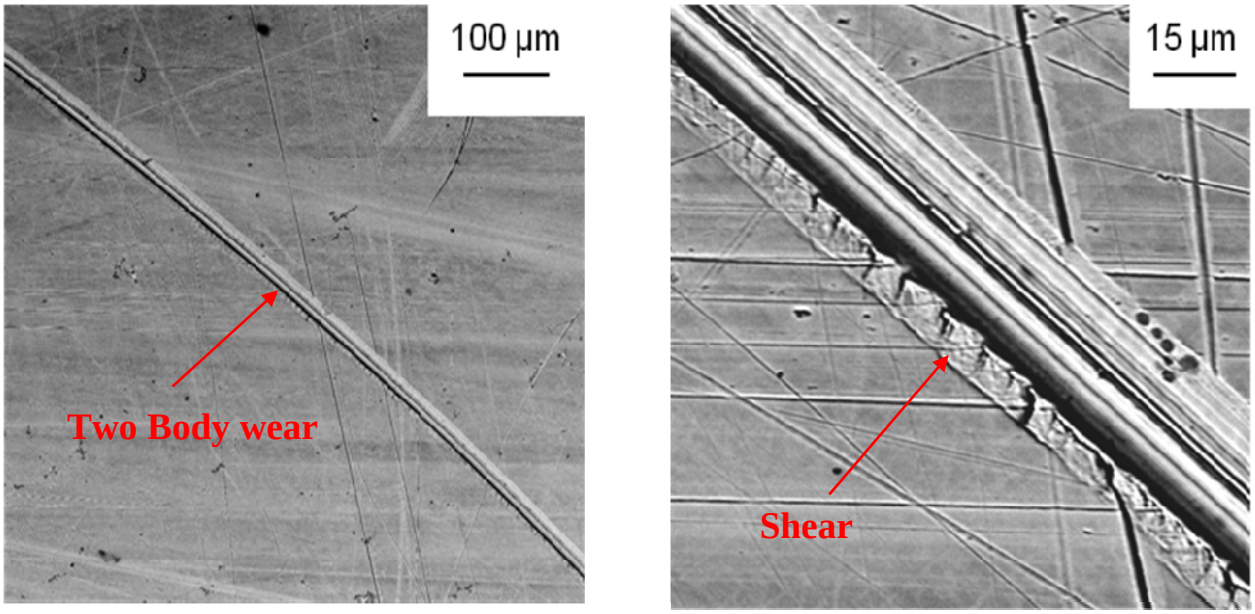

Figure 4.27: SEM images of a wear scar from WN AC 1 sample.

Figure 4.27 shows the wear tracks which result from articulation in the hip simulator. Two body wear is evident where a sharp peak or asperity has produced a deep groove in the bearing surface exposes the bare metal subsurface. On closer examination shear is evident on the edge of scratch which could represent a force coming in from the side causing fatigue and resulting in the formation of a scratch. It is important to note that these scratches represent a very small proportion of the surface exposed to the solution, indicating that a low fraction of the surface is active at any one time.

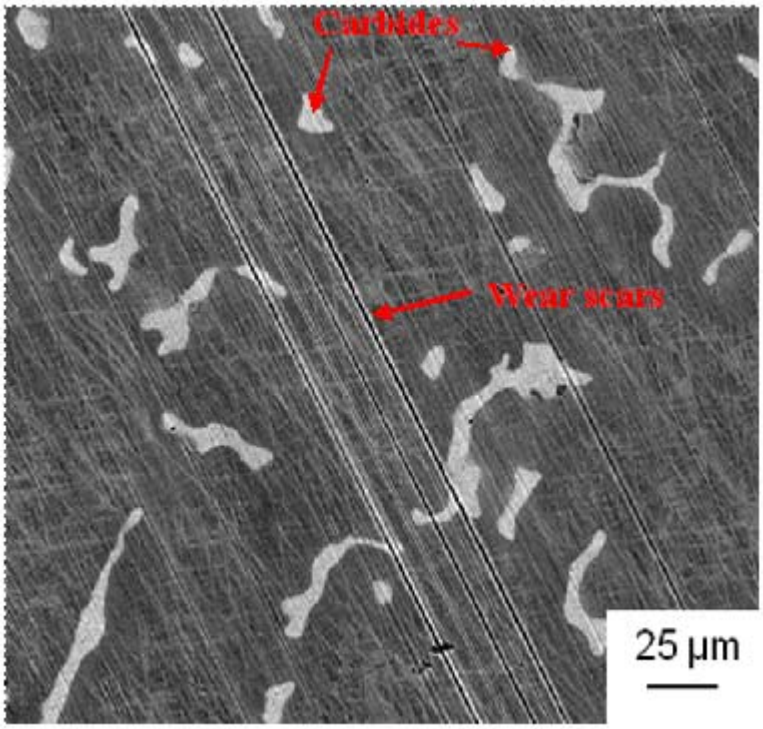

Figure 4.28: Typical SEM image of wear scars from NW AC 2.

Figure 4.28 also shows deep grooves in the surface of the sample head. This was typical for both as-cast samples. Again the grooves are the result of third body wear. Here, wear particles have made scratches into the surface of the bearing that are evident through the matrix and the more wear resistant carbides. As mentioned with Figure 4.27 these scratches represent a very small proportion of the surface exposed to the solution, which is sensitive function when looking at the corrosion susceptibility of the whole head and cup joint.

Discussion

5.1 Microstructure and composition differences of AC and DHT

It is well known in the literature that thermal treatment can affect the microstructure and composition of CoCrMo alloys [1, 17, 22, 72]. Leaving the alloy in the as-cast (AC) condition or subjecting it to "double heat-treatment" (DHT) can alter the microstructure, ultimately affecting its properties, as will be discussed in this section.

The AC material revealed a typical heterogeneous, coarse dendritic grain structure (shown in Figures 4.1a, 4.1c, 4.2a and 4.2c), which was consistent with the findings reported in the literature regarding microstructure [1, 13, 21, 73]. The microstructure also reveals large coarse carbides and shows evidence of interdendritic shrinkage porosity (Figure 4.1a). This could be detrimental in terms of an implant fracture by acting as initiation sites [74] for cracks or defects to develop under stress.

The double heat-treatment process involved a combination of solution annealing and HIPping (details shown in Table 3.2). This is performed in an attempt to remove any residual porosity from the casting process and improve homogenisation of the microstructure [1, 62, 75]. However, Figure 4.1 (b) shows that the double heat-treatment has not fully removed the porosity in the microstructure, which is expected to be removed if subjected to HIPping [1]. In both Kauser's study [1] and this study identical HIPping procedures were used. It is clear that the double heat-treatment causes dissolution of the carbides which is consistent with the literature [1, 18, 62]. It has been suggested that here, the carbon and molybdenum present in the carbides are dissolving back into the solid solution [74], which can cause the formation of small precipitates on cooling [1].

Figures 4.1b and 4.1d show that the double heat-treatment was not sufficient to fully dissolve the carbides. However the carbides were significantly reduced in size, demonstrating a significant reduction in carbide area fraction compared with Figure 4.1a and c, which is also consistent with the literature [1, 20].

5.2 Anodic polarisation curves – the difference of as-cast and double heat treated samples

The anodic reactivity of the AC and DHT samples was compared in different solutions. Both AC and DHT showed higher anodic reactivity in 28% serum (pH 8) compared with 3.5% NaCl (pH5) (Figures 4.3 and 4.4). For the measurements in serum, there was no

significant difference between the reactivity of the AC and DHT samples (Figure 4.5). However, in a more acidic solution containing serum (90% Ringers and 10% bovine serum acidified to pH 2), the DHT sample showed higher anodic reactivity (Figure 4.6).

These results for both pH 8 and pH2 solutions are consistent with those shown by Kauser [1] who used pH 7.6 Ringers solution and 90% Ringers with 10% bovine serum acidified to pH2 (the same as this study). The start potentials for the anodic reactions in both studies are of similar values for each solution and follow the same trend. This indicates some consistency that in acidified solutions the anodic polarisations occur at a less negative voltage. Kauser [1] also found that in both neutral and acidic solutions, the DHT sample was more susceptible to corrosion than the AC one, with more current flowing at the same potential. This backs up the results shown in Figure 4.6 where the DHT sample is shown to be more corrosion susceptible in the pH2 environment.

In neutral conditions, both AC and DHT samples show a higher reactivity in bovine serum than in NaCl solution (Figures 4.3 and 4.4). This could be attributed to the proteins forming complexes on the metal surface through charge transfer with the metal ions [76]. Proteins have a net charge according to their R-groups (side chains) and terminal groups all of which can be charged [1].

The results in Figure 4.6 suggest that under acidic conditions the bovine serum interacts with the metal surface of the AC and DHT alloys in a different manner than if they were at pH8 (Figure 4.5). This could be the effect of the proteins behaving differently but as no results were obtained without proteins in acidic conditions it cannot be reliably attributed as the reason why. It is widely considered that CoCrMo alloys show increased corrosion susceptibility in acidic environments as the solution is more aggressive making passivation more difficult [1, 14, 36]. It is suggested that in an acidic environment the repassivation rate of the alloy is slower than in a neutral environment. This is attributed to the formation of unstable cobalt oxide species as primary oxidation products and this hinders the formation of the chromium oxide passive film [1, 14, 77].

The role of proteins in an acidic environment is also an important factor in the corrosion susceptibility of the alloy, as the net charge mentioned can vary with pH and the environment. The pH at which the charge of the protein is zero is called the isoelectric point (pI). It is suggested that some proteins in serum are very acidic such as α-globulins (which make up approximately 30% of the protein fractions in serum, see Table 3.4) with a protein pI ranging from approximately 2-5. At pH 8 the solution is greater than the pI, meaning that the α-globulins will have a net negative charge. Alternatively, at pH2 solution is equal or less

than the pI of the α-globulins meaning that they will have a net positive charge. This could explain why the anodic polarisations at pH 2 in Figure 4.6 start at a less negative value than those done at pH 8 in Figure 4.5, which are at a more negative potential [1, 78, 79].

In acidic bovine serum DHT is more reactive than AC (Figure 4.6). This could be attributed to the molybdenum depleted regions that surround the molybdenum rich precipitates that are seen in the literature regarding DHT CoCrMo samples [1, 25]. As reported in the literature molybdenum gives good corrosion resistance [1, 3, 4, 13] and this depletion as a result of double heat treatment can leave the sample open to greater corrosive attack.

The clinical relevance of the difference seen in this experiment is that although the pH in the body is normally buffered to pH 7.4 [37, 43], during the time of an infection or inflammation a decrease to pH 4 can occur [37], which could then increase corrosion susceptibility. This may also apply to crevices in the implants [1].

5.3 Feasibility of electrochemical measurements in a Hip Simulator

5.3.1 The effect of temperature in hip simulator experiments

The measurements carried out in this project demonstrate that it is feasible to carry out electrochemical measurements in a hip simulator, as demonstrated by Yan et al., [42]. However, Yan et al., [42] did not look at the effect of temperature and this was where difficulties were encountered. The biggest problem was maintaining the temperature of the solution at both 20°C (room temperature) and 40°C. This is shown in Figures 4.13 and 4.15 where the solution is supposed to be at 20°C during the experiment but due to abrasion the temperature increases by approximately 12-16°C. As explained in Section 3.5.5 of the experimental method, prior to each test, the desired temperature was maintained for an hour prior to each experiment. However, when the solution came out of the incubator at 40°C it was immediately placed in an environment which was room temperature (20°C) and so would naturally cool over the course of the 1700 second experiment. In the case of the solution at 20°C the temperature was maintained more successfully due to the room temperature environment. However, increases were seen (shown in Figures 4.13 and 4.15), which can be attributed to the hot oil pumping around the machine to power articulation and the frictional heat resulting from articulation itself. The increase that resulted from this was

very minimal due to the short periods of abrasion but should be taken into account for the increase in temperature that can come from prolonged periods of articulation.

The results in section 4.3.2 regarding the difference in temperature show no major difference between 40°C and 20°C (room temperature). However, for the AC sample, in 3.5% NaCl there appeared to be a slightly higher OCP during repassivation at 20°C than at 40°C; this was less obvious in 28% bovine serum. Given the significant scatter observed, the data is not sufficiently robust to provide the basis for a detailed interpretation.

However contrary to what was found here, it is suggested in the literature that increased temperature can result in increased corrosion susceptibility of an alloy [80-82]. For example it is well known that at higher temperatures, chemical reactions can occur at an accelerated rate [83]. This means that the active dissolution processes would speed up as a result of temperature increase, which would speed up the loss of electrons. With body temperature being at 37°C, this could suggest that chemical reactions and diffusion processes could occur at a faster rate than if they were at room temperature and so could affect the OCP of the alloy. There is evidence that exists that a nickel based alloy, 690, shows a narrowing of its passive region as temperature exist from 20°C to 80°C in 5M NaCl [82]. This may imply that elevated temperatures affect the anodic reaction and this is what causes passivation of a metal surface. However, the effect of temperature on the corrosion potential of alloys in hip simulator experiments is not well developed. It is important to test the temperature value of 37°C in the laboratory so as to be as physiologically relevant as possible [38]. It was achieved in the anodic polarisation experiments where the parameters were easier to control and in some cases contrasting results were seen to the hip simulator results. Although various other variables listed in the method and appendix could also cause the inconsistency shown in Section 4.3.2, the results highlight the importance of at least monitoring temperature during tests. Ideally temperature regulation needs to be incorporated into the experiment and the use of a peristaltic pump as one of the possibilities. This would keep the solution at a constant temperature throughout experiments and would at least eliminate the possibility of it being a variable that could affect potential. Critically though, the results do not show that temperature has a consistent affect on the corrosion susceptibility in a hip simulator.

5.3.2 Hip Simulator results measuring OCP using new AC and DHT samples

5.3.2.1 Alternating cycles of stabilisation and abrasion

The experiments comparing AC and DHT samples with alternating periods of stabilisation and abrasion show a high amount of scatter with no convincing difference between the two heat-treatments (Section 4.4.1). As a general observation AC runs 1-8 are less negative than DHT runs 1-8. When looking at these results of brand new polished surfaces in comparison with the worn in parts in Section 4.3.2 very little consistency is seen between the OCPs of each sample. For every joint sample there are different articulating surfaces, which result in different areas of bare metal becoming exposed (shown in Figures 4.27 and 4.28). Each sample will give off different OCPs as a result of its bare metal surface that can vary from sample to sample.

As mentioned, literature exists attributing clinical failures and retrieval operations to the double heat-treating of the alloy [48]. Other literature suggests that DHT bearings have higher wear rates in comparison with AC bearings [20, 21]. However, little difference is shown in Figure 4.16, where very little difference is shown between AC run 8 and DHT run 8 suggesting that testing needs to take place over a much longer period. The reliability of this small difference in OCP also has to be questioned due to the scatter that occurs in runs 1-7 for both AC and DHT (Figures 4.12 and 4.14) prior to it. An explanation for there being no definite difference between AC and DHT over an 8 run period is that a general criticism of hip simulation testing is that there is a lack of severe testing in hip simulators and this leads to clinical failures not being picked up [17]. The ‘severe’ wear that is experienced in-vivo and then attempted to be replicated in hip simulators is still not fully understood [62]**.** It is thought that in-vivo a hip joint experiences higher and more variable wear as opposed to in a hip simulator [42]. Bowsher et al., [17] has criticised hip simulators for not being able to pick up clinical failures due to the lack ‘severe’ testing. To create ‘severe’ testing it is thought that a combination of microseperation and intermittent loading should be used, which results in higher metal-on-metal wear [62, 84]. Rieker et al., [71] also suggests that in-vivo running in can take a year to achieve, meaning much more test periods would be needed. Due to the short term constraints of the project and the relatively new concept of corrosion testing in a hip simulator a ‘severe’ testing regime was unable to take place. From this we can draw that it is not possible to make assumptions about the differences of running-in periods between AC and DHT samples from the results in Figures 4.12 and 4.14 due to the large amount of scatter shown.

5.3.2.2 Measuring the OCP over a 2.5 hour period

The results shown in Figure 4.19 are consistent with a study done by Yan et al., [42] whereby there is an initial stabilisation period in a static environment followed by a rapid shift in potential towards the active region. All four tests in Figure 4.19 show that when the abrasion period is over the OCP cannot recover to its starting value (what it was at 3000 seconds) until the test is stopped. This could indicate that the sample surface had been changed by tribological contact, which would then result in different corrosion properties. Alternatively, it could be that more than 3000 seconds is needed for the potential to repassivate to the start potential as the potential value is still moving in a more positive direction when the experiment is stopped. This is similar to what is seen by Yan et al., [30] whereby the rate at which the potential shifts in the active direction represents the rate and degree of damage to the passive film [30]. Based on the results shown in Figure 4.19, this would suggest that in run 1 the AC sample shifts to a more negative potential at a greater rate than the DHT sample in run 1 due to greater damage to the passive film. However, the damage to the passive film is only in the form of wear scars (examples shown in Section 4.7). The area exposed is in the scratches themselves and this represents a low fraction of the surface area of the bearing. It is important to take this into account, as the scratch itself may not give an accurate representation of the corrosion susceptibility once the passive film has been removed. The scratches may vary in depth and width or may be exposed to greater amounts of 3rd body wear between samples and experiments.

In the most relevant study done so far to date, Yan et al., [42] concluded that the ion release rate increases as the swing phase load increases. At higher loads more CoCr ions are released into the solution and this is consistent with the increased severity of metal-on-metal contact. This suggests that during the 3000 second abrasion period shown in Figure 4.19 the ion release rate is increasing, as the load and articulation has increased. As the AC sample appears to have experienced more damage to its passive film than the DHT sample, due to its more negative corrosion potential (Figure 4.19). This could suggest that the AC sample gives greater ion release in comparison with DHT sample due to the greater damage to the protective oxide film from the AC sample in this experiment. However, no measurements of ion release rate were able to be undertaken and this would need to be explored further for any definite conclusions to be drawn.

Another interesting aspect of the graph to consider is the gradient of the OCP during the 3000 second abrasion period. There is variation whereby two of them remain fairly flat whereas the other two runs show a gradual increase in OCP. Different gradients during abrasion were also seen by Yan et al., [42] who attributed this to the variation of a potential build up of a tribo-reaction layer, which could then affect the tribological interface and then ultimately the ion release

rate. This suggestion could help explain these gradients and is possibility another sensitive function of these tests, which give variable results.

When comparing these results with the worn-in samples (Figures 4.8-11) they too show differing start potentials which were attributed to sample to sample variability. Unlike the worn-in samples the variation seen in the start potentials cannot be attributed to previous experiments altering the surface properties of the alloy. However it could be argued that when comparing these two tests the stabilisation period for the alternating abrasion experiment was only 500 seconds, whereas the stabilisation period for the single abrasion experiment was 3000 seconds. If the alternating abrasion experiment had a 3000 second stabilisation period the potential may have levelled out to a similar value seen in the single abrasion experiment. However, based on the 3000 second stabilisation period seen in the single abrasion experiment, the OCP of the sample did not change enough to assume that this could be the reason for the difference in stabilisation potentials. A longer stabilisation period, greater than 3000 seconds could be required to obtain matching stabilisation potentials or it could be that sample to sample variation accounts for these differences in OCP.

The close up examination of the OCP in Figures 4.20-3 does show a general pattern of a backward and forward motion of the head in the cup. The pattern is roughly every 2 seconds, which is approximately the time taken for the head to do one forward and then backward motion at a speed of 0.5 Hz, however it should be noted that this pattern is not clearly defined. A reason for this could be the varying amounts of solution being washed in and out of the joint by the articulation of the head, which could then distort the signal being picked up by the reference electrode. It is also interesting to note that at the start of abrasion for each test a consistent pattern is not shown when articulation begins. Particularly, Figure 4.23 does not show any difference in the OCP when articulation starts. This suggests that not all changes in OCP as a result of articulation can be seen. At this moment, this is a relatively new test setup and so it may be that subtle changes in OCP are not picked up in the solution.

Yan et al., [42] did a comparable experiment closely examining the OCP in conjunction with the movement arm of the hip simulator. They used a speed of 1 Hz which gave a distinct pattern showing the backward and forward motion corresponding to a sharp dip and then a sharp increase in OCP. This shape was seen every second and so corresponds with the speed of the movement arm at 1 Hz.

5.3.3 Obtaining preliminary potentiostatic measurements using a hip simulator

The results in Figure 4.24 show that when a load and an angle of abrasion are applied to the two surfaces the current increases. The greater the angle of movement the greater amount of current is released by the joint. This can be attributed to the removal of the oxide film, exposing the bare metal surface, similar to what has been seen in the previous experiments measuring potential. This has also been seen in a study by Kauser [1] who performed scratch tests where a rapid increase in current was attributed to the exposure of the bare metal surface. The current also began to decay due to the reformation of the oxide film, which was also seen in Figure 4.24 when articulation was stopped. Currently, this is a relatively new experiment and as of yet no other studies have measured the current flowing from a metal-on-metal hip resurfacing joint in a hip simulator.

However, studies have looked at the current flowing using a ball-on-plate reciprocating tribo tester [13]. They found that the current increased in line with an increase in velocity of movement and that current then decreased with decreasing velocity. Similarly, with the results shown in Figure 4.24, the current increases with an increasing angle of movement and when the movement ceases the current decreases again. This indicates that once abrasion has stopped repassivation takes place after the passive film has been rubbed off during the articulation.

A comparison of AC and DHT samples was unable to be looked at in this preliminary experiment due to the constraints of the project. However, Kauser [1] looked at the current released for AC and DHT disc samples using scratch tests and concluded that once the maximum current had been reached the current decays were very similar, regardless of the electrolyte used.

5.3.4 The problem of variability within hip simulator experiments

The temperature and alternating cycles of abrasion experiments already discussed in this section (5.3.1) showed a lot of variability, meaning a reliable conclusion could not be drawn from the results. A hip simulator experiment measuring corrosion is a very complex one with many variables already outlined in section 3.4 of the experimental method. During the setup of each experiment care was taken to make sure that all of the variables for each experiment were uniform for each test.

A big source of variability which was difficult to control was the change in temperature during experiments (covered in section 5.3.1). A small source of variability may

arise from the movement of solution in the bag during articulation. The amount of solution in contact with the head and cup during each back and forth movement may give different readings to the reference electrode. However, this effect should be considered marginal as the same amount of solution was used for each experiment and the same type of articulation was used for each run in the experiment.

The biggest source of variability could be the extent of damage suffered to the sample head during articulation. Section 4.7 shows examples of the wear scars that result from the metal-on-metal articulation. The wear scars are the active part of the metal, which results in the potential fluctuations. However, these wear scars are only a very low fraction of the surface area of the joint. The vast majority of the surface area of the head does not have these deep scratches and so the surface would be less susceptible to corrosion.

Another source of variability and a concern with hip simulators in general is the head and cups are not in the appropriate anatomical position. Any wear debris or third body particles may stay imbedded in the joint whereas in the body the particles may fall out with time and be less of a problem. When third body wear takes place it can cause deep grooves in the implant surface such as the ones shown in Figures 4.27-8. This obviously exposes bare metal and can accelerate corrosion. It is possible to get the head and cup in the correct anatomical position in hip simulator experiments as demonstrated in a previous study [42].

5.4 The difference in solution using a Hip Simulator

There is a significant difference between the corrosion susceptibility of the same CoCrMo alloy when tested in 3.5% NaCl and 28% bovine serum. Figure 4.7 shows that when the joint experiences abrasive wear from the rubbing of the two articulating surfaces the potential decreases, making the joint more susceptible to corrosion. There is a distinct and consistent difference between the open circuit potentials of the two solutions with the measurements in NaCl giving more negative drops in potential than those in the serum. This could be because the proteins in the bovine serum adsorb to the bearings surfaces, creating ‘solid like’ films which rub together, protecting the surfaces from adhesion and abrasion and act as a transient lubricant [40-42]. This means the potential will not become as negative compared to the salt solution, which is free from biological species. Yan et al., [42] suggests that these ‘solid like’ films give a greater contribution to load support due to a greater viscosity than NaCl solution. It is also suggested that the more viscous serum solution has a lower ion release rate than the NaCl solution [42]. This could explain why the 3.5% NaCl solution has a more negative

potential then the 28% bovine serum solution. The protein concentration in bovine serum that can form this lubricating layer may be why not much of a difference was seen in the temperature experiments looking at bovine serum at 20°C and 40°C (Figures 4.8 and 4.10) as it may have buffered the effect that temperature can cause.

In contrast to this difference seen in solution, the anodic polarisation curves conducted with the same samples show the opposite, with calf serum being slightly more negative for both AC and DHT samples. This can be explained by the fact that there is no articulation in these experiments and highlights the effect that abrasive wear can have on the potential. The results suggest that when the passive film is worn away the NaCl has a more corrosive solution than the bovine serum, whereas when an experiment is performed with no abrasion to the surface there is less of a difference seen in the solutions with the serum being slightly more corrosive.

5.5 The clinical implications of this study

Throughout this study there has not been a consistent trend where one heat treatment has been superior to the other. Often AC has shown to have better corrosion resistance (Figures 4.3, 4.4, 4.6, 4.12 and 4.14), although DHT has shown to be superior in the experiment of longest duration (Figure 4.19). Alternatively no real difference between the heat treatments has been observed (Figure 4.5 and 4.8-11). From these results it cannot be said with any confidence that one heat treatment should be used over another for hip resurfacing joints.

Again, it cannot be said with any confidence that temperature affects the corrosion susceptibility of an alloy in a hip simulator. However, to be as clinically relevant as possible these types of experiments need to be developed so they can be conducted and maintained at 37°C.

The development of taking potentiostatic measurements in a hip simulator is more clinically relevant than doing static tests. Measuring the current that flows while the head and cup are articulating in a hip simulator makes it possible to see the fluctuations in current as a result of this movement which is more specific to what would happen in the body. If the sources of variability in the experiments carried out here can be overcome, it is a promising way to evaluate the corrosion suscepbility of hip prostheses.

6. Conclusions

The effect of heat treatment on the microstructure of CoCrMo alloys causes the matrix to become more homogenised with the carbides dissolving into the matrix. The carbides that remain after heat treatment are significantly reduced in size. Carbides are also richer in chromium and molybdenum compared with the matrix.

The change in microstructure between the two heat-treatments did not show any consistent differences in wear and corrosion behaviour.

After conducting anodic polarisation curves in a range of different environments the only consistent difference was seen in ringers and bovine serum solution acidified to pH2. Here double heat-treated was shown to be more susceptible to corrosion than the as-cast sample.

It is feasible to take both OCP and potentiostatic measurements using a hip simulator. However, in this study the sample to sample variation made it difficult to obtain consistent results regarding the effect of heat-treatment.

3.5% NaCl was consistently a more corrosive environment than 28% bovine serum for an as-cast worn-in part following experimentation in a hip simulator.

7. Future Work

- To further develop and devise a protocol for getting a consistent OCP and potentiostatic measurements in the hip simulator.
- Attempt a test setup that gets the head and cup in the anatomical position as in other studies.
- Introduce temperature regulation of the solution during hip simulator experiments.
- Under acidic conditions, conduct tests in solutions without proteins to be able to compare results of 90% Ringers solution with 10% bovine serum acidified to pH2. This would allow for investigation of the effect of proteins in corrosion tests.
- Increase the duration of the hip simulator tests to further investigate the difference between as-cast and double heat-treated samples.
- Undertake measurements of ion release rate into the solution after hip simulator tests. This could be another way of identifying any differences between as-cast and double heat-treated samples and could be related to any differences seen in corrosion potential.
- Measure pH2 acidic solutions in the hip simulator to compare with potentiodynamic anodic polarisation curves that saw a difference between AC and DHT with an acidic solution.

8. References

1. Kauser, F., *Corrosion of CoCrMo alloys for biomedical applications*, in *Department of Metallurgy and Materials, School of Engineering*. 2007, Univeristy of Birmingham: Birmingham. p. 4-285.
2. NHS, *Hip Replacements: Getting it right first time*, C.a.A. General, Editor. 2000, National Audit Office: London. p. 11-31.
3. McMinn, D. and J. Daniel, *History and modern concepts in surface replacement.* Proceedings of the Institution of Mechanical Engineers Part H-Journal of Engineering in Medicine, 2006. **220**(H2): p. 239-251.
4. McMinn, D.a.T., R., *Birmingham Hip Resurfacing (BHR) history, development and clinical results.* 2000, Midland Medical Technologies, Birmingham.
5. Sinnett-Jones, P.E., J.A. Wharton, and R.J.K. Wood, *Micro-abrasion-corrosion of a CoCrMo alloy in simulated artificial hip joint environments.* Wear, 2005. **259**: p. 898-909.
6. http://www.stanthonys.org.uk/Specialised_procedures/hip_resurfacing.html. 2009 [cited.
7. Resurfacing, B.H., *Hip Resurfacing Today: history, development and clinical results.* 2000.
8. Savarino, L., D. Granchi, G. Ciapetti, E. Cenni, M. Greco, R. Rotini, C.A. Veronesi, N. Baldini, and A. Giunti, *Ion release in stable hip arthroplasties using metal-on-metal articulating surfaces: A comparison between short-and medium-term results.* Journal Of Biomedical Materials Research Part A, 2003. **66A**(3): p. 450-456.
9. Yan, Y., A. Neville, and D. Dowson, *Biotribocorrosion - an appraisal of the time dependence of wear and corrosion interactions: II. Surface analysis.* Journal of Physics D-Applied Physics, 2006. **39**(15): p. 3206-3212.
10. Brooks, C.R., *Heat treatment, structure, and properties of nonferrous alloys.*, in *Metals park*. 1982: Ohio American Society for Metals. p. 229.
11. Crook, P., *Metals handbook. Nonferrous alloys and special-purpose materials*. 1990, Ohio American Society for Metals: ASM International: Materials Park. 447.
12. Codaro, E.N., P. Melnikov, I. Ramires, and A.C. Guastaldi, *Corrosion behavior of a cobalt-chromium-molybdenum alloy.* Russian Journal of Electrochemistry, 2000. **36**(10): p. 1117-1121.
13. Yan, Y., A. Neville, and D. Dowson, *Tribo-corrosion properties of cobalt-based medical implant alloys in simulated biological environments.* Wear, 2007. **263**: p. 1105-1111.
14. Contu, F., B. Elsener, and H. Bohni, *Electrochemical behavior of CoCrMo alloy in the active state in acidic and alkaline buffered solutions.* Journal Of The Electrochemical Society, 2003. **150**(9): p. B419-B424.
15. Sun, D., J.A. Wharton, R.J.K. Wood, L. Ma, and W.M. Rainforth. *Microabrasion-corrosion of cast CoCrMo alloy in simulated body fluids*. in *34th Leeds-Lyon Symposium on Tribology*. 2007. Lyon, FRANCE: Elsevier Sci Ltd.
16. Varma A., B.L., and Mukasyan A., *Advantages of Engineering Materials*. 2002. (7).
17. Bowsher, J.G., J. Nevelos, P.A. Williams, and J.C. Shelton, *'Severe' wear challenge to 'as-cast' and 'double heat-treated' large-diameter metal-on-metal hip bearings.* Proceedings of the Institution of Mechanical Engineers Part H-Journal of Engineering in Medicine, 2006. **220**(H2): p. 135-143.

18. Kinbrum, A. and A. Unsworth, *The wear of high-carbon metal-on-metal bearings after different heat treatments.* Proceedings of the Institution of Mechanical Engineers Part H-Journal of Engineering in Medicine, 2008. **222**(H6): p. 887-895.
19. Berry, G., J.D. Bolton, J.B. Brown, and S. McQuaide, *The production and properties of wrought high carbon Co-Cr-Mo alloys.* Cobalt-Base Alloys for Biomedical Applications, 1999. **1365**: p. 11-31.
20. Cawley, J., J.E.P. Metcalf, A.H. Jones, T.J. Band, and D.S. Skupien. *A tribological study of cobalt chromium molybdenum alloys used in metal-on-metal resurfacing hip arthroplasty*. in *14th International Conference on Wear of Materials*. 2003. Washington, D.C.: Elsevier Science Sa.
21. Wang, K.K., A. Wang, and L.J. Gustavson, *Metal-on-metal wear testing of Co-Cr alloys.* Cobalt-Base Alloys for Biomedical Applications, 1999. **1365**: p. 135-144.
22. Georgette, F.S. and J.A. Davidson, *The Effect Of Hiping On The Fatigue And Tensile-Strength Of A Cast, Porous-Coated Co-Cr-Mo Alloy.* Journal Of Biomedical Materials Research, 1986. **20**(8): p. 1229-1248.
23. McMinn, D., *Development of metal-on-metal hip resurfacing.* Hip International, 2003. **13**: p. S41-S53.
24. Hodgson, A.W.E., S. Kurz, S. Virtanen, V. Fervel, C.O.A. Olsson, and S. Mischler, *Passive and transpassive behaviour of CoCrMo in simulated biological solutions.* Electrochimica Acta, 2004. **49**(13): p. 2167-2178.
25. Gilbert, J.L., C.A. Buckley, and J.J. Jacobs, *IN-VIVO CORROSION OF MODULAR HIP-PROSTHESIS COMPONENTS IN MIXED AND SIMILAR METAL COMBINATIONS - THE EFFECT OF CREVICE, STRESS, MOTION, AND ALLOY COUPLING.* Journal of Biomedical Materials Research, 1993. **27**(12): p. 1533-1544.
26. Placko, H.E., S.A. Brown, and J.H. Payer, *Effects of microstructure on the corrosion behavior of CoCr porous coatings on orthopedic implants.* Journal of Biomedical Materials Research, 1998. **39**(2): p. 292-299.
27. Wang, K.K., R.M. Berlin, and L.J. Gustavson, *A dispersion strengthened Co-Cr-Mo alloy for medical implants.* Cobalt-Base Alloys for Biomedical Applications, 1999. **1365**: p. 89-97.
28. Mischler, S. *Triboelectrochemical techniques and interpretation methods in tribocorrosion: A comparative evaluation.* in *1st International Conference on Tribo-Conference*. 2006. Hyderabad, INDIA: Elsevier Sci Ltd.
29. Maffiotte, C., M. Navas, M.L. Castano, and A.M. Lancha. *XPS characterization of oxide films formed in cobalt-based alloys during corrosion tests at high temperature*. in *8th European Conference on Applications of Surface and Interface Analysis*. 1999. Seville, Spain: John Wiley & Sons Ltd.
30. Yan, Y., A. Neville, and D. Blowson, *Biotribocorrosion of CoCrMo orthopaedic implant materials - Assessing the formation and effectof the biofilm.* Tribology International, 2007. **40**(10-12): p. 1492-1499.
31. Khan, M., J.H. Kuiper, and J.B. Richardson, *Can cobalt levels estimate in-vivo wear of metal-on-metal bearings used in hip arthroplasty?* Proceedings Of The Institution Of Mechanical Engineers Part H-Journal Of Engineering In Medicine, 2007. **221**(H8): p. 929-942.
32. Geringer, J., B. Forest, and P. Combrade, *Fretting-corrosion of materials used as orthopaedic implants.* Wear, 2005. **259**: p. 943-951.
33. Hallab, N.J., C. Messina, A. Skipor, and J.J. Jacobs, *Differences in the fretting corrosion of metal-metal and ceramic-metal modular junctions of total hip replacements.* Journal of Orthopaedic Research, 2004. **22**(2): p. 250-259.

34. Yan, Y., A. Neville, and D. Dowson, *Understanding the role of corrosion in the degradation of metal-on-metal implants.* Proceedings of the Institution of Mechanical Engineers Part H-Journal of Engineering in Medicine, 2006. **220**(H2): p. 173-181.
35. Metikos-Hukovic, M. and R. Babic, *Passivation and corrosion behaviours of cobalt and cobalt-chromium-molybdenum alloy.* Corrosion Science, 2007. **49**(9): p. 3570-3579.
36. Lewis, A.C., M.R. Kilburn, I. Papageorgiou, G.C. Allen, and C.P. Case, *Effect of synovial fluid, phosphate-buffered saline solution, and water on the dissolution and corrosion properties of CoCrMo alloys as used in orthopedic implants.* Journal Of Biomedical Materials Research Part A, 2005. **73A**(4): p. 456-467.
37. Sun, D., Wharton, J.A. and Wood, R.J.W., *The effects of proteins and pH on tribo-corrosion performance of cast CoCrMo: a combined electrochemical and tribological study.* Tribology - Materials, Surfaces & Interfaces, 2008. **2**((3)): p. 150-160.
38. Bundy, K.J., *CORROSION AND OTHER ELECTROCHEMICAL ASPECTS OF BIOMATERIALS.* Critical Reviews in Biomedical Engineering, 1994. **22**(3-4): p. 139-251.
39. Hallab, N.J., A. Skipor, and J.J. Jacobs, *Interfacial kinetics of titanium- and cobalt-based implant alloys in human serum: Metal release and biofilm formation.* Journal Of Biomedical Materials Research Part A, 2003. **65A**(3): p. 311-318.
40. Scholes, S.C. and A. Unsworth, *The effects of proteins on the friction and lubrication of artificial joints.* Proceedings of the Institution of Mechanical Engineers Part H-Journal of Engineering in Medicine, 2006. **220**(H6): p. 687-693.
41. Wimmer, M.A., C. Sprecher, R. Hauert, G. Tager, and A. Fischer. *Tribochemical reaction on metal-on-metal hip joint bearings - A comparison between in-vitro and in-vivo results.* in *14th International Conference on Wear of Materials*. 2003. Washington, D.C.: Elsevier Science Sa.
42. Yan, Y., A. Neville, D. Dowson, S. Williams, and J. Fisher, *The influence of swing phase load on the electrochemical response, friction, and ion release of metal-on-metal hip prostheses in a friction simulator.* Proceedings Of The Institution Of Mechanical Engineers Part J-Journal Of Engineering Tribology, 2009. **223**(J3): p. 303-309.
43. Sargeant, A. and T. Goswami, *Hip implants - Paper VI - Ion concentrations.* Materials & Design, 2007. **28**(1): p. 155-171.
44. Mabilleau, G., Y.M. Kwon, H. Pandit, D.W. Murray, and A. Sabokbar, *Metal-on-metal hip resurfacing arthroplasty A review of periprosthetic biological reactions.* Acta Orthopaedica, 2008. **79**(6): p. 734-747.
45. Pandit, H., S. Glyn-Jones, P. McLardy-Smith, R. Gundle, D. Whitwell, C.L.M. Gibbons, S. Ostlere, N. Athanasou, H.S. Gill, and D.W. Murray, *Pseudotumours associated with metal-onmetal hip resurfacings.* Journal Of Bone And Joint Surgery-British Volume, 2008. **90B**(7): p. 847-851.
46. Amstutz, H.C., P. Campbell, H. McKellop, T.P. Schmalzried, W.J. Gillespie, D. Howie, J. Jacobs, J. Medley, and K. Merritt, *Metal on metal total hip replacement workshop consensus document.* Clinical Orthopaedics And Related Research, 1996(329): p. S297-S303.
47. Morlock, M.M., N. Bishop, F. Stahmer, J. Zustin, S. Breer, G. Sauter, M. Hahn, M. Krause, W. Ruther, and M. Amling, *Reasons for failure of hip resurfacing implants. A failure analysis based on 250 revision specimens.* Orthopade, 2008. **37**(7): p. 695-+.
48. Eisner, W., *Corin CEO Paling Responds to OTW FDA Panel Story, Fires Salvo at Smith and Nephew*, in *Orthopedics, This Week*. 2007. p. 10-14.

49. Cobb, A.G. and T.P. Schmalzreid, *The clinical significance of metal ion release from cobalt-chromium metal-on-metal hip joint arthroplasty.* Proceedings Of The Institution Of Mechanical Engineers Part H-Journal Of Engineering In Medicine, 2006. **220**(H2): p. 385-398.
50. Benson, M.K.D., P.G. Goodwin, and J. Brostoff, *METAL SENSITIVITY IN PATIENTS WITH JOINT REPLACEMENT ARTHROPLASTIES.* British Medical Journal, 1975. **4**(5993): p. 374-375.
51. Campbell, P., A. Shimmin, L. Walter, and M. Solomon, *Metal Sensitivity as a Cause of Groin Pain in Metal-on-Metal Hip Resurfacing.* Journal of Arthroplasty, 2008. **23**(7): p. 1080-1085.
52. Toms, A.P., T.J. Marshall, J. Cahir, C. Darrah, J. Nolan, S.T. Donell, T. Barker, and J.K. Tucker, *MRI of early symptomatic metal-on-metal total hip arthroplasty: a retrospective review of radiological findings in 20 hips.* Clinical Radiology, 2008. **63**(1): p. 49-58.
53. Kwon, Y.M., Z. Xia, S. Glyn-Jones, D. Beard, H.S. Gill, and D.W. Murray, *Dose-dependent cytotoxicity of clinically relevant cobalt nanoparticles and ions on macrophages in vitro.* Biomedical Materials, 2009. **4**(2).
54. Boardman, D.R., F.R. Middleton, and T.G. Kavanagh, *A benign psoas mass following metal-on-metal resurfacing of the hip.* Journal of Bone and Joint Surgery-British Volume, 2006. **88B**(3): p. 402-404.
55. Clayton, R.A.E., I. Beggs, D.M. Salter, M.H. Grant, J.T. Patton, and D.E. Porter, *Inflammatory pseudotumor associated with femoral nerve palsy following metal-on-metal resurfacing of the hip.* Journal of Bone and Joint Surgery-American Volume, 2008. **90A**(9): p. 1988-1993.
56. Jeanrot, C., M. Ouaknine, P. Anract, M. Forest, and B. Tomeno, *Massive pelvic and femoral pseudotumoral osteolysis secondary to an uncemented total hip arthroplasty.* International Orthopaedics, 1999. **23**(1): p. 37-40.
57. Malviya, A. and J.P. Holland, *Pseudotumours associated with metal-on-metal hip resurfacing: 10-year Newcastle experience.* Acta Orthopaedica Belgica, 2009. **751**(4): p. 477-483.
58. Wang, A., J.D. Bobyn, S. Yue, J.B. Medley, and F.W. Chan, *Residual abrasive material from surface grinding of metal-metal hip implants: A source of third-body wear?* Cobalt-Base Alloys for Biomedical Applications, 1999. **1365**: p. 125-134.
59. Yan, Y., A. Neville, D. Dowson, and S. Williams. *Tribocorrosion in implants - assessing high carbon and low carbon Co-Cr-Mo alloys by in situ electrochemical measurements*. in *32nd Leeds-Lyon Symposium on Tribiology*. 2006. Lyon, FRANCE: Elsevier Sci Ltd.
60. Contu, F., B. Elsener, and H. Bohni, *Corrosion behaviour of CoCrMo implant alloy during fretting in bovine serum.* Corrosion Science, 2005. **47**(8): p. 1863-1875.
61. Vassitiou, K., A.P.D. Elfick, S.C. Scholes, and A. Unsworth, *The effect of 'running-in' on the tribology and surface morphology of metal-on-metal Birmingham hip resurfacing device in simulator studies.* Proceedings of the Institution of Mechanical Engineers Part H-Journal of Engineering in Medicine, 2006. **220**(H2): p. 269-277.
62. Bowsher, J.G., A. Hussain, P.A. Williams, and J.C. Shelton, *Metal-on-metal hip simulator study of increased wear particle surface area due to 'severe' patient activity.* Proceedings of the Institution of Mechanical Engineers Part H-Journal of Engineering in Medicine, 2006. **220**(H2): p. 279-287.
63. Rieker, C.B., R. Schon, R. Konrad, G. Liebentritt, P. Gnepf, M. Shen, P. Roberts, and P. Grigoris, *Influence of the clearance on in-vitro tribology of large diameter metal-*

on-metal articulations pertaining to resurfacing hip implants. Orthopedic Clinics of North America, 2005. **36**(2): p. 135-+.
64. Park, S.H., H. McKellop, B. Lu, F. Chan, and R. Chiesa, *Wear morphology of metal-metal implants: Hip simulator tests compared with clinical retrievals.* Alternative Bearing Surfaces in Total Joint Replacement, 1998. **1346**: p. 129-143.
65. Scholes, S.C., S.M. Green, and A. Unsworth, *The wear of metal-on-metal total hip prostheses measured in a hip simulator.* Proceedings of the Institution of Mechanical Engineers Part H-Journal of Engineering in Medicine, 2001. **215**(H6): p. 523-530.
66. Smith, S.L., D. Dowson, and A.A.J. Goldsmith, *The effect of femoral head diameter upon lubrication and wear of metal-on-metal total hip replacements.* Proceedings of the Institution of Mechanical Engineers Part H-Journal of Engineering in Medicine, 2001. **215**(H2): p. 161-170.
67. Nevelos, J., Shelton, J., Fisher, J., *Metallurgical considerations in the wear of metal-on-metal hip bearings.* Hip International, 2004. **14**: p. 1-10.
68. 14242-1, I.S.I., *Implants for surgery- Wear of total hip-joint prostheses- Part 1: Loading and displacement parameters for wear-testing machines and corresponding environmental conditions for test*. 2002.
69. ISO, *Implants for surgery - Wear of total hip-joint prostheses- Part: Loading and displacement parameters for wear-testing machines and corresponding environmental conditions for test*, ISO, Editor. 2002: Switzerland. p. 1-8.
70. Essner, A., G. Schmidig, and A. Wang, *The clinical relevance of hip joint simulator testing: In vitro and in vivo comparisons.* Wear, 2005. **259**: p. 882-886.
71. Rieker, C.B., R. Schon, and P. Kottig. *Development and validation of a second-generation metal-on-metal bearing - Laboratory studies and analysis of retrievals*. in *2nd International Conference on Metal-On-Metal Hip Prostheses - Past Performance and Future Directions*. 2003. Montreal, CANADA: Churchill Livingstone Inc Medical Publishers.
72. Mancha, H., E. Carranza, J.I. Escalante, G. Mendoza, M. Mendez, F. Cepeda, and E. Valdes, *M23C6 carbide dissolution mechanisms during heat treatment of ASTM f-75 implant alloys.* Metallurgical and Materials Transactions a-Physical Metallurgy and Materials Science, 2001. **32**(4): p. 979-984.
73. Mancha, H., F. Cepeda, M. Castro, M. Mendez, and J. Mendez, *Effect of casting parameters on the microstructure of ASTM F-75 alloy.* Light Metals 1996, 1996: p. 1095-1101.
74. Sullivan, C.P., J.D. Varin, and M.J. Danachie, *RELATIONSHIP OF PROPERTIES TO MICROSTRUCTURE IN COBALT-BASE SUPERALLOYS.* Metals Engineering Quarterly, 1969. **9**(2): p. 16-&.
75. Berlin, R.M., L.J. Gustavson, and K.K. Wang, *Influence of post processing on the mechanical properties of investment cast and wrought Co-Cr-Mo alloys.* Cobalt-Base Alloys for Biomedical Applications, 1999. **1365**: p. 62-70.
76. Payer, J.H., K. Merrit, S.K. Chawla, and S. A. Brown. Biological Interactions in localised Corrosion Phenomena of Orthopaedic Implants. in Advances in Localised Corrosion. 1987. Orlando, Florida NACE., *Biological Interactions in localised Corrosion Phenomena of Orthopaedic Implants.* Advances in Localised Corrosion, 1987.
77. Goldberg, J.R., C.A. Buckley, J.J. Jacobs, and J.L. Gilbert, *Corrosion testing of modular hip implants.* Modularity of Orthopedic Implants, 1997. **1301**: p. 157-176.
78. Putnam, F.W., *The plasma proteins.* 1975.
79. Devlin, T.M., *Textbook of biochemistry with clinical correlations*. Fourth Edition ed. 1997: New York: Wiley and Sons Ltd.24.

80. Bayoumi, F.M., *Kinetics of high temperature corrosion of a low Cr-Mo steel in aqueous NaCl Solution.* Materials And Corrosion-Werkstoffe Und Korrosion, 2007. **58**(6): p. 422-426.
81. El Aal, E.E.A., S.A. El Wanees, A. Diab, and S.M.A. El Haleem, *Environmental factors affecting the corrosion behavior of reinforcing steel III. Measurement of pitting corrosion currents of steel in Ca(OH)(2) solutions under natural corrosion conditions.* Corrosion Science, 2009. **51**(8): p. 1611-1618.
82. Chen, Y.Y., L.B. Chou, and H.C. Shih, *Factors affecting the electrochemical behavior and stress corrosion cracking of Alloy 690 in chloride environments.* Materials Chemistry And Physics, 2006. **97**(1): p. 37-49.
83. http://www.corrosionsource.com/technicallibrary/corrdoctors/Modules/Aircraft/tempera.htm. 2009.
84. Bowsher, J.G., Nevelos, J., Pickard, J., and Shelton, J. C., *Do heat treatments influence the wear of large diameter metal-on-metal hip joints? - an in vitro study under normal and adverse gait conditions.* Transactions of the 49th Orthopaedic Research Society Meeting, New Orleans, Louisianna, USA, 2003. **28**: p. p1398.

9. Appendix

9.1 Clearance values of test pieces

Clearance values were only taken for the new test parts used to examine the difference in heat-treatments. This was to eliminate the variability that clearance could cause on the behaviour of each heat-treatment.

Femoral head diameter		**Acetabular cup diameter**			
		NW AC 1	**NW DHT 1**	**NW AC 2**	**NW DHT 2**
		50.027 mm	50.038 mm	50.026 mm	50.035 mm
NW AC 1	49.771 mm	254 microns	-	-	-
NW DHT 1	49.798 mm	-	240 microns	-	-
NW AC 2	49.776 mm	-	-	247 microns	-
NW DHT 2	49.788 mm	-	-	-	247 microns